

## GENERATION OF CENOZOIC GRANITOIDS IN HOKKAIDO (JAPAN): CONSTRAINTS FROM ZIRCON GEOCHRONOLOGY, Sr-Nd-Hf ISOTOPIC AND GEOCHEMICAL ANALYSES, AND IMPLICATIONS FOR CRUSTAL GROWTH

BOR-MING JAHN\*<sup>†</sup>, MASAKO USUKI\*, TADASHI USUKI\*\*,  
and SUN-LIN CHUNG\*

**ABSTRACT.** The island of Hokkaido is a young accretionary terrane, basically built with a Jurassic accretionary complex and Cretaceous arc in the west (= NE Japan arc terrane), a Cretaceous-Paleogene forearc basin and accretionary complex with the Hidaka metamorphic belt in the center, and a Cenozoic island arc with Cretaceous basement in the east (= Chishima or Kuril arc terrane). Though volumetrically small, Paleogene and Neogene granitoids are widespread in central Hokkaido (Hidaka Belt). Granitoids are the most representative component of the continental crust, so in this work we aimed to study the mode of generation and source characteristics of these granitoids in order to assess the crustal composition of Hokkaido and examine the general problem of continental growth. New zircon geochronology on nine granitic and one gabbroic rocks from the Hidaka Belt reveals three distinct magmatic episodes, two in the Eocene at 45–46 Ma (3 granites), and  $37.0 \pm 0.5$  Ma (1 granite), and one in the Miocene at 18 to 19 Ma (5 granites and 1 gabbro). The Miocene episode represents the most important granitic emplacement in Hokkaido. The early Eocene zircon ages of 45 to 46 Ma are identified for the first time for granitoids that occur in the northern part of the Hidaka Belt. The zircon age of 37 Ma for a granite from Shirataki is rather rare in Hokkaido, but similar ages had been reported for a tonalite and a granite from the Hidaka metamorphic belt. Geochemically, all granites are slightly peraluminous but not S-type, and they possess volcanic arc granitoid characteristics. Their REE distribution patterns are typically “granitic,” showing fractionated patterns with LREE enrichment and distinct negative Eu anomaly. The whole-rock isotopic signatures [ $I_{Sr} = 0.7044$  to  $0.7061$ ;  $\epsilon_{Nd}(t) = +1.0$  to  $+4.7$ ;  $T_{DM-1} = 400$ - $1000$  Ma] reveal their largely juvenile characteristics. This is corroborated by the zircon Hf isotopic compositions [ $\epsilon_{Hf}(t) = +8$  to  $+19$ ]. The Eocene granites were most probably generated by melting of subducted accretionary complex in a prolonged period from 46 to 37 Ma in supra-subduction zone; whereas the Miocene granites were also generated by melting of accretionary complex in a back-arc rifting setting. In both cases, the involved accretionary complex was probably dominated by the mantle-derived lithological component with little Paleozoic or older crustal material. Hokkaido provides an excellent example of juvenile crust addition to the continental crust.

Key words: Accretionary orogen, accretionary complex, Japanese Islands, Hokkaido, zircon dating, Sr-Nd-Hf isotope tracers, granitoids, Nipponides, crustal growth, juvenile/recycled crust, Central Asian Orogenic Belt (CAOB)

### INTRODUCTION

The Japanese Islands represent a Phanerozoic subduction-related orogen developed along the western Pacific convergent margin. The formation of the Japanese Islands has been taken as the classic model for accretionary orogeny (for example, Cawood and others, 2009). According to Maruyama and associates (Maruyama, 1997; Maruyama and others, 1997), the most important cause of the orogeny is the subduction of an oceanic ridge, by which the continental mass increases through the transfer of granitic melt from the subducting oceanic crust to the orogenic belt.

\* Department of Geosciences, National Taiwan University, Taipei 106, Taiwan

\*\* Institute of Earth Sciences, Academia Sinica, Nangang, Taipei 115, Taiwan

<sup>†</sup> Corresponding author: (bmjahn@ntu.edu.tw)

Sengor and Natal'in (1996) named the orogenic complex the "Nipponides," and pointed out the resemblance in orogenic style between Japan and the Central Asian Orogenic Belt (CAOB). Using the newly acquired and literature Sr-Nd isotopic data, Jahn (2010) tested the models made by the above authors. The test reveals that a large proportion of the granitoids from SW Japan in fact show high initial  $^{87}\text{Sr}/^{86}\text{Sr}$  ratios, negative  $\epsilon_{\text{Nd}}(\text{T})$  values and Proterozoic Sm-Nd model ages. These data are in strong contrast with those of two celebrated accretionary orogens, the CAOB (for example, Jahn, 2004) and Arabian-Nubian Shield (ANS; for example, Stern, 1994; Eyal and others, 2014), but are quite comparable with those observed in SE China and Taiwan (Jahn and others, 1990; Chen and Jahn, 1998; Jahn, 2010). This raises questions about the bulk composition of the continental crust in SW Japan, or the type of material accreted in accretionary complexes. The finding of Jahn (2010) also negates the hypothesis that the Nipponides contains very few fragments of older continental crust. It appears that the subduction-accretion complexes in SW Japan represent only the upper portion of the bulk crust, which is probably underlain by a Proterozoic basement.

A continuous study on other parts of the Japanese Islands reveals that the crustal development in NE Japan (= NE Honshu and Hokkaido) is quite distinguished from that of SW Japan (fig. 1). In NE Japan the granitoids show the lithological types (more TTG, or tonalite-trondhjemite-granodiorite suite, and adakitic rocks) and Sr-Nd isotopic compositions with significantly more "juvenile" signatures. Since granitic rocks are commonly generated in the P-T conditions of middle to lower crust, they are ideal materials to be used to probe the nature and architecture of the middle to lower continental crust. Besides, the radiogenic isotopic compositions of granitoids preserve the crustal history of their protoliths and constrain their formation time. In this paper, we employ the conventional geochemical and isotopic tracer techniques, together with zircon dating and Hf isotope analyses, to examine the petrogenesis of the Tertiary granitoids from Hokkaido. We will then compare the results with that of the massive granitoids from SW Japan and other celebrated accretionary orogens (for example, CAOB and ANS), and discuss the implications for crust growth and the tectonic evolution of the Japanese accretionary orogens.

#### GENERAL GEOLOGIC SETTING OF JAPAN AND HOKKAIDO

The evolution of the Japanese Islands results from the interaction of four tectonic plates: the Eurasian, Philippine Sea, Pacific and Okhotsk. The southwestern part of Japan (SW Japan) is an eastern margin of the Eurasian Plate, but separated from the Asian continent by the Japan Sea. The northeastern part of Honshu and Hokkaido (= NE Japan) belong to the Okhotsk plate. The Okhotsk plate was formerly considered as a part of the North American Plate, but recent studies indicate that it is an independent mini-plate, bounded on the north by the North American Plate (Seno and others, 1996; Apel and others, 2006). The Philippine Sea plate is subducting northwestwards at a rate of 4 to 6 cm/a under SW Japan along the Nankai Trough and Ryukyu trench. The Pacific plate is subducting at a rate of 9 to 10 cm/a beneath NE Japan, with its leading slab reaching a depth of 660 km underneath the area of Beijing, China, as revealed by a tomographic study (Zhao and others, 2007, 2011; see also a review by Isozaki and others, 2010).

An incipient subduction zone appears to be developed in the eastern Japan Sea (Nakamura, 1983; Tamaki and Honza, 1985). Its onland extension, the Itoigawa-Shizuoka Suture (fig. 1), separates the Japanese Islands in two parts, NE and SW Japan. However, this subduction zone is not universally accepted as the geophysical evidence is still not so convincing. On the other hand, many workers consider that the true geological or tectonic boundary between NE and SW Japan in the Pre-Tertiary time is located within NE Honshu, termed as "the Tanakura Tectonic Line" (fig. 1).

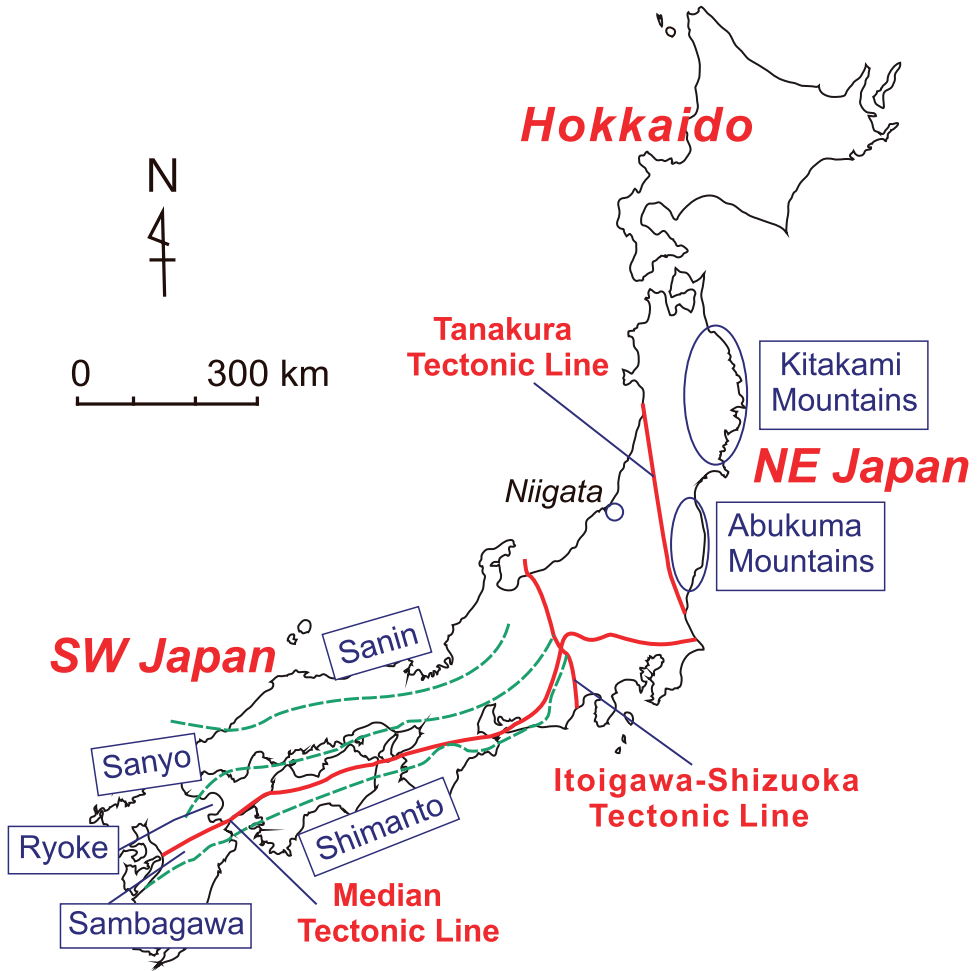


Fig. 1. Index map of Japan showing major tectonic units discussed in this paper. NE Japan is separated from SW Japan by a major fault or tectonic boundary, which is controversially represented by the Itoigawa-Shizuoka or Tanakura Tectonic Line. SW Japan comprises five tectonic belts: three granitic belts (Sanin, Sanyo and Ryoke) are separated by two accretionary belts (Sambagawa and Shimanto) by the Median Tectonic Line. In NE Japan, granitic rocks mainly occur in the Kitakami and Abukuma Mountains.

The predominance of accretionary complexes and the association of detached continental fragments in Japan suggest that the Japanese Islands have developed mainly through convergence between oceanic and continental plates along active margins (Isozaki, 1997; Isozaki and others, 2010). Isozaki (1996) stated that several major oceanic plates have subducted beneath the South China Block margin, leaving more than 10 distinct accretionary complex (AC) belts (now reduced to 9 AC belts, based on the latest reappraisal of the geotectonic framework of Japan by Isozaki and others, 2010). All the AC belts occur as thin subhorizontal fault-bounded geologic units, that is, nappes, and show a clear downward and oceanward younging polarity (Isozaki and Itaya, 1991; Isozaki and Maruyama, 1991). Numerous oceanic fragments derived from subducted oceanic plates, including deep-sea sediments and seamount basalts and reef limestone, were accreted to Japan. According to Isozaki and others (2010), five orogenic phases had occurred in the last 500 Ma, namely, at 450 Ma

(Oeyama), 340 Ma (Renge), 240 Ma (Akiyoshi), 140 to 130 Ma and 80 to 60 Ma. The Permo-Triassic event in Japan was thought to be related to the continental collision between the North and South China Blocks as recorded in the Dabie-Sulu terrane of China (Oh, 2006; Isozaki and others, 2010), or due to the collision of a Proto-Japan block with the Eurasian margin (de Jong and others, 2009). In summary, the model of accretionary orogeny developed for the Japanese Islands (= Miyashiro-type orogeny, Maruyama, 1997) underlines the prime role of continuous ocean-floor and episodic ocean-ridge subduction.

**Geology of Hokkaido.** The island of Hokkaido is a young accretionary terrane with little or no rocks of Paleozoic ages and older. Kiminami and others (1986) presented the first tectonic framework of the island's evolution, which was followed by other workers (for example, Komatsu and others, 1992). According to Ueda and others (2000) and Ueda (2005), Hokkaido comprises five roughly N-S running tectonic units or orogenic belts, from west to east (fig. 2): (1) the Oshima Belt, a Jurassic accretionary complex and an overlying Cretaceous arc; (2) the Sorachi-Yezo Belt, a Cretaceous-Paleogene forearc basin and accretionary complex; (3) the Hidaka Belt, a Paleogene arc complex in the north and the Hidaka metamorphic belt in the south; originally, the Hidaka Belt was defined to contain a Hidaka Supergroup (clastic accretionary complex) and a Hidaka Metamorphic Belt (metamorphosed accretionary complex, up to granulite facies); (4) the Tokoro Belt, a Cretaceous and Paleogene accretionary complex; and (5) the Nemuro Belt, a Cretaceous and Paleogene arc/forearc complex (fig. 2). Tectonically, the Oshima Belt has been considered as the northern extension of NE Honshu and formed the same tectonic collage with Sikhote-Alin of the Russian Far East (= Honshu-Sikhote-Alin Tectonic Collage), and the Sorachi-Yezo and Hidaka Belts formed a second tectonic collage or continental-margin arc with Sakhalin (= Sakhalin-Hokkaido Tectonic Collage; Rodionov and others, 2011). This arc was interpreted as having formed during subduction of the ancestral Pacific plate (Izanagi). The Tokoro and Nemuro belts belong to the Kuril Arc Terrane.

The accretionary complexes of the Oshima, Sorachi-Yezo and Hidaka Belts show a generally eastward younging polarity formed by westward subduction (Ueda and others, 2000; Kawamura, 2004). U-Pb SHRIMP dating of detrital zircon from the Oshima sandstone revealed some Precambrian ages of 1.88 and 2.5 Ga, hence suggesting that the Oshima sandstone had a share of clastic source from Precambrian terranes of the Asian continent or the Sino-Korean Craton (Kawamura and others, 2000).

The Sorachi-Yezo Belt comprises four tectonic units (GSJ, 2010): (1) the Sorachi Group, in the western part of the belt, composed essentially of greenstones in the lower part and greenstone, chert and pyroclastic rocks in the upper part; (2) the Yezo Group, to the east of the Sorachi group, characterized by a Cretaceous forearc basin sequence dominantly of marine siliciclastic deposits; (3) the Kamuikotan Zone, consisting of Cretaceous accretionary complexes, which have undergone various grades of metamorphism from the blueschist to epidote amphibolite facies; and (4) the Idonnappu Zone, consisting also of Cretaceous accretionary complexes, but only feebly metamorphosed. Kimura and others (1994) proposed that the greenstones of the Sorachi Group represented the remnants of an accreted Late Jurassic oceanic plateau formed on the Izanagi (Paleo-Pacific) plate based on the large volume of basaltic flows and hyaloclastic deposits. However, it has also been proposed that the Sorachi-Yezo belt represents a normal oceanic crust (Niida and Kito, 1986) or a marginal basin crust (Takashima and others, 2002). As a whole, Hokkaido is characterized by the latest Cretaceous to early Paleogene rapid growth of accretionary complex and exhumation of high pressure metamorphic rocks in the northwestern Pacific margin (Kimura, 1994).

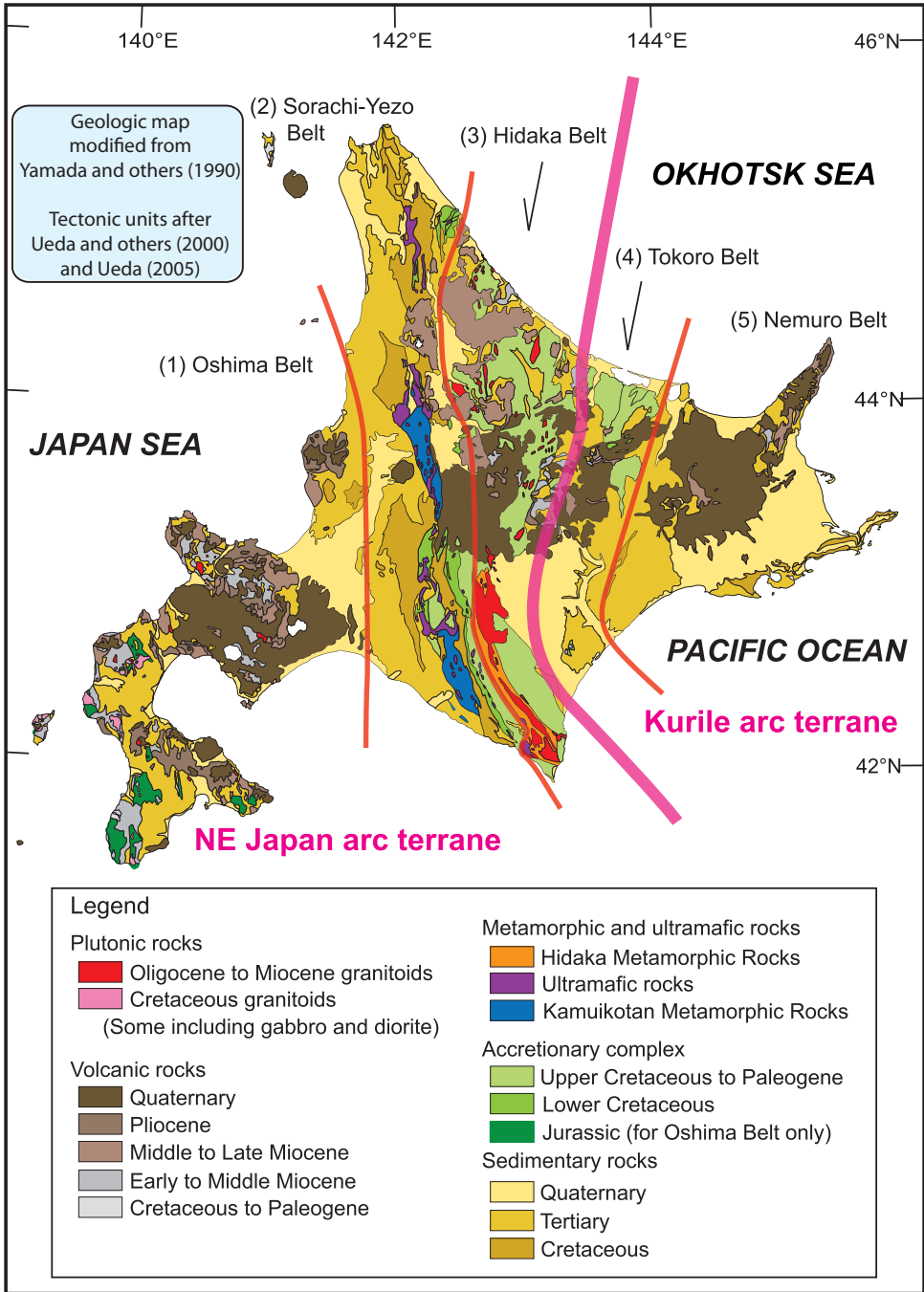


Fig. 2. General geologic map of Hokkaido (modified after Yamada and others, 1990). The division of tectonic units follows Ueda and others (2000) and Ueda (2005).

The Hidaka Belt in central Hokkaido is characterized by the vast distribution of Cretaceous accretionary complexes and Tertiary metamorphic belts and ophiolites (for example, Osanai and others, 1991, 1992). The Hidaka Supergroup consists mainly of sandstone and shale, with minor chert and volcanic tuffs. Basaltic lava is also found to erupt on or intruded into unconsolidated mudstone (Miyashita and Katsushima, 1986; Kiminami and others, 1999). Based on microfossil studies, these sediments were mostly deposited in the Paleogene. The Supergroup was intruded by granitoids of Eocene to Miocene ages. All the samples analyzed in this work came from this belt.

The Hidaka Metamorphic Belt (HMB) in south-central Hokkaido consists of high-angle east-dipping thrust sheets composed of metamorphic (pelitic-psammitic rocks, intermediate and mafic rocks), igneous (layered gabbro, massive gabbro-diorite and granitoids), and alpine-type ultramafic rocks (Arai and Takahashi, 1989; Arai, 1994; Shimura and others, 2004). In fact, the southern part of the Hidaka belt was considered to have formed by upthrusting of the eastern main block toward the western block due to oblique subduction of the Pacific Plate along the Kuril Trench since Miocene (Kimura, 1986). Thus, some workers considered that the zone along the Hidaka Main Thrust is a distinct suture between the western (Eurasian plate) and eastern (Okhotsk Plate) blocks (for example, Iwasaki and others, 2004). On the other hand, Ueda (2005) considered that the boundary between the Kurile and NE Japan arc terranes is situated to the east of the Hidaka Belt.

The base of the HMB is the Hidaka Main Thrust, where the metamorphic and igneous rocks are mylonitized with dextral shear sense. Almost all igneous rocks are intruded into the metamorphic layers as syn-metamorphic suites. The HMB is thought to represent an eastward dipping island-arc type crustal section (Komatsu and others, 1989, 1994; Owada and others, 2003). Based on the reconstruction of Shimura and others (2004), the unexposed "lowermost part" of the "Hidaka crust," from *ca.* 23 km to the Moho (30 km?) is probably composed of mafic granulites as inferred from petrological studies. The "lower Hidaka crust" (15–23 km) is likely represented by garnet-2-pyroxene mafic granulite, garnet-orthopyroxene aluminous granulite and gabbro. The mafic granulites and gabbros show MORB-like composition (Maeda and Kagami, 1994, 1996; Mikoshiba, 1999).

The Hidaka Mountains show a positive gravity anomaly zone, which was probably due to the tectonic uplift of the basement rocks that occurred during the collision of the Kuril forearc sliver with the northern extension of the Honshu arc (Kimura, 1986; Taira, 2001). In addition, the crustal thickness of the Hidaka Mountains is *ca.* 30 to 50 km (Ogawa and others, 1994), which is the thickest in Hokkaido.

The celebrated Horoman Peridotite occurs in the southernmost of the Hidaka belt. It is a fault-bounded mantle slice of 8 km × 10 km × 3 km, emplaced at *ca.* 23 Ma (Rb–Sr isotopes on a phlogopite-bearing spinel lherzolite, Yoshikawa and others, 1993). The peridotite consists of several lithological sequences of plagioclase lherzolite–lherzolite–harzburgite ± dunite–harzburgite–lherzolite–plagioclase lherzolite (for example, Takahashi, 1991; Takazawa and others, 1999, 2000). As the Horoman Peridotite is not directly related to the present work, no further details will be given. Similarly, the two tectonic units of the Kuril Arc, the Tokoro and Nemuro belts, are unrelated to the petrogenesis of the granitoids concerned, their description is not further presented. We proceed to introduce the geological setting and essential points relevant to the studied granitoids.

#### OCCURRENCE OF GRANITOIDS

Though volumetrically small, Cenozoic granitoids are widespread in the Hidaka Belt. They are scattered in the axial belt of central Hokkaido for an area of 300 km N-S and 60 km E-W (Ishihara and Terashima, 1985). The granitoids commonly crop out to the east of the high-grade metamorphic belt in the south, but scattered widely in the

non-metamorphosed Hidaka Supergroup in the north. Spatially, the granitoids do not accompany coeval volcanic rocks, but are closely associated with the contemporaneous gabbroids.

The Cenozoic granitoids of the Hidaka Belt are mostly fine-grained massive I-type granitoids (Ishihara and Terashima, 1985). Since they are associated with gabbroids, especially in the westernmost zone, the plutonism is of a bimodal nature. S-type granitoids also occur, and both S- and I-type granitoids contain ilmenite but not magnetite, so they belong to the ilmenite series (Ishihara and others, 1998). Ishihara (2007) considered that the granitoids were generated within the accretionary complex of the Hidaka Supergroup and its basement, by heat provided by these gabbroids.

Tonalitic granitoids, commonly known to be generated by partial melting of mafic sources, such as amphibolites, at lower crustal conditions, are conspicuously present in abundance in the Hidaka Metamorphic Belt. Based on the ASI (aluminum saturation index) or A/CNK (=  $\text{Al}_2\text{O}_3/(\text{CaO}+\text{Na}_2\text{O}+\text{K}_2\text{O})$  molar ratio), many of them have been classified as “S-type tonalities,” and the peraluminous variety (S-type) predominates over the metaluminous I-type (Shimura and others, 2004). Furthermore, the tonalities, especially the S-type, entrain a large number of enclaves of various rock types, including para-granulites (gt-opx-bi granulite and gt-opx-cord granulite), mafic granulites, and meta-harzburgite. Mafic enclaves comprise gabbro, hornblende amphibolite and mafic granulites (opx granulite and two-px granulite). Enclave-melt reactions are commonly observed.

Kemp and others (2007a) studied a suite of rocks including opx-bearing granulites, tonalites and gabbros from the Hidaka metamorphic belt and attempted to clarify the magmatic-metamorphic connection in this area. Their zircon geochronology revealed that the granulite and amphibolite facies metamorphism and the emplacement of garnet-opx tonalites and gabbros took place at about 19 Ma; whereas a hornblende-tonalite and a granite were emplaced at  $37.5 \pm 0.3$  Ma. With these zircon age data, they concluded that the Hidaka metamorphic belt has recorded a two-stage evolution, with the first stage of supra-subduction zone magmatism in late Eocene (*ca.* 37 Ma) and the second stage of back-arc extension in the Miocene (*ca.* 19 Ma). The second stage coincides with the opening of the Japan Sea, and the tectonic activity resulted in the granulite metamorphism and generation of grt-opx tonalite and gabbro, probably all related to the underplating of basic magma.

#### SAMPLING LOCALITIES AND SAMPLE DESCRIPTION

The granitoid samples of this study were collected from the Hidaka Belt of central Hokkaido, in a N-S traverse along about  $143^\circ\text{E}$  (fig. 3). A simple petrographic description of all the samples is given in table 1. Note that the rock types assigned for the granitoids were determined after the QAPF classification scheme of Streckeisen and Le Maitre (1979) based on normative abundances of quartz and feldspars. The modal analysis indicates that in addition to quartz and feldspars, biotite is present in all and hornblende in most granitoid samples. The only gabbro sample is composed of plagioclase, orthopyroxene and clinopyroxene.

#### ANALYTICAL METHODS

##### *Zircon U-Pb Geochronology and Lu-Hf Isotopic Analysis*

Zircon grains were separated from samples of about 1 to 3 kg using the conventional heavy-liquid and magnetic separation techniques at the Langfang Mineral Separation Laboratory, near Beijing. Cathodoluminescence (CL) images were taken at the Beijing SHRIMP Center, Institute of Geology, Chinese Academy of Geological Sciences, for examination of zircon internal structures and for selection of analytical spots.

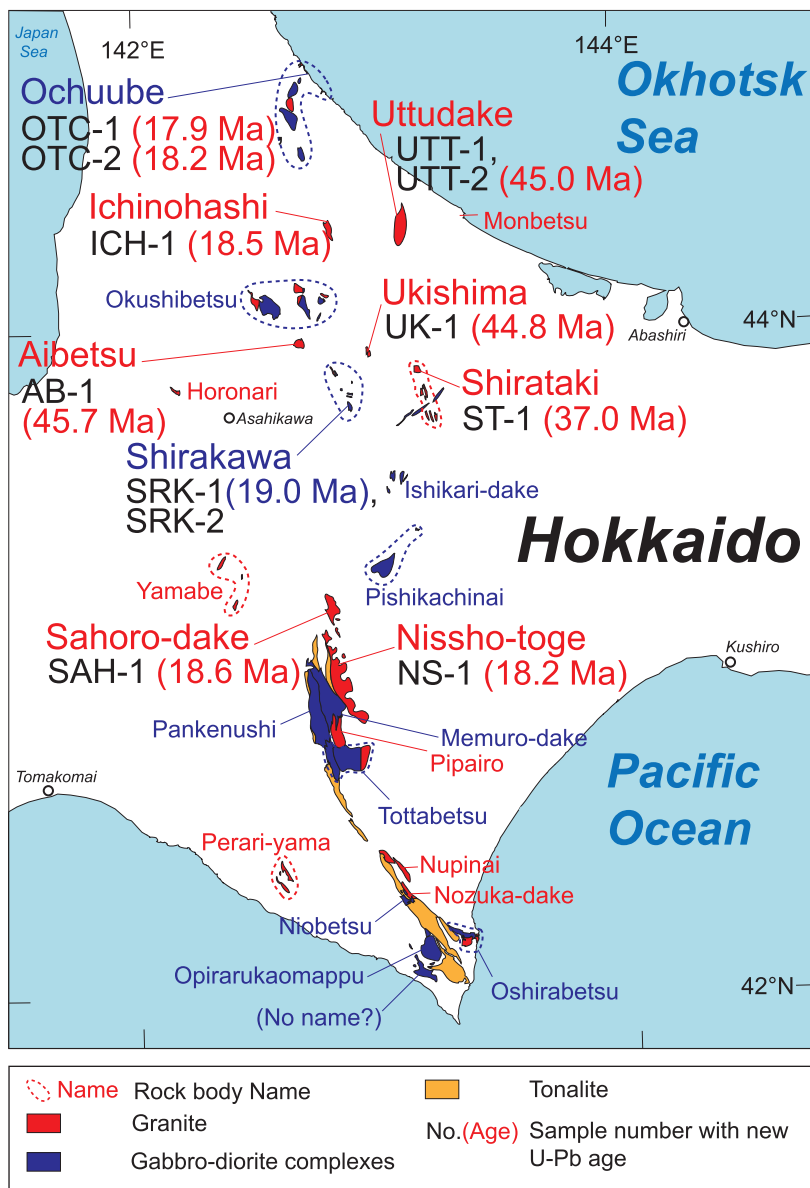


Fig. 3. Sampling localities of the granitoid samples from central Hokkaido. The Yamabe and Perari-yama intrusions are of granite porphyry. The new zircon ages obtained in this study are shown next to the sample numbers. Map based on GSJ, AIST, editor (2003), Maeda and others (1986), Editorial committee of Hokkaido (1990), Editorial committee of Geology of Japan (2005), Osanai and others (2006, 2007), Suetake (1997), and Nakagawa (1992).

Zircon U-Pb isotopic analyses were performed using a New Wave UP213 laser ablation system combined with an Agilent 7500s quadrupole ICPMS (inductively coupled plasma mass spectrometer) at the Department of Geosciences, National Taiwan University (NTU-Geosciences). The LA-ICPMS operating conditions and analytical procedures were the same as those reported in Chiu and others (2009). We

TABLE 1

*Petrographic description of granitoid and gabbro samples from Hokkaido, Japan*

Sample No.	Rock type	Major phases (approx. proportion)	Accessory phases	Secondary phases
NS-1	syenogranite	Kf (35%), Qtz (23%), Bt (20%), Pl (19%), Hbl (Chl) (3%)	opaque, zircon, apatite, titanite	Limonite?
SAH-1	syenogranite	Kf (40%), Qtz (36%), Pl (14%), Hbl (5%), Bt (5%)	opaque, zircon, apatite	
SRK-1	gabbro	Pl (60%), Opx (35%), Cpx (5%)	opaque	Hb, Bt, Chl
SRK-2	granodiorite	Pl (45%), Kf (23%), Qtz (22%), Hbl (3%), Bt (7%)	opaque, titanite, zoisite	
UTT-1	monzogranite	Qtz (26%), Kf (26%), Pl (23%), probably Hbl or Bt in original (25%)	opaque, apatite, zircon	Chl
UTT-2	monzogranite	Qtz (32%), Kf (28%), Pl (20%), Bt? In original (15%), green Hbl (5%)	opaque, apatite, zircon	
OTC-1	monzogranite	Kf (36%), Qtz (31%), Pl (23%), Bt (10%)	zircon, apatite	
OTC-2	monzogranite	Qtz (36%), Pl (31%), Kf (23%), Bt (10%)	opaque, zircon, apatite	
ICH-1	syenogranite	Kf (49%), Pl (24%), Qtz (24%), Bt (3%)	opaque, titanite, zircon, apatite	Chl
ST-1	monzogranite	Qtz (42%), Pl (26%), Kf (17%), probably Hbl or Bt in original (15%)	opaque, titanite, zircon, apatite	
UK-1	monzogranite	Pl (36%), Qtz (31%), Kf (23%), Hbl (5%), Bt (5%)	opaque, zircon, apatite	
AB-1	monzogranite	Bt (40%), Pl (21%), Kf (21%), Qtz (18%)	opaque, zircon, apatite	

have followed a common practice in reporting zircon ages of young, particularly Cenozoic, rocks; for example, Wen and others (2008) and Chiu and others (2009). Generally, precise measurement of  $^{207}\text{Pb}/^{235}\text{U}$  and  $^{207}\text{Pb}/^{206}\text{Pb}$  ratios is feasible for Precambrian zircons, but not for very young zircons, due to the fact that in young zircons  $^{235}\text{U}$  comprises less than 1 percent of natural U, thus little  $^{207}\text{Pb}$  can be produced in zircons (for example, Ireland and Williams, 2003). For this reason, the weighted mean of pooled  $^{206}\text{Pb}/^{238}\text{U}$  ages are taken to represent the crystallization ages of the dated samples. The  $^{206}\text{Pb}/^{238}\text{U}$  ages are reported with uncertainties at two-standard deviation ( $2\sigma$ ) or 95 percent confidence level.

*In-situ* Lu-Hf isotopic analyses of zircon were performed using a multi-collector ICP-MS (Neptune), also at NTU-Geosciences. A New Wave UP193FX laser ablation system was used for spot vaporization. The Lu-Hf isotope analyses were done on the same zircon grains that were previously analyzed for U-Pb dating. Ablation time was about 26 s for each measurement with a beam diameter of *ca.* 40  $\mu\text{m}$ , an 8 Hz repetition rate, and energy of 100 mJ. The detailed descriptions for the analytical techniques can be found in Wu and others (2006) and Xie and others (2008). The Harvard reference zircon 91500 and Australian Mud Tank carbonatite zircon were used as secondary standards for data quality assessment. During the data acquisition of this study,  $^{176}\text{Hf}/^{177}\text{Hf}$  ratio of  $0.282511 \pm 25$  ( $2\sigma$ ,  $n = 39$ ) for Mud Tank and  $0.282293 \pm 22$  ( $2\sigma$ ,  $n = 16$ ) for 91500 were obtained. These values are in good agreement with those obtained by solution and ICPMS methods reported in the literature (Goolaerts and others, 2004; Woodhead and others, 2004; Woodhead and Hergt, 2005; Griffin and others, 2006; Wu and others, 2006).

*Major and Trace Element Analyses*

All major and trace element analyses were performed at NTU-Geosciences. Samples were crushed in a stainless steel jaw crusher and then powdered in an agate

mill. Major elements were determined by X-ray fluorescence (XRF) spectroscopy on fused glass beads, using a Rigaku RIX-2000 spectrometer. For trace-element analyses, about 200 mg of powdered sample was dissolved in a mixture of HF and HNO<sub>3</sub> (2:1) in a screw-top Teflon beaker (Savillex) for 5 to 7 days at ~100 °C. This was followed by evaporation to dryness, refluxing in 6N HCl and drying twice, and finally re-dissolution in 1N HCl. The procedure was repeated until complete dissolution. The final solution was split in two parts; a small aliquot (about 10%) was used for subsequent trace element analysis by ICP-MS, and the rest for further chemical separation of Sr and Nd for isotopic analysis using a thermo-ionization mass spectrometer (TIMS). Trace element analysis was performed using an Agilent 7500s. The standard reference materials used for trace element analyses are AGV-2, BCR-2, BHVO-2, BIR-1 and DNC-1. The details of analytical procedures may be found in Lin and others (2012). Analytical errors are 0.5 to 3 percent for major elements and 1 to 10 percent for trace elements, depending on the concentrations.

#### *Whole-Rock Sr-Nd Isotopic Analyses*

For Sr-Nd isotopic analysis, the chemical preparation and mass analysis were performed at Institute of Earth Sciences (IES), Academia Sinica. Approximately 150 to 175 mg of rock powder was dissolved using a HF-HNO<sub>3</sub> (2:1) mixture in a screw-top Teflon beaker for 5 to 7 days at ~100 °C. This same procedure was followed by evaporation to dryness, refluxing in 6N HCl and drying twice, and then dissolution in 1N HCl. The procedure was repeated until complete dissolution. Chemical separation was carried out using the conventional ion exchange techniques. Strontium and REEs were separated in polyethylene columns with a 2.5 ml resin bed of AG50W-X8, 100 to 200 mesh. Strontium was further purified through 1 ml resin bed of AG50W-X8, 100 to 200 mesh. Neodymium was separated from other REEs on 1 ml polyethylene columns using Eichrom Ln resin (Ln-B25-A) as a cation exchange medium. Sr and Nd isotope ratios were measured using a Finnigan MAT 262 and a TRITON mass spectrometer. For the isotopic measurement, Sr was loaded on a single Ta filament with H<sub>3</sub>PO<sub>4</sub> and TaF<sub>5</sub>; but Nd was loaded on a Re filament with H<sub>3</sub>PO<sub>4</sub> and measured using a double-Re-filament configuration. The effect of mass fractionation in Sr and Nd isotopic measurements was corrected by normalizing to  $^{86}\text{Sr}/^{88}\text{Sr} = 0.1194$  and  $^{146}\text{Nd}/^{144}\text{Nd} = 0.7219$ , respectively. Analyses of NBS 987 Sr and JMC Nd standard throughout the period of analysis yielded  $^{86}\text{Sr}/^{87}\text{Sr} = 0.710238 \pm 0.000016$  ( $2\sigma$ ) and  $^{143}\text{Nd}/^{144}\text{Nd} = 0.511812 \pm 0.000007$  ( $2\sigma$ ). Procedural blanks were *ca.* 330 pg Sr and 300 pg Nd. Within-run precision, expressed as  $2\sigma_m$ , was better than 0.000010 for both Sr and Nd. The procedures of chemical separation and mass analysis can be found in Jahn and others (2009).

### ANALYTICAL RESULTS

#### *Zircon U-Pb Data*

The CL images of the ten analyzed zircon samples are shown in figure 4. The sizes of zircon grains could be estimated from the round laser-abraded spots that have a diameter of about 50 μm. Zircon grains are in general prismatic and euhedral. A total of 104 images were taken. Since all the images are very similar, only two images from each sample are displayed in this figure. All zircon crystals show simple internal structure with clear oscillatory zonings, thus their magmatic origin can be certified. The results of U-Pb isotopic analyses are given in table 2. The errors for individual spot analyses are quoted at  $1\sigma$ , whereas those for the weighted mean ages represent  $2\sigma$  (95% confidence level).

Figure 5 shows a plot of Th/U ratios vs U concentrations in zircon samples. The variation in both parameters are quite impressive; the U concentrations vary from less

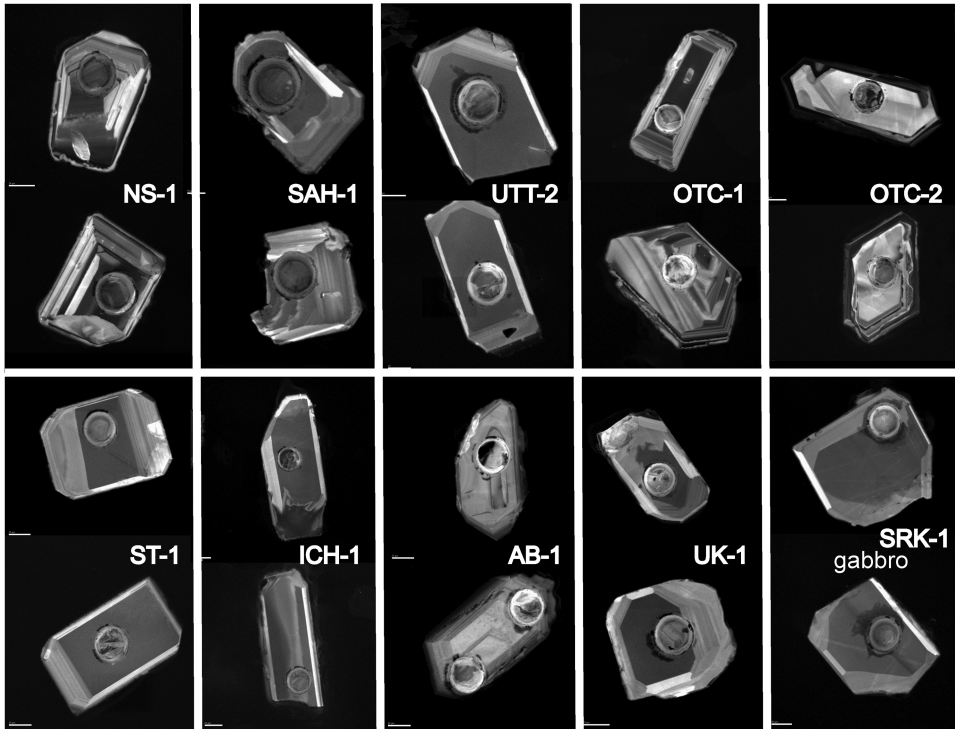


Fig. 4. Representative CL images of the dated granitoids and a gabbro. The round spot size is about 50  $\mu\text{m}$  (diameter).

than 100 ppm to 2000 ppm or more, and most Th/U ratios are greater than 0.5. Since metamorphic zircons commonly have low to very low Th/U ratios ( $<0.1$ ; Hoskin and Black, 2000), the present Th and U concentration data corroborate the magmatic origin of the zircon crystals of the Hokkaido granites.

Figure 6 illustrates the U-Pb isotopic compositions in the Concordia diagrams. We underline that almost all individual analyses fall on or near the Concordia. For the obvious reason that the ratios of  $^{206}\text{Pb}/^{238}\text{U}$  are more precisely measured than those of  $^{207}\text{Pb}/^{235}\text{U}$  and  $^{207}\text{Pb}/^{206}\text{Pb}$  (table 2), the weighted mean values of  $^{206}\text{Pb}/^{238}\text{U}$  dates are taken to be the crystallization ages of the analyzed zircon crystals. The obtained ages fall in three groups: (1) 45 to 46 Ma (3 granite samples), (2)  $37.0 \pm 0.5$  Ma (1 granite sample), and (3) 18 to 19 Ma (5 granite samples and 1 gabbro sample).

#### Whole-Rock Geochemical Data

The chemical analyses of the granitoids are presented in table 3. The principal characteristics are illustrated in figures 7 and 8. In the Q'-ANOR classification scheme of Streckeisen and Le Maitre (1979), all the Hokkaido granitoids fall in the class of "granite" (monzogranite + syenogranite) with only one exception, sample SRK-2, in granodiorite (fig. 7A). The granitoid samples show a range of  $\text{SiO}_2$  contents from *ca.* 65 to 75 percent, and  $\text{K}_2\text{O}$  from 2.7 to 5.0 percent (table 3). In the A/NK vs A/CNK diagram (fig. 7B), most samples are shown slightly peraluminous; all but one sample (AB-1) have A/CNK ratios less than 1.1, which is the value suggested by Chappell and White (1992) to be the boundary between I- and S-type granitoids. Consequently, most granitoids may be considered as I-type granitoids, but not S-type as commonly referred to in the literature.

TABLE 2  
Zircon U-Pb isotopic compositions, Th-U concentrations and calculated ages

Analysis No.	Th (ppm)	U (ppm)	Th/U	RATIO S (common-Pb corrected)				AGE S (common-Pb corrected, Ma)											
				$\frac{^{207}\text{Pb}}{^{235}\text{U}} \pm 1\sigma$	$\frac{^{207}\text{Pb}}{^{238}\text{U}} \pm 1\sigma$	$\frac{^{208}\text{Pb}}{^{232}\text{Th}} \pm 1\sigma$	$\frac{^{207}\text{Pb}}{^{206}\text{Pb}} \pm 1\sigma$	$\frac{^{207}\text{Pb}}{^{233}\text{U}} \pm 1\sigma$	$\frac{^{206}\text{Pb}}{^{238}\text{U}} \pm 1\sigma$	$\frac{^{206}\text{Pb}}{^{232}\text{Th}} \pm 1\sigma$	$\frac{^{208}\text{Pb}}{^{232}\text{Th}} \pm 1\sigma$								
<b>OTC-1 wt. mean = 17.9 ± 0.3 Ma (2σ)</b>																			
OTC-1-2	3099	1979	1.57	0.04617	0.00073	0.01712	0.00056	0.00269	0.00006	0.00089	0.00002	6	32	17.2	0.6	17.3	0.4	18.0	0.4
OTC-1-3	684	909	0.75	0.04732	0.00092	0.01816	0.00066	0.00278	0.00006	0.00095	0.00003	65	45	18.3	0.7	17.9	0.4	19.2	0.6
OTC-1-4	1147	1381	0.83	0.04609	0.00025	0.01797	0.00046	0.00283	0.00007	0.00100	0.00003	2	13	18.1	0.5	18.2	0.4	20.2	0.7
OTC-1-5	1794	2001	0.90	0.04617	0.00107	0.01698	0.00066	0.00267	0.00006	0.00087	0.00003	6	45	17.1	0.7	17.2	0.4	17.6	0.5
OTC-1-6	480	832	0.58	0.04548	0.00085	0.01828	0.00068	0.00292	0.00007	0.00098	0.00003	-30	36	18.4	0.7	18.8	0.4	19.8	0.6
OTC-1-7	260	375	0.69	0.04940	0.00172	0.01984	0.00109	0.00291	0.00007	0.00096	0.00004	167	82	20.0	1.0	18.7	0.4	19.4	0.8
OTC-1-8	165	179	0.92	0.05191	0.00367	0.02059	0.00195	0.00288	0.00008	0.00094	0.00005	281	160	21.0	2.0	18.5	0.5	19.0	1.0
OTC-1-9	896	1092	0.82	0.04613	0.00061	0.01811	0.00059	0.00285	0.00007	0.00095	0.00003	5	27	18.2	0.6	18.3	0.5	19.1	0.6
OTC-1-13	597	883	0.68	0.04761	0.00097	0.01847	0.00069	0.00281	0.00006	0.00105	0.00003	80	48	18.6	0.7	18.1	0.4	21.2	0.6
OTC-1-14	505	686	0.74	0.04604	0.00106	0.01772	0.00076	0.00279	0.00007	0.00100	0.00003	0	45	17.8	0.8	18.0	0.4	20.2	0.6
OTC-1-15	238	475	0.50	0.05011	0.00204	0.01874	0.00117	0.00271	0.00007	0.00099	0.00005	200	93	19.0	1.0	17.4	0.5	20.0	1.0
OTC-1-16	1158	1904	0.61	0.04785	0.00062	0.01791	0.00051	0.00272	0.00006	0.00098	0.00002	92	30	18.0	0.5	17.5	0.4	19.8	0.4
OTC-1-17	1155	794	1.45	0.04813	0.00106	0.01862	0.00073	0.00281	0.00006	0.00091	0.00002	106	51	18.7	0.7	18.1	0.4	18.4	0.4
OTC-1-18	690	588	1.17	0.04471	0.00121	0.01741	0.00082	0.00283	0.00007	0.00093	0.00003	-34	52	17.5	0.8	18.2	0.4	18.8	0.6
OTC-1-19	610	411	1.48	0.04614	0.00208	0.01701	0.00109	0.00267	0.00007	0.00090	0.00004	5	94	17.0	1.0	17.2	0.5	18.2	0.9
OTC-1-21	591	482	1.23	0.04750	0.00145	0.01790	0.00092	0.00273	0.00007	0.00092	0.00003	74	68	18.0	0.9	17.6	0.5	18.6	0.6
OTC-1-24	673	775	0.87	0.04576	0.00109	0.01729	0.00072	0.00274	0.00006	0.00089	0.00003	-15	47	17.4	0.7	17.6	0.4	18.0	0.6
<b>OTC-2 wt. mean = 18.2 ± 0.2 Ma (2σ)</b>																			
OTC-2-1	1257	773	1.63	0.04616	0.00149	0.00149	0.01761	0.00277	0.00006	0.00090	0.00002	6	65	17.7	0.8	17.8	0.4	18.1	0.4
OTC-2-2	503	740	0.68	0.04688	0.00229	0.00229	0.01809	0.00280	0.00007	0.00089	0.00004	43	105	18.0	1.0	18.0	0.4	18.0	0.9
OTC-2-5	898	1055	0.85	0.04612	0.00066	0.00066	0.01742	0.00274	0.00006	0.00092	0.00003	4	28	17.5	0.5	17.6	0.4	18.5	0.6
OTC-2-6	156	233	0.67	0.05064	0.00298	0.00298	0.02008	0.00288	0.00007	0.00096	0.00005	224	134	20.0	2.0	18.5	0.4	19.0	1.0
OTC-2-7	716	871	0.82	0.04669	0.00153	0.00153	0.01827	0.00284	0.00007	0.00090	0.00003	33	69	18.4	0.9	18.3	0.5	18.3	0.5
OTC-2-8	528	723	0.73	0.04738	0.00164	0.00164	0.01834	0.00281	0.00007	0.00089	0.00002	68	77	18.0	1.0	18.1	0.5	18.0	0.4
OTC-2-9	437	522	0.84	0.04773	0.00221	0.00221	0.01894	0.00288	0.00007	0.00091	0.00003	86	100	19.0	1.0	18.5	0.5	18.5	0.5
OTC-2-10	835	911	0.92	0.05487	0.00104	0.00104	0.02139	0.00283	0.00006	0.00117	0.00003	407	42	21.5	0.8	18.2	0.4	23.6	0.6
OTC-2-11	1248	1411	0.88	0.04610	0.00019	0.00019	0.01881	0.00296	0.00007	0.00102	0.00003	3	10	18.9	0.5	19.1	0.4	20.7	0.7
OTC-2-12	402	562	0.72	0.04743	0.00199	0.00199	0.01847	0.00282	0.00007	0.00090	0.00003	71	92	19.0	1.0	18.2	0.4	18.1	0.6
OTC-2-13	403	562	0.72	0.04688	0.00123	0.00123	0.01853	0.00287	0.00007	0.00102	0.00003	43	56	18.6	0.8	18.5	0.4	20.6	0.6
OTC-2-15	1304	1913	0.68	0.04809	0.00061	0.00061	0.01816	0.00274	0.00006	0.00103	0.00003	104	30	18.3	0.5	17.6	0.4	20.8	0.6
OTC-2-16	256	337	0.76	0.04538	0.00216	0.00216	0.01841	0.00294	0.00007	0.00100	0.00004	0	98	19.0	1.0	18.9	0.4	20.2	0.8

TABLE 2  
(continued)

Analysis No.	Th (ppm)	U (ppm)	Th/U	RATI OS (common-Pb corrected)			AGE S (common-Pb corrected, Ma)											
				$\frac{^{207}\text{Pb}}{^{235}\text{U}} \pm 1\sigma$	$\frac{^{206}\text{Pb}}{^{238}\text{U}} \pm 1\sigma$	$\frac{^{208}\text{Pb}}{^{232}\text{Th}} \pm 1\sigma$	$\frac{^{207}\text{Pb}}{^{206}\text{Pb}} \pm 1\sigma$	$\frac{^{207}\text{Pb}}{^{233}\text{U}} \pm 1\sigma$	$\frac{^{206}\text{Pb}}{^{238}\text{U}} \pm 1\sigma$	$\frac{^{208}\text{Pb}}{^{232}\text{Th}} \pm 1\sigma$								
<b>OTC-2 wt. mean = 18.2 ± 0.2 Ma (2σ)</b>																		
OTC-2-17	3783	2041	1.85	0.04614	0.00063	0.01763	0.00277	0.00006	0.00092	0.00002	5	28	17.7	0.5	17.8	0.4	18.6	0.4
OTC-2-19	562	506	1.11	0.04609	0.00044	0.00044	0.00281	0.00007	0.00097	0.00004	2	20	18.0	0.5	18.1	0.4	19.6	0.7
OTC-2-20	133	337	0.39	0.04928	0.00215	0.01875	0.00276	0.00007	0.00105	0.00006	161	98	19.0	1.0	17.8	0.5	21.0	1.0
OTC-2-21	237	247	0.96	0.04673	0.00474	0.01847	0.00287	0.00010	0.00117	0.00007	35	212	19.0	2.0	18.5	0.6	24.0	1.0
OTC-2-22	158	287	0.55	0.05296	0.00379	0.02007	0.00275	0.00008	0.00130	0.00008	327	164	20.0	2.0	17.7	0.5	26.0	2.0
OTC-2-24	552	591	0.93	0.04608	0.00021	0.00021	0.00297	0.00007	0.00108	0.00005	2	11	19.0	0.4	19.1	0.4	21.9	1.0
<b>ICH-1 wt. mean = 18.5 ± 0.2 Ma (2σ)</b>																		
ICH-1-1	192	157	1.22	0.04911	0.00443	0.01862	0.00275	0.00008	0.00087	0.00004	153	200	19.0	2.0	17.7	0.5	17.6	0.7
ICH-1-2	367	267	1.37	0.05008	0.00210	0.01964	0.00284	0.00007	0.00094	0.00003	199	98	20.0	1.0	18.3	0.4	19.0	0.6
ICH-1-4	1151	415	2.77	0.04662	0.00151	0.01816	0.00282	0.00006	0.00090	0.00002	30	68	18.3	0.9	18.2	0.4	18.2	0.4
ICH-1-6	157	142	1.10	0.05807	0.00509	0.02223	0.00278	0.00009	0.00095	0.00005	532	196	22.0	3.0	17.9	0.6	19.0	1.0
ICH-1-7	1278	700	1.82	0.04842	0.00096	0.01874	0.00281	0.00006	0.00095	0.00002	120	47	18.9	0.7	18.1	0.4	19.2	0.4
ICH-1-8	1772	850	2.08	0.04612	0.00035	0.01860	0.00292	0.00006	0.00098	0.00002	4	17	18.7	0.4	18.8	0.4	19.9	0.4
ICH-1-9	1030	585	1.76	0.04637	0.00114	0.01856	0.00290	0.00006	0.00095	0.00002	17	51	18.7	0.8	18.7	0.4	19.2	0.4
ICH-1-10	215	195	1.11	0.04543	0.00300	0.00300	0.01817	0.00290	0.00100	0.00004	-32	140	18.0	2.0	18.7	0.4	20.2	0.8
ICH-1-11	219	206	1.06	0.04945	0.00317	0.00317	0.01884	0.00276	0.00007	0.00004	169	143	19.0	2.0	17.8	0.5	20.6	0.8
ICH-1-12	204	195	1.04	0.04607	0.00032	0.00032	0.01867	0.00294	0.00007	0.00008	1	16	18.8	0.5	18.9	0.5	23.0	2.0
ICH-1-13	884	474	1.86	0.04620	0.00242	0.0242	0.01848	0.00290	0.00007	0.00003	8	108	19.0	1.0	18.7	0.4	18.8	0.5
ICH-1-14	1113	579	1.92	0.04672	0.00113	0.00113	0.01846	0.00287	0.00006	0.00094	35	51	18.6	0.8	18.5	0.4	19.0	0.4
ICH-1-16	287	232	1.23	0.04938	0.00371	0.00371	0.02013	0.00296	0.00008	0.00093	166	168	20.0	2.0	19.0	0.5	18.9	0.5
ICH-1-17	2563	1060	2.42	0.04797	0.00098	0.00098	0.01845	0.00279	0.00006	0.00092	98	48	18.6	0.7	18.0	0.4	18.6	0.4
ICH-1-18	1259	651	1.93	0.04390	0.00104	0.00104	0.01751	0.00289	0.00006	0.00096	-76	50	17.6	0.7	18.6	0.4	19.4	0.4
ICH-1-19	1200	621	1.93	0.04673	0.00097	0.00097	0.01876	0.00291	0.00007	0.00097	35	44	18.9	0.7	18.7	0.4	19.6	0.4
ICH-1-21	159	161	0.98	0.04905	0.00332	0.00332	0.02015	0.00298	0.00008	0.00102	150	150	20.0	2.0	19.2	0.5	20.6	0.8
ICH-1-24	173	163	1.07	0.04998	0.00346	0.00346	0.02043	0.00297	0.00008	0.00100	194	157	21.0	2.0	19.1	0.5	20.2	0.8
<b>UTT-2 wt. mean = 45.0 ± 0.5 Ma (2σ)</b>																		
UTT-2-1	353	239	1.48	0.04730	0.00205	0.00205	0.04479	0.00687	0.00017	0.00220	64	94	44	3	44	1	44	1
UTT-2-2	399	268	1.49	0.04607	0.00107	0.00107	0.04524	0.00712	0.00015	0.00237	1	46	45	2	46	1	48	1
UTT-2-3	169	139	1.21	0.05105	0.00237	0.00237	0.04970	0.00706	0.00017	0.00245	243	109	49	3	45	1	49	2
UTT-2-4	176	164	1.07	0.04867	0.00210	0.00210	0.04737	0.00706	0.00017	0.00249	132	98	47	3	45	1	50	2
UTT-2-5	257	244	1.05	0.04846	0.00145	0.00145	0.04862	0.00728	0.00016	0.00251	122	71	48	2	47	1	51	1

TABLE 2  
(continued)

Analysis No.	Th (ppm)	U (ppm)	Th/U	RATIOS (common-Pb corrected)				AGES (common-Pb corrected, Ma)										
				$\frac{^{207}\text{Pb}}{^{206}\text{Pb}} \pm 1\sigma$	$\frac{^{207}\text{Pb}}{^{235}\text{U}} \pm 1\sigma$	$\frac{^{206}\text{Pb}}{^{238}\text{U}} \pm 1\sigma$	$\frac{^{208}\text{Pb}}{^{232}\text{Th}} \pm 1\sigma$	$\frac{^{207}\text{Pb}}{^{206}\text{Pb}} \pm 1\sigma$	$\frac{^{207}\text{Pb}}{^{235}\text{U}} \pm 1\sigma$	$\frac{^{206}\text{Pb}}{^{238}\text{U}} \pm 1\sigma$	$\frac{^{208}\text{Pb}}{^{232}\text{Th}} \pm 1\sigma$							
<b>UTT-2 wt. mean = 45.0 ± 0.5 Ma (2σ)</b>																		
UTT-2-6	129	137	0.94	0.04921	0.00283	0.04870	0.00718	0.00018	0.00239	0.00010	158	128	48	4	46	1	48	2
UTT-2-7	301	217	1.38	0.04727	0.00161	0.04686	0.00719	0.00017	0.00242	0.00007	63	74	46	2	46	1	49	1
UTT-2-8	225	226	1.00	0.04859	0.00162	0.04765	0.00711	0.00016	0.00254	0.00007	128	78	47	2	46	1	51	1
UTT-2-9	457	311	1.47	0.04616	0.00196	0.04504	0.00708	0.00016	0.00227	0.00005	6	89	45	3	45	1	46	1
UTT-2-10	204	189	1.08	0.04648	0.00234	0.04391	0.00685	0.00016	0.00218	0.00008	22	105	44	3	44	1	44	2
UTT-2-11	413	276	1.49	0.04756	0.00135	0.04722	0.00720	0.00016	0.00242	0.00006	77	63	47	2	46	1	49	1
UTT-2-12	220	188	1.17	0.04663	0.00192	0.04485	0.00698	0.00016	0.00234	0.00007	30	88	45	3	45	1	47	1
UTT-2-13	239	175	1.36	0.04882	0.00149	0.04742	0.00705	0.00017	0.00230	0.00006	139	71	47	2	45	1	46	1
UTT-2-14	754	431	1.75	0.04613	0.00167	0.04491	0.00707	0.00017	0.00232	0.00005	4	73	44	2	45	1	45	1
UTT-2-16	310	228	1.35	0.04609	0.00128	0.04537	0.00680	0.00016	0.00229	0.00008	119	84	45	3	44	1	46	2
UTT-2-17	115	146	0.78	0.04840	0.00182	0.04537	0.00680	0.00016	0.00229	0.00008	119	84	45	3	44	1	46	2
UTT-2-19	147	167	0.88	0.04411	0.00149	0.04403	0.00724	0.00017	0.00232	0.00008	-65	70	44	2	47	1	47	2
UTT-2-20	655	431	1.52	0.04610	0.00178	0.04359	0.00686	0.00017	0.00223	0.00006	3	80	43	2	44	1	45	1
UTT-2-21	604	345	1.75	0.05116	0.00091	0.04709	0.00668	0.00015	0.00220	0.00005	248	41	47	2	43	1	44	1
UTT-2-22	822	508	1.62	0.04807	0.00080	0.04486	0.00677	0.00015	0.00226	0.00005	103	39	45	1	44	1	46	1
UTT-2-23	150	155	0.97	0.04678	0.00217	0.04334	0.00672	0.00016	0.00214	0.00007	38	100	43	3	43	1	43	1
UTT-2-25	143	138	1.04	0.04615	0.00255	0.04421	0.00695	0.00018	0.00222	0.00009	5	115	44	3	45	1	45	2
<b>AB-1 wt. mean = 45.7 ± 0.5 Ma (2σ); old core excluded</b>																		
AB-1-4	118	208	0.57	0.04265	0.00191	0.04076	0.00694	0.00018	0.00231	0.00011	-142	98	41	3	45	1	47	2
AB-1-7	100	160	0.63	0.04660	0.00247	0.04447	0.00693	0.00018	0.00256	0.00012	29	112	44	3	45	1	52	2
AB-1-8	510	443	1.15	0.04704	0.00094	0.04454	0.00687	0.00017	0.00217	0.00006	51	45	44	2	44	1	44	1
AB-1-10	136	250	0.54	0.04592	0.00163	0.04362	0.00689	0.00018	0.00208	0.00009	-6	73	43	2	44	1	42	2
AB-1-11	159	167	0.95	0.05231	0.00223	0.05255	0.00729	0.00019	0.00228	0.00009	299	97	52	3	47	1	46	2
AB-1-12	165	251	0.66	0.04977	0.00156	0.04856	0.00708	0.00018	0.00254	0.00009	184	72	48	2	45	1	51	2
AB-1-13	53	156	0.34	0.04211	0.00323	0.04084	0.00703	0.00020	0.00224	0.00021	-171	148	41	4	45	1	45	4
AB-1-14	85	164	0.52	0.04212	0.00280	0.04161	0.00717	0.00020	0.00284	0.00015	-170	136	41	4	46	1	49	3
AB-1-15	213	234	0.91	0.05938	0.00190	0.05804	0.00709	0.00019	0.00243	0.00008	581	106	57	3	46	1	57	3
AB-1-16	115	169	0.68	0.04829	0.00268	0.04691	0.00705	0.00019	0.00219	0.00011	114	120	47	4	45	1	44	2
AB-1-17	166	220	0.75	0.04197	0.00199	0.04217	0.00729	0.00019	0.00231	0.00009	-179	106	42	3	47	1	47	2
AB-1-18(c)	425	303	1.40	0.04826	0.00065	0.20836	0.03132	0.00077	0.01021	0.00023	112	32	192	5	199	5	205	5
AB-1-19(r)	95	218	0.43	0.04730	0.00210	0.04732	0.00726	0.00020	0.00249	0.00014	64	98	47	3	47	1	50	3

TABLE 2  
(continued)

Analysis No.	Th (ppm)	U (ppm)	Th/U	RATIOS (common-Pb corrected)				AGES (common-Pb corrected, Ma)											
				$\frac{^{207}\text{Pb}}{^{206}\text{Pb}} \pm 1\sigma$	$\frac{^{207}\text{Pb}}{^{235}\text{U}} \pm 1\sigma$	$\frac{^{206}\text{Pb}}{^{238}\text{U}} \pm 1\sigma$	$\frac{^{208}\text{Pb}}{^{232}\text{Th}} \pm 1\sigma$	$\frac{^{207}\text{Pb}}{^{206}\text{Pb}} \pm 1\sigma$	$\frac{^{207}\text{Pb}}{^{235}\text{U}} \pm 1\sigma$	$\frac{^{206}\text{Pb}}{^{238}\text{U}} \pm 1\sigma$	$\frac{^{208}\text{Pb}}{^{232}\text{Th}} \pm 1\sigma$								
<b>AB-1 wt. mean = 45.7 ± 0.5 Ma (2σ); old core excluded</b>																			
AB-1-20	78	141	0.55	0.04578	0.00319	0.04394	0.00696	0.00020	0.00238	0.00014	-14	150	44	4	45	1	48	3	
AB-1-21	715	924	0.77	0.04756	0.00065	0.04724	0.00721	0.00018	0.00230	0.00006	77	32	47	1	46	1	46	1	
AB-1-22	75	198	0.38	0.05325	0.00223	0.05247	0.00715	0.00019	0.00226	0.00015	339	97	52	3	46	1	46	3	
AB-1-23	71	164	0.43	0.04575	0.00272	0.04615	0.00732	0.00020	0.00226	0.00016	-15	126	46	4	47	1	46	3	
AB-1-24	56	122	0.46	0.05247	0.00359	0.00359	0.05196	0.00021	0.00237	0.00019	306	153	51	5	46	1	48	4	
AB-1-26	105	195	0.54	0.04986	0.00244	0.00244	0.04889	0.00019	0.00251	0.00013	188	113	48	3	46	1	51	3	
AB-1-27	87	200	0.44	0.04509	0.00240	0.00240	0.04255	0.00018	0.00238	0.00014	-15	113	42	3	44	1	48	3	
AB-1-28	160	221	0.72	0.04806	0.00209	0.00209	0.04570	0.00018	0.00247	0.00010	102	96	45	3	44	1	50	2	
AB-1-29	81	178	0.45	0.04607	0.00247	0.00247	0.04641	0.00020	0.00264	0.00016	1	111	46	3	47	1	53	3	
AB-1-30(c)	162	140	1.15	0.04573	0.00224	0.00224	0.10231	0.00046	0.00530	0.00020	-16	103	99	7	104	3	107	4	
AB-1-32	249	966	0.26	0.04705	0.00064	0.00064	0.04721	0.00728	0.00018	0.00286	0.00009	52	32	47	1	47	1	58	2
AB-1-33(c)	220	203	1.08	0.04820	0.00178	0.00178	0.06116	0.00920	0.00307	0.00010	109	86	60	3	59	2	62	2	
AB-1-34(r)	89	170	0.52	0.04227	0.00275	0.00275	0.04191	0.00719	0.00020	0.00256	-162	132	42	4	46	1	52	3	
AB-1-35	634	335	1.89	0.04842	0.00316	0.00316	0.04909	0.00735	0.00020	0.00233	120	145	49	4	47	1	47	1	
<b>UK-1 wt. mean = 44.8 ± 0.5 Ma (2σ)</b>																			
UK-1-1	288	239	1.21	0.04639	0.00226	0.00226	0.04305	0.00673	0.00017	0.00215	18	104	43	3	43	1	43	1	
UK-1-2	175	174	1.01	0.04394	0.00299	0.00299	0.04104	0.00677	0.00020	0.00203	-74	141	41	4	43	1	41	2	
UK-1-3	296	208	1.42	0.04609	0.00167	0.00167	0.04500	0.00708	0.00017	0.00232	2	74	45	2	45	1	47	1	
UK-1-4	466	347	1.34	0.04970	0.00101	0.00101	0.04859	0.00709	0.00017	0.00232	181	47	48	2	46	1	47	1	
UK-1-5	248	228	1.09	0.05143	0.00149	0.00149	0.04923	0.00694	0.00017	0.00228	260	67	49	2	45	1	46	1	
UK-1-6	241	181	1.33	0.05087	0.00361	0.00361	0.04872	0.00695	0.00019	0.00219	235	159	48	4	45	1	44	1	
UK-1-7	203	255	0.80	0.05062	0.00260	0.00260	0.04762	0.00682	0.00018	0.00215	223	117	47	3	44	1	43	1	
UK-1-9	226	221	1.02	0.04915	0.00254	0.00254	0.04862	0.00718	0.00019	0.00227	155	117	48	3	46	1	46	1	
UK-1-10	355	246	1.45	0.04611	0.00240	0.00240	0.04348	0.00684	0.00018	0.00221	3	110	43	3	44	1	45	1	
UK-1-11	332	273	1.21	0.04980	0.00131	0.00131	0.04832	0.00704	0.00017	0.00237	186	62	48	2	45	1	48	1	
UK-1-12	162	166	0.98	0.04608	0.00192	0.00192	0.04517	0.00711	0.00018	0.00231	2	85	45	3	46	1	47	2	
UK-1-13	255	185	1.38	0.05126	0.00173	0.00173	0.04959	0.00702	0.00018	0.00222	253	77	49	3	45	1	45	1	
UK-1-14	171	157	1.09	0.04608	0.00293	0.00293	0.04254	0.00670	0.00019	0.00224	2	136	42	3	43	1	45	3	
UK-1-15	179	167	1.08	0.05046	0.00186	0.00186	0.05006	0.00720	0.00018	0.00245	216	86	50	3	46	1	49	2	
UK-1-16	832	473	1.76	0.05049	0.00092	0.00092	0.04862	0.00698	0.00017	0.00222	218	42	48	2	45	1	45	1	
UK-1-17	691	446	1.55	0.04434	0.00080	0.00080	0.04343	0.00710	0.00017	0.00223	-53	37	43	2	46	1	45	1	

TABLE 2  
(continued)

Analysis No.	Th (ppm)	U (ppm)	Th/U	RATIOS (common-Pb corrected)				AGES (common-Pb corrected, Ma)										
				$\frac{^{207}\text{Pb}}{^{206}\text{Pb}} \pm 1\sigma$	$\frac{^{207}\text{Pb}}{^{235}\text{U}} \pm 1\sigma$	$\frac{^{206}\text{Pb}}{^{238}\text{U}} \pm 1\sigma$	$\frac{^{208}\text{Pb}}{^{232}\text{Th}} \pm 1\sigma$	$\frac{^{207}\text{Pb}}{^{206}\text{Pb}} \pm 1\sigma$	$\frac{^{207}\text{Pb}}{^{235}\text{U}} \pm 1\sigma$	$\frac{^{206}\text{Pb}}{^{238}\text{U}} \pm 1\sigma$	$\frac{^{208}\text{Pb}}{^{232}\text{Th}} \pm 1\sigma$							
<b>UK-1 wt. mean = 44.8 ± 0.5 Ma (2σ)</b>																		
UK-1-18	927	532	1.74	0.04821	0.00076	0.00076	0.00076	0.00688	0.00016	0.00218	110	37	45	1	44	1	44	1
UK-1-19	182	162	1.12	0.05064	0.00191	0.00191	0.00191	0.00703	0.00018	0.00246	224	86	49	3	45	1	50	2
UK-1-20	382	290	1.31	0.05339	0.00120	0.00120	0.00120	0.00673	0.00016	0.00220	345	51	49	2	43	1	44	1
UK-1-22	560	362	1.55	0.04703	0.00221	0.00221	0.00221	0.00696	0.00017	0.00221	51	102	45	3	45	1	45	1
UK-1-23	295	233	1.27	0.04564	0.00141	0.00141	0.00141	0.00712	0.00017	0.00224	-21	62	44	2	46	1	45	1
UK-1-24	283	231	1.22	0.04894	0.00141	0.00141	0.00141	0.00711	0.00017	0.00234	145	67	48	2	46	1	47	1
<b>ST-1 wt. mean = 37.0 ± 0.5 Ma (2σ)</b>																		
ST-1-1	75	148	0.51	0.05255	0.00185	0.00185	0.00185	0.00606	0.00014	0.00281	309	80	44	2	39	1	57	2
ST-1-2	785	530	1.48	0.04799	0.00077	0.00077	0.00077	0.00580	0.00013	0.00190	99	38	38	1	37	1	38	1
ST-1-3	173	144	1.20	0.04607	0.00160	0.00160	0.00160	0.00591	0.00015	0.00199	2	70	37	2	38	1	40	2
ST-1-4	1607	788	2.04	0.04609	0.00240	0.00240	0.00240	0.00590	0.00014	0.00191	3	110	37	3	38	1	39	1
ST-1-5	689	464	1.48	0.04673	0.00075	0.00075	0.00075	0.00558	0.00012	0.00185	35	36	36	1	36	1	37	1
ST-1-6	335	249	1.34	0.04774	0.00116	0.00116	0.00116	0.00556	0.00013	0.00179	86	56	37	2	36	1	36	1
ST-1-8	175	220	0.79	0.05082	0.00130	0.00130	0.00130	0.00578	0.00013	0.00194	233	58	40	2	37	1	39	1
ST-1-9	103	129	0.80	0.04657	0.00223	0.00223	0.00223	0.00597	0.00015	0.00190	27	100	38	2	38	1	38	2
ST-1-11	275	225	1.22	0.04546	0.00127	0.00127	0.00127	0.00577	0.00013	0.00187	-31	54	36	2	37	1	38	1
ST-1-12	251	296	0.85	0.04674	0.00138	0.00138	0.00138	0.00559	0.00013	0.00188	36	62	36	2	36	1	38	1
ST-1-13	332	361	0.92	0.04706	0.00156	0.00156	0.00156	0.00564	0.00013	0.00179	52	72	37	2	36	1	36	1
ST-1-14	378	266	1.42	0.04690	0.00117	0.00117	0.00117	0.00576	0.00013	0.00191	44	53	37	2	37	1	39	1
ST-1-16	298	221	1.35	0.04904	0.00139	0.00139	0.00139	0.00561	0.00013	0.00180	150	66	38	2	36	1	36	1
ST-1-19	71	186	0.38	0.04676	0.00157	0.00157	0.00157	0.00591	0.00014	0.00194	37	71	38	2	38	1	39	2
ST-1-22	243	254	0.96	0.04898	0.00120	0.00120	0.00120	0.00573	0.00013	0.00177	147	57	39	2	37	1	36	1
ST-1-23	369	282	1.31	0.04920	0.00117	0.00117	0.00117	0.00559	0.00012	0.00181	157	55	38	2	36	1	37	1
ST-1-24	177	241	0.73	0.05099	0.00121	0.00121	0.00121	0.00594	0.00013	0.00196	240	55	42	2	38	1	40	1
<b>SRK-1 wt. mean = 19.0 ± 0.2 Ma (2σ)</b>																		
SRK-1-1	769	324	2.37	0.05708	0.00220	0.00220	0.00220	0.00296	0.00008	0.00097	495	87	23.0	1.0	19.1	0.5	19.6	0.6
SRK-1-2	353	149	2.37	0.04800	0.00516	0.00516	0.00516	0.00301	0.00009	0.00096	99	227	20.0	3.0	19.4	0.6	19.4	0.8
SRK-1-3	359	158	2.27	0.04686	0.00561	0.00561	0.00561	0.00285	0.00009	0.00091	42	237	19.0	3.0	18.4	0.6	18.3	0.8
SRK-1-4	194	104	1.87	0.05949	0.00893	0.00893	0.00893	0.00279	0.00011	0.00109	585	328	23.0	4.0	18.0	0.7	22.0	1.0
SRK-1-5	320	136	2.36	0.04521	0.00588	0.00588	0.00588	0.00291	0.00009	0.00096	-9	233	19.0	3.0	19.2	0.6	19.4	0.8
SRK-1-6	274	139	1.97	0.05000	0.00561	0.00561	0.00561	0.00301	0.00009	0.00094	195	242	21.0	3.0	19.4	0.6	19.0	0.8

TABLE 2  
(continued)

Analysis No.	Th (ppm)	U (ppm)	Th/U	RATIO S (common-Pb corrected)				AGE S (common-Pb corrected, Ma)												
				$\frac{^{207}\text{Pb}}{^{206}\text{Pb}} \pm 1\sigma$	$\frac{^{207}\text{Pb}}{^{235}\text{U}} \pm 1\sigma$	$\frac{^{206}\text{Pb}}{^{238}\text{U}} \pm 1\sigma$	$\frac{^{208}\text{Pb}}{^{232}\text{Th}} \pm 1\sigma$	$\frac{^{207}\text{Pb}}{^{206}\text{Pb}} \pm 1\sigma$	$\frac{^{207}\text{Pb}}{^{235}\text{U}} \pm 1\sigma$	$\frac{^{206}\text{Pb}}{^{238}\text{U}} \pm 1\sigma$	$\frac{^{208}\text{Pb}}{^{232}\text{Th}} \pm 1\sigma$									
<b>SRK-1 wt. mean = 19.0 ± 0.2 Ma (2σ)</b>																				
SRK-1-7	185	93	1.99	0.05367	0.02206	0.00408	0.00298	0.00010	0.00093	0.00004	357	331	22.0	4.0	19.2	0.6	18.8	0.8		
SRK-1-8	97	76	1.27	0.03396	0.01076	0.00501	0.00307	0.00011	0.00108	0.00009	-116	400	14.0	5.0	19.8	0.7	22.0	2.0		
SRK-1-9	712	271	2.63	0.05371	0.00293	0.02122	0.00166	0.00008	0.00095	0.00003	359	124	21.0	2.0	18.5	0.5	19.2	0.6		
SRK-1-10	822	386	2.13	0.04615	0.00402	0.01860	0.00196	0.00008	0.00094	0.00004	5	181	19.0	2.0	18.8	0.5	19.1	0.7		
SRK-1-11	353	147	2.40	0.04074	0.00572	0.01642	0.00275	0.00009	0.00094	0.00004	-247	221	17.0	3.0	18.8	0.6	19.0	0.8		
SRK-1-12	151	89	1.70	0.06256	0.01235	0.02652	0.00616	0.00307	0.00094	0.00004	693	419	27.0	6.0	19.8	0.8	19.1	0.7		
SRK-1-13	176	85	2.07	0.03636	0.01112	0.01413	0.00481	0.00282	0.00097	0.00006	-19	416	14.0	5.0	18.2	0.7	20.0	1.0		
SRK-1-14	818	286	2.87	0.03728	0.00313	0.01494	0.00161	0.00008	0.00095	0.00003	-454	276	15.0	2.0	18.7	0.5	19.2	0.6		
SRK-1-16	929	385	2.41	0.04619	0.00307	0.01802	0.00155	0.00008	0.00092	0.00003	7	142	18.0	2.0	18.2	0.5	18.6	0.6		
SRK-1-17	271	144	1.88	0.04559	0.00607	0.01886	0.00301	0.00009	0.00088	0.00004	-24	248	19.0	3.0	19.3	0.6	17.8	0.8		
SRK-1-18	337	214	1.57	0.04794	0.00417	0.01931	0.00214	0.00008	0.00094	0.00004	96	189	19.0	2.0	18.8	0.5	19.0	0.8		
SRK-1-19	193	112	1.73	0.04139	0.00825	0.01654	0.00380	0.00290	0.00010	0.00090	-211	296	17.0	4.0	18.7	0.6	18.0	1.0		
SRK-1-20	165	91	1.81	0.04259	0.00899	0.01847	0.00447	0.00315	0.00106	0.00006	-145	314	19.0	4.0	20.3	0.7	21.0	1.0		
SRK-1-21	265	130	2.04	0.04984	0.00662	0.02054	0.00333	0.00299	0.00090	0.00004	188	274	21.0	3.0	19.2	0.6	18.2	0.8		
SRK-1-22	293	131	2.23	0.05789	0.00650	0.02362	0.00328	0.00296	0.00099	0.00004	526	248	24.0	3.0	19.1	0.6	20.0	0.8		
SRK-1-23	446	192	2.32	0.03914	0.00446	0.01643	0.00230	0.00304	0.00098	0.00003	-340	220	17.0	2.0	19.6	0.6	19.8	0.6		
SRK-1-24	353	175	2.02	0.04038	0.00530	0.01607	0.00255	0.00289	0.00099	0.00004	-268	211	16.0	3.0	18.6	0.6	18.8	0.8		
<b>SAH-1 wt. mean = 18.6 ± 0.2 Ma (2σ)</b>																				
SAH-1-1	754	465	1.62	0.04927	0.00210	0.01943	0.00123	0.00286	0.00007	0.00095	161	96	20.0	1.0	18.4	0.4	19.2	0.6		
SAH-1-2	716	443	1.62	0.04798	0.00196	0.01936	0.00118	0.00293	0.00007	0.00098	98	91	19.0	1.0	18.9	0.4	19.8	0.6		
SAH-1-3	929	587	1.58	0.04733	0.00268	0.01900	0.00143	0.00291	0.00007	0.00093	66	122	19.0	1.0	18.7	0.5	18.7	0.5		
SAH-1-4	744	430	1.73	0.04613	0.00114	0.01912	0.00076	0.00301	0.00007	0.00101	5	50	19.2	0.8	19.3	0.4	20.5	0.7		
SAH-1-5	1463	718	2.04	0.04628	0.00275	0.01877	0.00142	0.00294	0.00007	0.00094	12	127	19.0	1.0	18.9	0.5	19.0	0.5		
SAH-1-7	1382	761	1.82	0.04611	0.00115	0.01861	0.00082	0.00293	0.00007	0.00098	3	49	18.7	0.8	18.9	0.4	19.8	0.4		
SAH-1-8	1701	923	1.84	0.04615	0.00152	0.01870	0.00095	0.00294	0.00007	0.00095	6	67	18.8	0.9	18.9	0.5	19.2	0.4		
SAH-1-9	398	127	1.26	0.04868	0.00367	0.01938	0.00184	0.00289	0.00007	0.00091	133	166	19.0	2.0	18.6	0.5	18.5	0.6		
SAH-1-10	2588	1212	2.14	0.04796	0.00088	0.01911	0.00066	0.00289	0.00006	0.00102	97	44	19.2	0.7	18.6	0.4	20.6	0.4		
SAH-1-12	817	506	1.62	0.04609	0.00040	0.01819	0.00045	0.00286	0.00106	0.00005	2	19	18.3	0.4	18.4	0.4	21.0	1.0		
SAH-1-14	878	490	1.79	0.04629	0.00423	0.01764	0.00196	0.00276	0.00008	0.00088	13	189	18.0	2.0	17.8	0.5	17.9	0.8		
SAH-1-15	3777	1461	2.59	0.04611	0.00032	0.01873	0.00043	0.00295	0.00006	0.00099	3	16	18.8	0.4	19.0	0.4	20.1	0.4		
SAH-1-16	2445	1184	2.06	0.04624	0.00158	0.01766	0.00087	0.00277	0.00006	0.00090	10	70	17.8	0.9	17.8	0.4	18.1	0.4		

TABLE 2  
(continued)

Analysis No.	Th (ppm)	U (ppm)	Th/U	RATIO S (common-Pb corrected)				AGE S (common-Pb corrected, Ma)												
				$\frac{^{207}\text{Pb}}{^{206}\text{Pb}}$	$\pm 1\sigma$	$\frac{^{207}\text{Pb}}{^{235}\text{U}}$	$\pm 1\sigma$	$\frac{^{206}\text{Pb}}{^{238}\text{U}}$	$\pm 1\sigma$	$\frac{^{207}\text{Pb}}{^{206}\text{Pb}}$	$\pm 1\sigma$	$\frac{^{206}\text{Pb}}{^{238}\text{U}}$	$\pm 1\sigma$							
<b>SAH-1 wt. mean = 18.6 ± 0.2 Ma (2σ)</b>																				
SAH-1-17	1054	594	1.78	0.04616	0.00157	0.01829	0.00093	0.00287	0.00007	0.00095	0.00003	6	68	18.4	0.9	18.5	0.4	19.2	0.6	0.6
SAH-1-18	1065	675	1.58	0.04785	0.00149	0.01921	0.00098	0.00291	0.00007	0.00098	0.00003	92	71	19.3	1.0	18.7	0.4	19.8	0.6	0.6
SAH-1-19	902	609	1.48	0.04612	0.00183	0.01777	0.00101	0.00279	0.00007	0.00092	0.00003	4	81	18.0	1.0	18.0	0.4	18.5	0.6	0.6
SAH-1-20	1354	785	1.72	0.04616	0.00183	0.01795	0.00101	0.00282	0.00007	0.00093	0.00003	6	81	18.0	1.0	18.2	0.4	18.8	0.6	0.6
SAH-1-21	502	322	1.56	0.04998	0.00267	0.01976	0.00147	0.00287	0.00007	0.00100	0.00003	194	123	20.0	1.0	18.5	0.4	20.2	0.6	0.6
SAH-1-22	2582	996	2.59	0.05191	0.00088	0.02147	0.00074	0.00300	0.00007	0.00097	0.00002	281	39	21.6	0.7	19.3	0.4	19.6	0.4	0.4
SAH-1-23	682	407	1.68	0.05160	0.00404	0.02059	0.00207	0.00289	0.00008	0.00091	0.00002	268	177	21.0	2.0	18.6	0.5	18.4	0.3	0.3
SAH-1-24	471	346	1.36	0.04952	0.00238	0.02023	0.00138	0.00296	0.00007	0.00098	0.00003	173	108	20.0	1.0	19.1	0.4	19.8	0.6	0.6
<b>NS-1 wt. mean = 18.2 ± 0.3 Ma (2σ)</b>																				
NS-1-3	869	623	1.39	0.04613	0.00161	0.01870	0.00095	0.00294	0.00007	0.00096	0.00003	5	72	18.8	1.0	18.9	0.4	19.4	0.6	0.6
NS-1-5	963	864	1.11	0.04793	0.00237	0.01946	0.00134	0.00294	0.00007	0.00093	0.00002	96	108	20.0	1.0	19.0	0.5	18.9	0.4	0.4
NS-1-6	944	785	1.20	0.04610	0.00094	0.01720	0.00059	0.00271	0.00006	0.00091	0.00003	3	40	17.3	0.6	17.4	0.4	18.5	0.7	0.7
NS-1-8	559	529	1.06	0.04619	0.00257	0.01777	0.00128	0.00279	0.00007	0.00090	0.00004	8	118	18.0	1.0	18.0	0.4	18.2	0.9	0.9
NS-1-9	384	298	1.29	0.04611	0.00072	0.01854	0.00057	0.00292	0.00006	0.00104	0.00005	3	31	18.7	0.6	18.8	0.4	21.0	1.0	1.0
NS-1-10	1932	1013	1.91	0.04610	0.00025	0.01876	0.00039	0.00295	0.00006	0.00103	0.00003	3	13	18.9	0.4	19.0	0.4	20.7	0.6	0.6
NS-1-11	1094	1028	1.06	0.04611	0.00039	0.01741	0.00045	0.00274	0.00006	0.00092	0.00002	3	19	17.5	0.5	17.6	0.4	18.6	0.5	0.5
NS-1-13	280	324	0.86	0.05497	0.00445	0.02031	0.00217	0.00268	0.00008	0.00093	0.00006	411	184	20.0	2.0	17.3	0.5	19.0	1.0	1.0
NS-1-14	251	217	1.15	0.04690	0.00585	0.01782	0.00273	0.00276	0.00009	0.00104	0.00006	44	242	18.0	3.0	17.8	0.6	21.0	1.0	1.0
NS-1-15	390	274	1.42	0.04715	0.00362	0.01830	0.00176	0.00282	0.00007	0.00090	0.00003	57	170	18.0	2.0	18.1	0.4	18.1	0.7	0.7
NS-1-16	4118	1201	3.43	0.05289	0.00474	0.02000	0.00223	0.00274	0.00007	0.00086	0.00001	324	201	20.0	2.0	17.7	0.5	17.4	0.3	0.3
NS-1-17	576	487	1.18	0.04649	0.00472	0.01801	0.00210	0.00281	0.00007	0.00090	0.00006	23	206	18.0	2.0	18.1	0.4	18.0	1.0	1.0
NS-1-18	1274	703	1.81	0.04714	0.00137	0.01786	0.00084	0.00275	0.00006	0.00091	0.00002	56	64	18.0	0.8	17.7	0.4	18.4	0.4	0.4
NS-1-20	170	156	1.09	0.05652	0.00560	0.02279	0.00287	0.00292	0.00009	0.00100	0.00005	473	221	23.0	3.0	18.8	0.6	20.0	1.0	1.0
NS-1-21	1002	644	1.55	0.05189	0.00156	0.02043	0.00097	0.00286	0.00006	0.00110	0.00003	281	69	20.5	1.0	18.4	0.4	22.2	0.6	0.6
NS-1-22	2049	2360	0.87	0.04854	0.00211	0.01885	0.00114	0.00282	0.00006	0.00089	0.00002	126	98	19.0	1.0	18.1	0.4	18.0	0.4	0.4
NS-1-23	206	190	1.08	0.04694	0.00578	0.01820	0.00275	0.00281	0.00009	0.00094	0.00006	46	239	18.0	3.0	18.1	0.6	19.0	1.0	1.0
NS-1-24	376	290	1.30	0.04767	0.00391	0.01866	0.00194	0.00284	0.00008	0.00090	0.00004	83	178	19.0	2.0	18.3	0.5	18.2	0.7	0.7
NS-1-25	807	516	1.56	0.04639	0.00252	0.01870	0.00095	0.00276	0.00007	0.00088	0.00003	18	116	18.0	1.0	17.8	0.4	17.8	0.5	0.5

c = core; r = rim

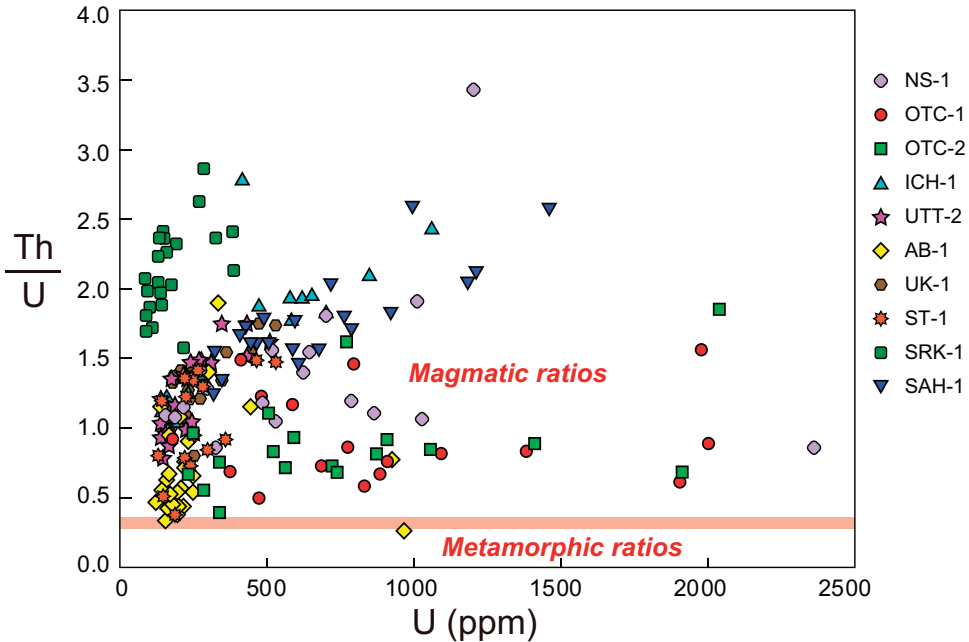


Fig. 5. Th and U concentrations in zircon crystals of the Hokkaido granitoids. The generally high Th/U ratios ( $>0.5$ ) suggest that the zircon crystals are of magmatic origin.

Chondrite-normalized REE patterns are shown in figures 8A and 8B. They are typical of granitic rocks, with light REE enrichment and conspicuous negative Eu anomaly. The REE abundances of the older Eocene granitoids (fig. 8A) may be slightly lower and less fractionated than those of the younger Miocene granitoids (fig. 8B), but the difference is quite subtle. The only gabbro sample exhibits a quasi-flat REE pattern with about 10x chondritic abundances. In a sense it looks like an atypical N-MORB with small LREE depletion.

Primitive-mantle-normalized spidergrams of the granitoids are shown in figures 8C and 8D. In the spidergrams the trace elements are arranged in the ascending order, from left to right, of their compatibilities with the basaltic liquid. Nevertheless, the application of such diagrams to granitic rocks also serves to identify fractionation of particular mineral phases during the generation and differentiation of granitic liquids. Figure 8C shows that in the Eocene granitoids, depletion or negative anomaly is observed in Nb-Ta, Sr, P, Zr and Ti. The phenomenon of the “TNT (Ti-Nb-Ta) anomaly” is most characteristic of granitic rocks, island arc volcanics and the continental crust in general.

The spidergrams of the Miocene granitoids are shown in figure 8D. The general enrichment/depletion patterns are grossly similar to those of the Eocene granitoids. The only gabbro shows negative anomalies in Nb and Ta, but positive anomaly in Sr. Such an elemental distribution may favor an interpretation of its origin in an island arc setting, but not in mid-ocean ridge.

#### Whole-Rock Sr-Nd Isotopic Data

The whole-rock Sr and Nd isotopic analyses are given in table 4, and further illustrated in figure 9A. The Rb concentrations in all samples range from 50 to 143 ppm, which are “normal” for granitic rocks. However, the Sr contents vary from *ca.* 50 to 190 ppm, which are somewhat lower than the normal range of granitic rocks. The

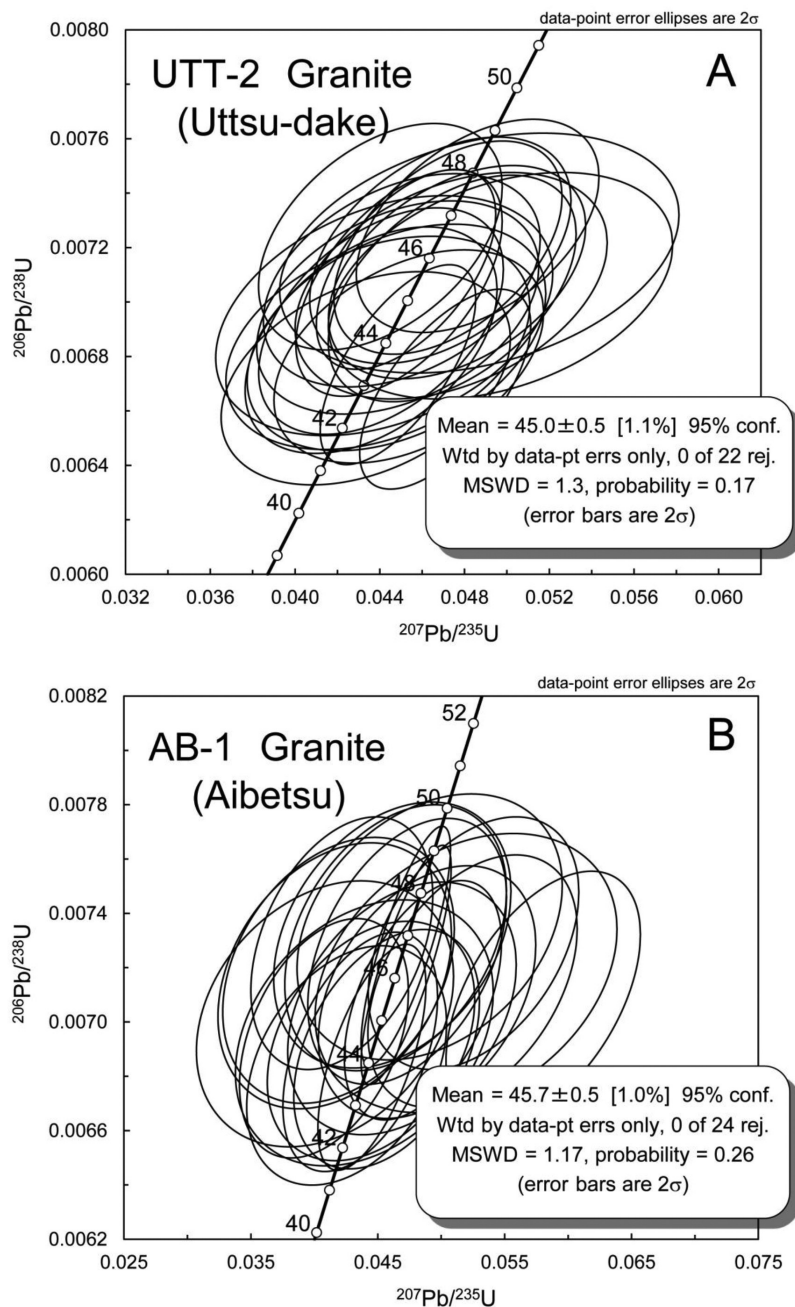


Fig. 6. U-Pb Concordia diagrams for the zircon grains from the Hokkaido granitoids and a gabbro.

calculated initial  $^{87}\text{Sr}/^{86}\text{Sr}$  ratios ( $I_{\text{Sr}}$  values) range from 0.7044 to 0.7061; and the age-corrected initial  $^{143}\text{Nd}/^{144}\text{Nd}$  ratios, expressed as  $\epsilon_{\text{Nd}}(t)$  values, are all positive, ranging from +1.0 to +4.7. Single-stage Sm-Nd model ages are between 400 to 1000 Ma (table 4).

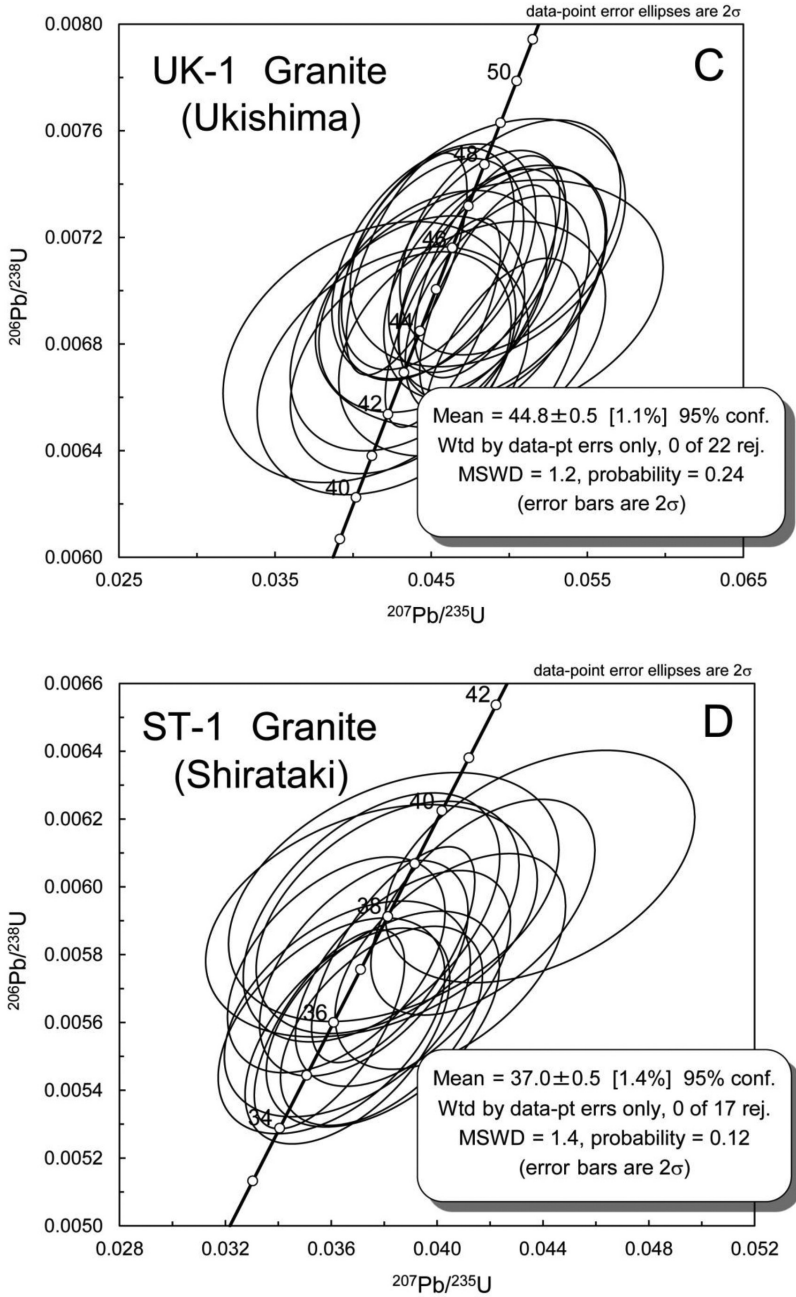


Fig. 6. (continued).

In figure 9B, the literature Sr-Nd isotopic data of Cenozoic felsic-intermediate magmatic rocks are also shown for comparison. The isotopic data of Miocene rhyolitic rocks are predominant and they refer to those occurring in four areas—northern Hokkaido (4-15 Ma; Takagi and others, 1999), central Hokkaido (15-17 Ma; Furukata

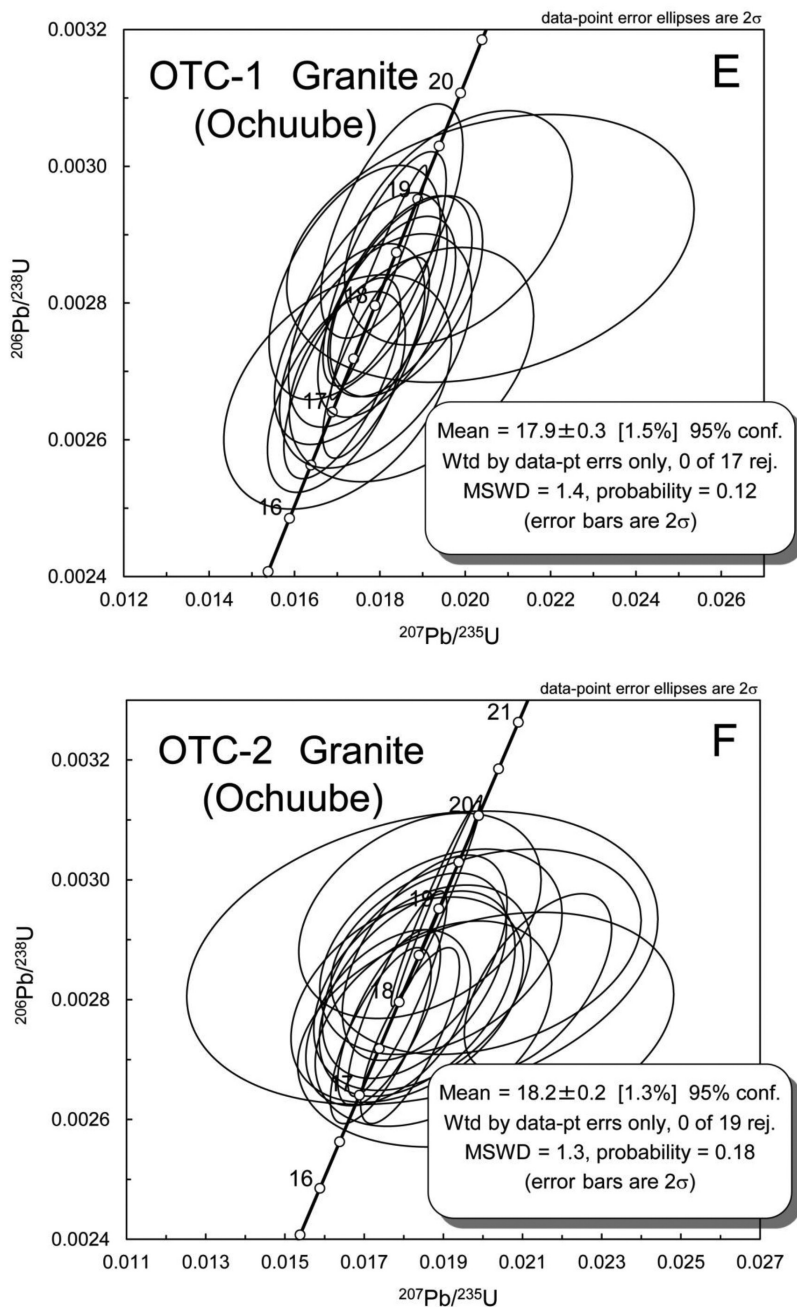


Fig. 6. (continued).

and others, 2010), SW and NE Hokkaido (2-18 Ma; Takanashi and others, 2011, 2012). Note that all the rocks from the Hidaka metamorphic belt show positive  $\epsilon_{\text{Nd}}(t)$  values except for four tonalitic rocks, two of them defined as tonalitic xenoliths and two as S-type tonalities (shown in blue diamonds in fig. 9B; Owada and others, 2006). The

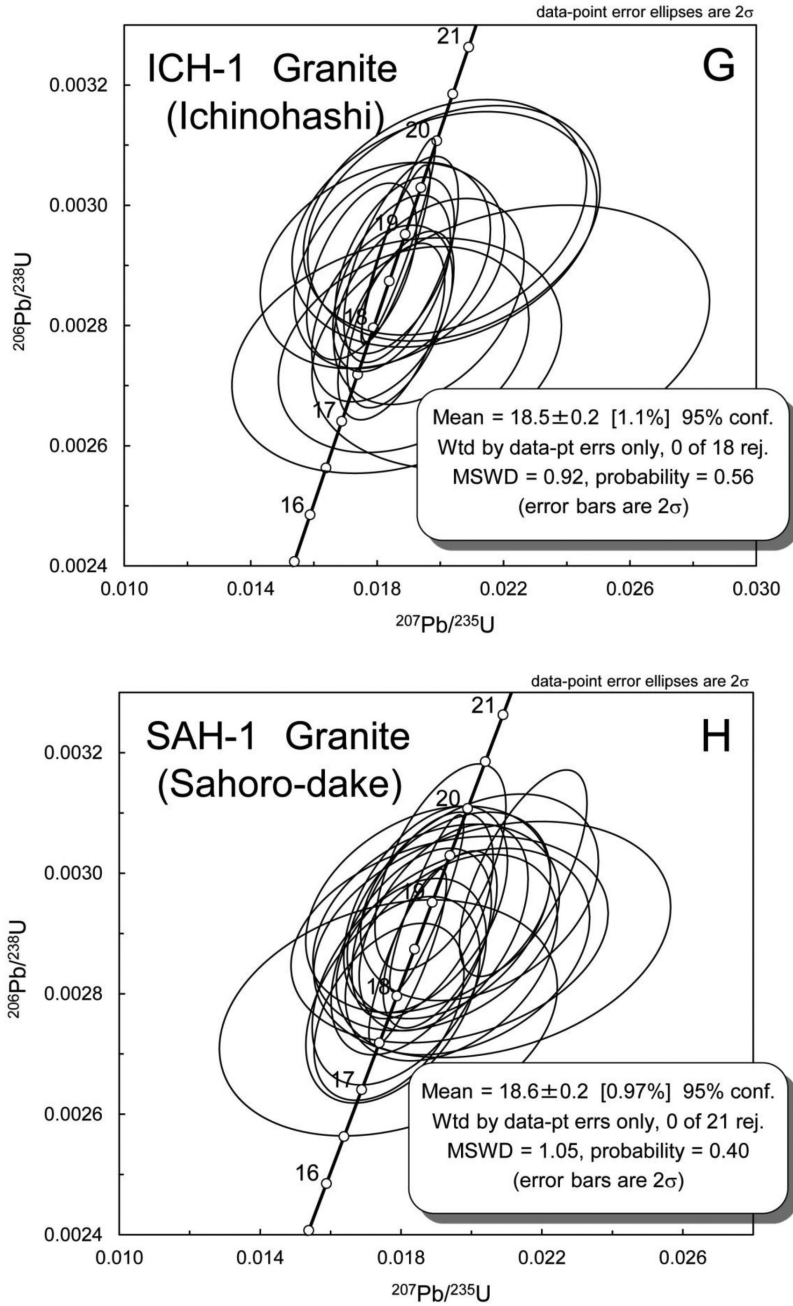


Fig. 6. (continued).

entire data set also shows an anti-correlation between  $\epsilon_{Nd}(t)$  and  $I_{Sr}$  values. Note that the ensemble of our new granitoid data points (shown in red solid dots, fig. 9B) appears to lie slightly above the bulk array.

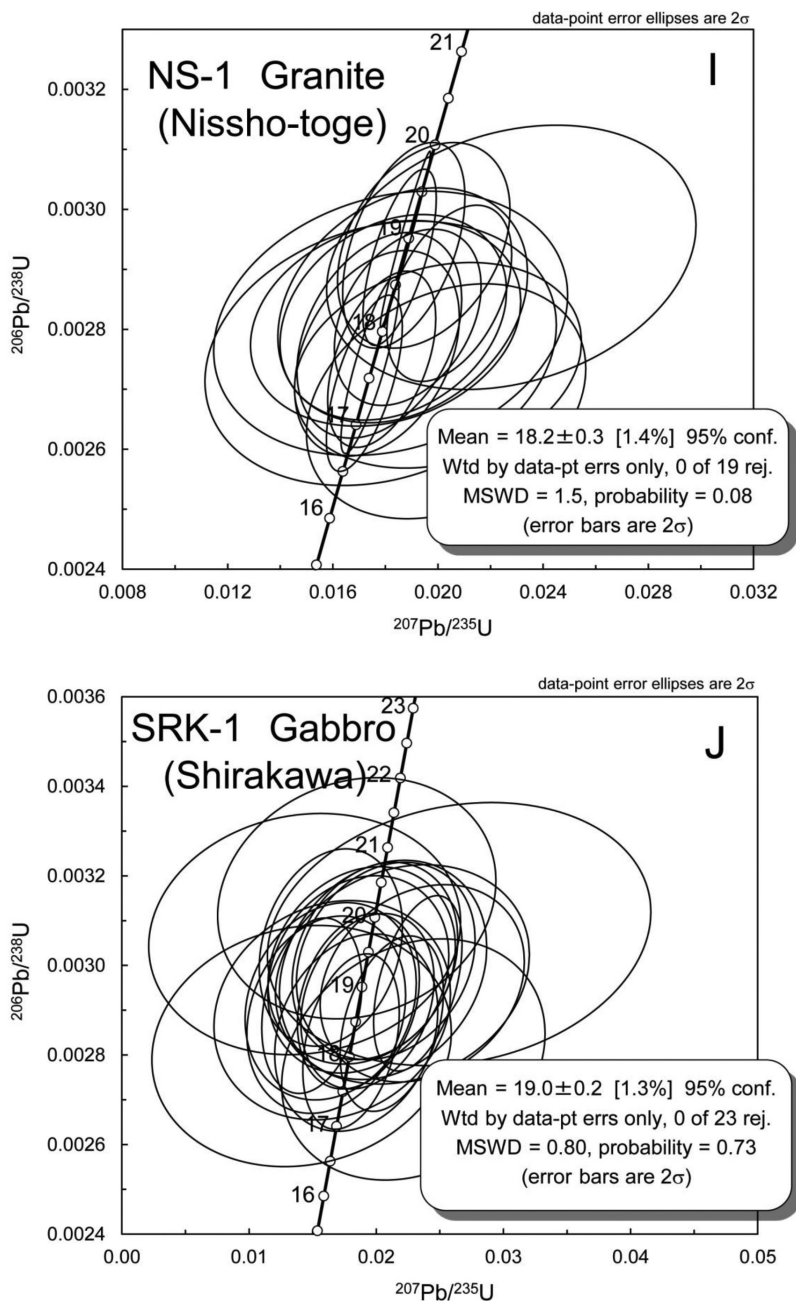


Fig. 6. (continued).

#### Zircon Hf Isotopic Data

The zircon Hf isotopic compositions of the Hokkaido granitoids are given in table 5, and further illustrated in figures 10A and 10B. Note that all individual samples have a range of  $\epsilon_{\text{Hf}}(t)$  values; for example, sample UK-1 (*ca.* 45 Ma) shows a range of  $\epsilon_{\text{Hf}}(t)$

from +8.9 to +17.3, and ST-1 (37 Ma) from +11.0 to +18.1 (table 5). The ranges are beyond the analytical uncertainty of 0.5 to 1.0 epsilon unit. In a study of zircon chemistry and Hf isotopic compositions from two igneous complexes (Pingtan and Tonglu) in SE China, Griffin and others (2002) observed that a large variation in  $^{176}\text{Hf}/^{177}\text{Hf}$  (up to 15  $\epsilon_{\text{Hf}}$  units) was found between zircon grains of different growth stages within a single rock, and between zones within single zircon grains (up to 9  $\epsilon_{\text{Hf}}$  units). Such variation suggests that each of the observed magmas in both complexes developed through hybridization of two or more magma batches with different sources. They conclude that this mixing has produced similar Sr and Nd isotopic compositions in the different rock types of each complex, but the zircons have functioned as “tape recorders” and preserved details of the assembly of the different magmas. We agree with the above observation and interpretation of Griffin and others (2002), however, we like to offer a supplementary explanation as follows.

Zircon crystallizes at a given time in an evolving granitic magma that would likely preserve the chemical and isotopic compositions in equilibrium with the magma at that time. The bulk composition of a magma chamber would change through fractional crystallization, but such closed system chemical fractionation will probably not modify the isotopic compositions. A change of isotopic compositions could only be achieved through an open-system behavior, such as influx of a foreign magma or assimilation of country rocks in the magma chamber. Zircon crystals formed at any given stage would register the Hf isotopic composition of the evolving magma at that stage. Since zircon crystals do not grow at the same time, the individual grains from a single rock could have recorded the Hf isotopic compositions of different stages of magma evolution.

Kemp and others (2007b) conducted an elaborate study of Hf isotopic change with magma generation and evolution of the I-type granites from the Lachlan Fold Belt of Australia. They analyzed U-Pb, Hf and O isotopic compositions in zircons to reveal the nature of the crustal component. They reached a novel conclusion that the I-type granites were in fact formed by the reworking of sedimentary materials by mantle-like magmas, but not by remelting of older metamorphosed igneous rocks as widely believed. Nonetheless, the authors also concluded that I-type magmatism critically involves continental growth, this being camouflaged to some extent by the non-mantle-like isotope ratios of the bulk rocks. The overall proportion of juvenile material added by the Lachlan I-type suites was between 85 percent and 50 percent in different plutons.

Despite the large range of  $\epsilon_{\text{Hf}}(t)$  values observed in the Hokkaido granitoids (fig. 10A), the entire data set shows that all of them is exclusively positive, similar to the whole-rock  $\epsilon_{\text{Nd}}(t)$  values. The two-stage Lu-Hf model ages are shown in figure 10B. All model ages are younger than 550 Ma, and a few give negative or future age values. Similar to the whole-rock Sm-Nd model ages, the zircon Hf model ages are consistent with their juvenile characteristics. No Precambrian heritage is identified.

#### DISCUSSION

##### *Significance of the New Zircon U-Pb Ages and Literature Age Data*

Our new zircon age data and those from Kemp and others (2007a) indicate three distinct intrusive events in Hokkaido at *ca.* 45, 37 and 18 Ma. In order to reach a better understanding of the significance of the newly obtained zircon ages and the tectonomagmatic evolution of Hokkaido, we compiled the available age data of Tertiary plutonic rocks from the literature, and they are summarized in a histogram (fig. 11). Among the 108 dates reported in the literature, a half of them (54) were obtained on biotite by the conventional K-Ar method, and a quarter (29) were fission-track (FT) dates on zircon (18) and apatite (11). Prior to the present work, zircon U-Pb dates are rare (total = 6),

TABLE 3

*Chemical compositions of granitoids and a gabbro from Hokkaido*

Sample No.	NS-1	SAH-1	SRK-1	SRK-2	AB-1	UK-1
Locality	Nissho-toge	Sahoro-dake	Shirakawa	Shirakawa	Aibetsu	Ukishima
Rock type	granite	granite	gabbro	grano-diorite	granite	granite
Zircon age (Ma)	18.2	18.6	19.0	(19.0)	45.7	44.8
Major element contents (in %)						
SiO <sub>2</sub>	74.48	73.34	48.29	64.89	67.87	68.48
Al <sub>2</sub> O <sub>3</sub>	13.57	13.65	19.58	14.55	15.31	13.52
Fe <sub>2</sub> O <sub>3</sub>	1.40	1.91	7.31	6.87	4.03	2.97
MnO	0.03	0.04	0.13	0.11	0.09	0.05
MgO	0.29	0.14	7.24	1.35	1.33	0.75
CaO	1.02	0.87	12.12	2.69	2.27	2.04
Na <sub>2</sub> O	3.20	4.17	2.75	3.96	3.46	4.76
K <sub>2</sub> O	5.01	4.37	0.15	2.72	3.23	3.02
TiO <sub>2</sub>	0.25	0.23	0.81	1.07	0.65	0.38
P <sub>2</sub> O <sub>5</sub>	0.06	0.05	0.08	0.25	0.16	0.09
LOI	0.40	0.37	1.02	0.91	1.04	2.41
Total	99.71	99.14	99.48	99.36	99.44	98.46
Parameters used for classification of Streckisen and Le Maitre (1979):						
ANOR	12.74	12.64	97.72	40.44	33.21	25.59
Q'	34.96	30.72	0.00	25.49	31.38	26.10
Parameters (molar ratios) for calculation of aluminum saturation index:						
A/NK	1.27	1.18	4.18	1.54	1.67	1.22
A/CNK	1.08	1.03	0.73	1.01	1.15	0.91
Trace elements (in ppm):						
Cs	4.0	5.1	3.0	6.1	6.1	2.6
Rb	108.6	143.2	5.6	109.8	88.8	94.8
Sr	75.2	47.8	211.2	151.5	163.7	67.0
Ba	476	679	29.3	541	659	346
Nb	4.17	6.64	1.05	8.59	9.31	4.63
Ta	0.35	0.58	0.08	0.65	0.72	0.39
Th	9.58	12.32	0.35	6.85	12.59	7.41
U	1.45	2.28	0.1	1.54	2.52	2.3
Pb	18.3	17.9	2.0	10.4	18.7	16.2
Zr	14.1	42.9	53.3	38.8	15.6	37.7
Hf	0.66	1.58	1.37	1.11	0.65	1.51
Y	16.85	40.11	15.38	43.9	34.21	26.73
V	9.3	6.2	150.1	102.5	67.5	15.9
Co	5.6	4.8	36.3	11.8	10.5	6.5
Ni	2.8	2.6	74.4	12.5	13.4	4.5
Cr	6.5	5.3	253.9	24.9	29.3	8.8
Mo	0.59	1.48	0.67	1.03	0.87	1.29
W	0.16	0.96	0.13	1.05	1.17	0.69
Cu	3.1	3.8	65.0	9.4	21.0	8.5
Zn	25.1	43.3	47.0	67.6	61.2	43.7
Cd	0.01	0.02	0.03	0.02	0.02	0.02
Ga	15.5	19.5	14.9	21.4	20.2	13.9
Ge	0.3	0.4	1.0	1.0	0.7	0.4
Sn	2.13	4.28	0.79	2.06	4.25	3.58
As	0.81	1.89	0.53	3.23	5.46	0.85
Sb	0.28	0.27	0.16	0.4	0.24	0.29
La	30.49	31.11	2.19	26.00	23.60	15.22
Ce	61.73	66.10	6.60	61.12	55.07	37.51
Pr	6.80	7.88	1.14	7.61	6.49	4.49
Nd	23.95	29.74	5.98	31.03	25.27	17.75
Sm	4.30	6.81	2.03	7.54	5.97	4.29
Eu	0.58	0.78	0.84	1.45	0.95	0.55
Gd	4.18	6.89	2.46	7.89	6.09	4.46
Tb	0.55	1.09	0.44	1.24	0.93	0.72
Dy	3.14	6.82	2.96	7.75	5.73	4.58
Ho	0.63	1.43	0.64	1.61	1.17	0.97
Er	1.71	3.94	1.74	4.35	3.11	2.69
Tm	0.26	0.59	0.26	0.64	0.44	0.41
Yb	1.70	3.76	1.66	4.02	2.67	2.61
Lu	0.24	0.53	0.24	0.58	0.36	0.38

TABLE 3  
(continued)

Sample No.	ST-1	ICH-1	UTT-1	UTT-2	OTC-1	OTC-2
Locality	Shirataki	Ichinohashi	Utsu-dake	Utsu-dake	Ochuube	Ochuube
Rock type	granite	granite	granite	granite	granite	granite
Zircon age (Ma)	37.0	18.5	(45.0)	45.0	17.9	18.2
Major element contents (in %)						
SiO <sub>2</sub>	65.93	73.76	70.86	70.46	72.46	72.36
Al <sub>2</sub> O <sub>3</sub>	15.49	13.48	14.46	14.46	14.53	13.95
Fe <sub>2</sub> O <sub>3</sub>	4.24	1.56	2.95	3.20	1.60	2.10
MnO	0.07	0.03	0.03	0.04	0.04	0.04
MgO	1.77	0.34	0.57	0.62	0.40	0.67
CaO	2.06	1.04	1.09	1.89	1.45	1.50
Na <sub>2</sub> O	4.49	3.17	4.45	4.13	3.89	3.43
K <sub>2</sub> O	2.83	4.92	3.46	3.43	4.23	4.27
TiO <sub>2</sub>	0.64	0.28	0.45	0.49	0.24	0.33
P <sub>2</sub> O <sub>5</sub>	0.15	0.06	0.09	0.11	0.08	0.10
LOI	1.79	0.66	1.08	0.72	0.37	0.53
Total	99.46	99.30	99.49	99.54	99.29	99.28
Parameters used for classification of Streckisen and Le Maitre (1979):						
ANOR	33.92	13.18	17.90	28.32	19.80	19.97
Q'	23.89	34.89	29.95	29.57	30.89	33.52
Parameters (molar ratios) for calculation of aluminum saturation index:						
A/NK	1.48	1.28	1.31	1.38	1.32	1.36
A/CNK	1.09	1.08	1.11	1.04	1.07	1.07
Trace elements (in ppm):						
Cs	2.4	3.8	3.5	3.5	8.0	8.6
Rb	92.5	103.0	75.3	83.3	50.4	50.8
Sr	128.3	69.2	188.7	138.9	85.8	129.4
Ba	465	653	725	623	571	1056
Nb	6.26	5.12	6.92	7.19	9.37	8.95
Ta	0.53	0.58	0.69	0.55	0.44	0.68
Th	8.3	13.87	9.22	9.84	17.44	11.07
U	1.91	2.65	1.94	2.3	2.27	2.66
Pb	10.4	25.0	7.2	9.1	21.5	25.1
Zr	22.4	39.5	71.1	72.5	15.8	26.4
Hf	0.98	1.55	2.55	2.59	0.7	0.95
Y	33.07	25.95	35.17	42.48	17.03	26.12
V	61.4	14.3	17.7	21.2	10.3	27.9
Co	13.8	6.2	6.8	7.4	6.0	7.5
Ni	20.8	3.2	3.9	8.6	3.6	7.4
Cr	28.3	6.1	8.9	18.8	6.4	13.4
Mo	0.63	0.85	0.66	0.76	0.63	0.59
W	0.68	0.29	0.64	0.96	0.65	0.66
Cu	5.6	26.8	2.3	3.9	1.8	7.7
Zn	58.8	14.9	19.8	26.4	38.0	36.5
Cd	0.01	0.01	0.02	0.02	0.01	0.01
Ga	19.1	16.3	18.1	18.6	19.2	17.2
Ge	0.6	0.3	0.5	0.5	0.4	0.4
Sn	2.27	1.66	2.67	3.52	1.79	4.86
As	1.09	2.30	0.84	1.07	1.30	7.86
Sb	0.19	0.36	0.25	0.27	0.32	0.53
La	17.56	21.70	20.99	25.13	33.39	25.05
Ce	41.30	46.90	34.74	54.97	71.53	52.88
Pr	5.25	5.20	6.27	6.86	8.10	6.23
Nd	21.19	18.70	25.02	26.87	29.10	23.56
Sm	5.24	4.13	5.68	6.36	5.69	5.24
Eu	0.78	0.56	0.71	0.76	0.59	0.89
Gd	5.45	4.24	5.69	6.75	5.45	5.29
Tb	0.87	0.66	0.91	1.10	0.68	0.79
Dy	5.50	4.16	5.92	7.00	3.64	4.75
Ho	1.16	0.87	1.23	1.49	0.69	0.95
Er	3.19	2.46	3.43	4.11	1.69	2.54
Tm	0.47	0.38	0.54	0.61	0.21	0.38
Yb	3.00	2.52	3.48	3.80	1.24	2.38
Lu	0.43	0.36	0.46	0.55	0.17	0.34

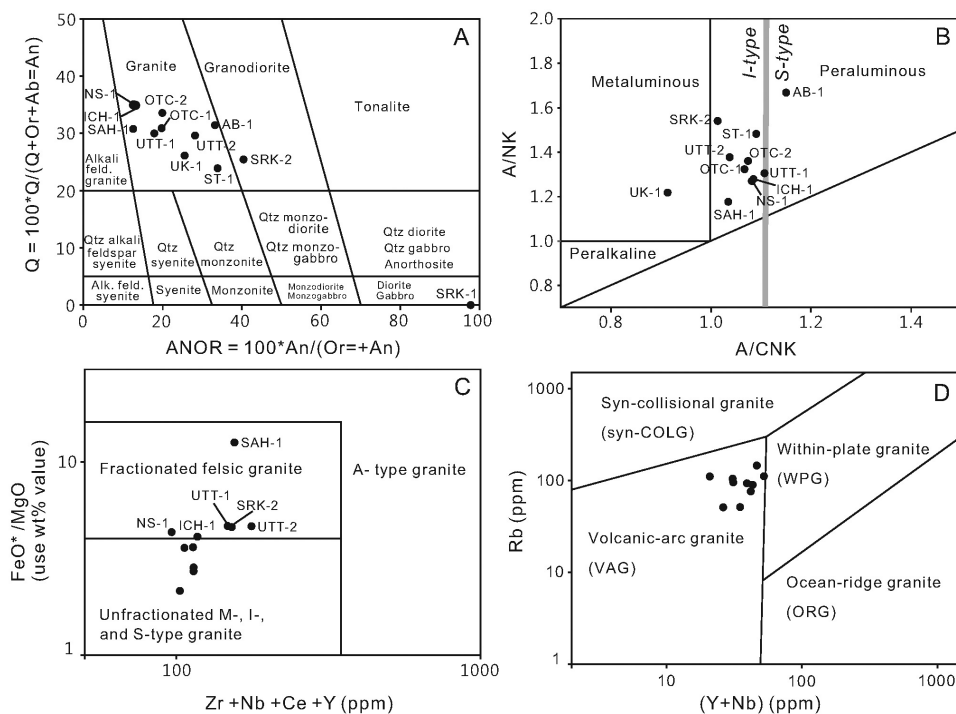


Fig. 7. Chemical characterization of the Hokkaido granitoids. (A) In the Q'-ANOR classification scheme of Streckeisen and Le Maitre (1979), the granitoids fall in the fields of granodiorite and "granite" (= monzogranite and syenogranite). (B) Most granitoid samples are slightly peraluminous and all but one has A/CNK values (Shand's index) less than 1.1. Thus, the granitoids are of I-type. (C) In a binary plot of Zr+Nb+Ce+Y vs. FeO\*/MgO (Whalen and others, 1987), the granitoids show various degrees of fractional crystallization. No rocks belong to A-type granite. (D) In a geotectonic classification of granitoids by Pearce and others (1984), all the Hokkaido granitoids fall in the field of volcanic-arc granites.

and Kemp and others (2007a) gave 5 out of 6 dates. As demonstrated earlier, the clear magmatic zoning, the range of Th/U ratios ( $>0.5$ ) in zircon crystals and the simple clustering of concordant or near-concordant data points provide strong evidence for the zircon crystallization in magmatic liquids. The three distinct age groups must represent three significant granitic intrusive episodes at 45, 37 and 18 Ma (fig. 11).

The majority of the K-Ar and fission-track (FT) dates can in principle be interpreted as the time of magmatic cooling but not the time of magmatic emplacement. This is probably true for the cases of Otchube (U-Pb age = 18, K-Ar (biotite/WR) = 16.5/16.0 Ma), Aibetsu (U-Pb = 45.5, FT (zircon) = 38.9, FT (apatite) = 16.5 Ma), and Nissho-toge (U-Pb = 18.6, K-Ar (biotite) = 16.0 Ma). On the other hand, a few K-Ar (biotite) ages are identical within the error limits with their corresponding zircon U-Pb ages, such as those of Ichinohashi and Uttsu-dake. This may suggest that the plutons cooled very fast from magmatic to Ar isotope closure temperature of biotite at about 250 to 300 °C. In this case, the K-Ar ages can be regarded as the time of magma emplacement.

In any case, figure 11 suggests that the Miocene peak at about 18 Ma must represent the most pre-eminent tectonothermal event in Hokkaido. The age spectrum (fig. 11) appears to show a continuous magmatic activity since 52 Ma, but we incline to think that many of the "intermediate ages" do not represent significant thermal events.

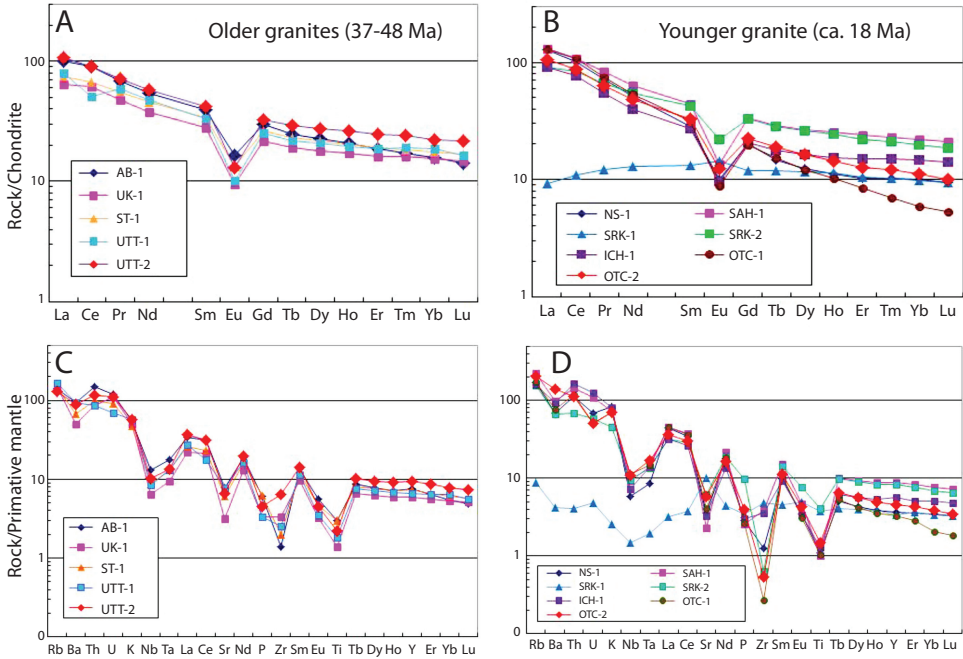


Fig. 8. REE distribution patterns and spidergrams for the Hokkaido granitoids and a gabbro. Note that the older Eocene granitoids and the younger Miocene granitoids are quite similar in the trace element distributions.

However, late Miocene granitic emplacements during 12 to 8 Ma have been well documented (Ishihara and others, 1998; Ishihara, 2007).

#### *Petrogenesis of the Granitoids—Constrained by Geochemical and Sr-Nd-Hf Isotopic Compositions*

The generation of these granitic rocks has been debated. In the northern half of the chains, two models have been proposed for the generation of the Eocene granite: one is related to ridge subduction and the other to arc magmatism due to change of subduction polarity. For the Miocene granites no model has been proposed.

In the southern half, a model for the Eocene granitoids is also related to ridge subduction, and a model for the Miocene granitoids calls for a mantle upwelling related to the opening of the Japan and Kurile basins (Kimura and Kusunoki, 1997; Usuki and others, 2006; Kemp and others, 2007a). In addition, some granitic rocks that intruded into a regional metamorphic zone are thought to be derived by mixing of a basic-to-intermediate magma and an acid magma of crustal partial melting (Owada and others, 2006).

The granitoids of the present study were collected from several areas in the central zone of Hokkaido extending N-S for more than 300 km. Besides, they were formed in three magmatic stages; thus, any petrogenetic model attempting to relate all the rocks is not realistic. However, it is possible to discuss the general mode of magma generation based on the geochemical and isotopic characteristics documented in preceding sections. The validity of proposed models can be tested with the geochemical and isotopic data.

In general, the granitoids show the typical arc magma signatures, including light-REE enriched rare earth patterns with strong negative Eu anomalies, distinctive

TABLE 4  
Rb-Sr and Sm-Nd isotopic compositions of granitoids and a gabbro from Hokkaido, Japan

Sample No.	Rock type	Age (Ma)	[Rb] (ppm)	[Sr] (ppm)	<sup>87</sup> Rb/ <sup>86</sup> Sr	± 2σm	I(Sr)	[Sm] (ppm)	[Nd] (ppm)	<sup>147</sup> Sm/ <sup>144</sup> Nd	<sup>143</sup> Nd/ <sup>144</sup> Nd	± 2σm	εNd(0)	εNd(T)	f <sub>s</sub>	T <sub>DM-1</sub> (Ma)
NS-1	Granite	18	108.6	75.2	4.18	0.705441	7	0.70437	4.30	0.1085	0.512867	8	4.5	4.7	-0.45	411
SAH-1	Granite	19	143.2	47.8	8.66	0.706768	7	0.70443	6.81	0.1384	0.512865	6	4.4	4.6	-0.30	578
SRK-1	Gabbro	19	5.6	211.2	0.076	0.702961	7	0.70294	2.03	0.2052	0.513059	6	8.2	8.2	0.04	1638
SRK-2	Granodiorite	19	109.8	151.5	2.10	0.705955	7	0.70539	7.54	0.1469	0.512781	6	2.8	2.9	-0.25	843
AB-1	Granite	46	88.8	163.7	1.57	0.707121	9	0.70610	5.97	0.1428	0.512672	6	0.7	1.0	-0.27	1028
UK-1	Granite	45	94.8	67.0	4.09	0.707017	11	0.70440	4.29	0.1461	0.512820	6	3.5	3.8	-0.26	745
ST-1	Granite	37	92.5	128.3	2.09	0.705564	7	0.70447	5.24	0.1495	0.512806	8	3.3	3.5	-0.24	818
ICH-1	Granite	19	103.0	69.2	4.31	0.706636	8	0.70547	4.13	0.1335	0.512738	6	2.0	2.1	-0.32	783
UTT-1	Granite	45	75.3	188.7	1.15	0.705666	7	0.70493	5.68	0.1372	0.512781	6	2.8	3.1	-0.30	735
UTT-2	Granite	45	83.3	138.9	1.74	0.705946	7	0.70484	6.36	0.1431	0.512785	6	2.9	3.2	-0.27	788
OTC-1	Granite	18	50.4	85.8	1.70	0.705575	8	0.70514	5.69	0.1182	0.512731	6	1.8	2.0	-0.40	670
OTC-2	Granite	18	50.8	129.4	1.14	0.705753	7	0.70546	5.24	0.1345	0.512709	6	1.4	1.5	-0.32	849

\*SRK-2; Use same age with SRK-1 because sampling points are close  
 \*UTT-1; Use same age with UTT-2 because sampling points are close  
 $I(Sr) = ({}^{87}Sr/{}^{86}Sr)_{sample(0)} - ({}^{87}Rb/{}^{86}Sr)_{sample(0)} \times (e^{\lambda t} - 1)$   
 $\epsilon_{Nd}(0) = 10^4 * (({}^{143}Nd/{}^{144}Nd)_{sample(0)} / ({}^{143}Nd/{}^{144}Nd)_{CHUR(0)} - 1)$   
 $\epsilon_{Nd}(T) = 10^4 * (({}^{143}Nd/{}^{144}Nd)_{sample(0)} - {}^{147}Sm/{}^{144}Nd_{sample(0)}) \times (e^{\lambda_{147}t} - 1) / ({}^{143}Nd/{}^{144}Nd)_{CHUR(0)} \times (e^{\lambda_{147}t} - 1) - 1)$   
 $f_s = f_{Sm/Nd, sample(0)} = ({}^{147}Sm/{}^{144}Nd)_{sample(0)} / ({}^{147}Sm/{}^{144}Nd)_{CHUR(0)} - 1$   
 $T_{DM-1} = (1/\lambda_{147}) \times \log_2(1 + [({}^{143}Nd/{}^{144}Nd)_{sample(0)} - ({}^{143}Nd/{}^{144}Nd)_{DM(0)}] / [({}^{147}Sm/{}^{144}Nd)_{sample(0)} - ({}^{147}Sm/{}^{144}Nd)_{DM(0)}])$   
 Constants and parameters used in calculations:  
 $\lambda ({}^{87}Rb) = 1.42 \times 10^{-5}/Ma$   
 $\lambda ({}^{147}Sm) = 6.54 \times 10^{-6}/Ma$  (Lugmair and Marti, 1978)  
 $({}^{143}Nd/{}^{144}Nd)_{CHUR(0)} = 0.512638$  (Goldstein and others, 1984)  
 $({}^{147}Sm/{}^{144}Nd)_{CHUR(0)} = 0.1967$  (Jacobsen and Wasserburg, 1980)  
 $({}^{143}Nd/{}^{144}Nd)_{DM(0)} = 0.51315$ ;  $({}^{147}Sm/{}^{144}Nd)_{DM(0)} = 0.2137$

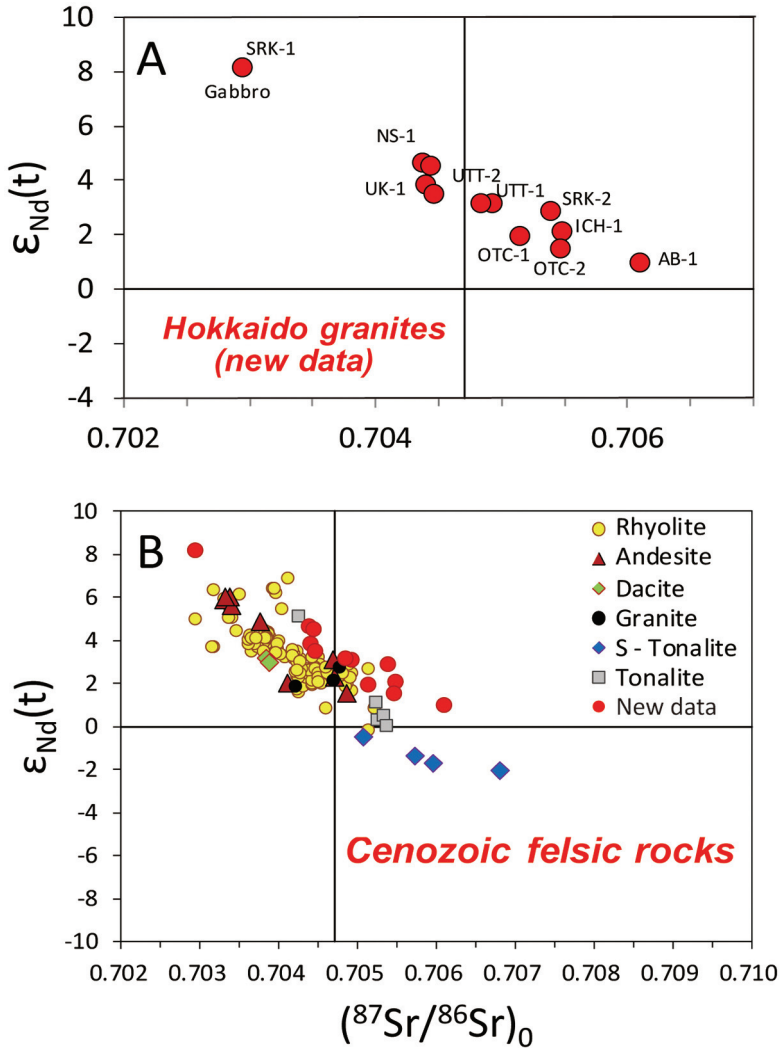


Fig. 9. (A) Whole-rock Sr-Nd isotopic compositions of the analyzed granitoids showing that all  $\epsilon_{\text{Nd}}(t)$  values are positive. The same scenario is found for Cenozoic volcanic rocks in Hokkaido (B). In (B), the four data point showing slightly negative  $\epsilon_{\text{Nd}}(t)$  values are for the “S-type tonalite” xenoliths from the Nozuka-dake area, Hidaka metamorphic belt (Owada and others, 2006).

negative Ta-Nb-Ti anomalies in the spidergrams, positive whole-rock  $\epsilon_{\text{Nd}}(t)$  values (+1 to +5), positive zircon  $\epsilon_{\text{Hf}}(t)$  values (+10 to +18), and young whole rock Sm-Nd model ages (400-1000 Ma), as well as young zircon Lu-Hf model ages (<400 Ma). Note that little geochemical and isotopic difference exists between the Eocene and Miocene granitoids. This suggests that their mode of generation and source rock nature were rather similar but not differentiated by the age factor. The overall isotopic signatures indicate that the granitoids and the bulk crust of Hokkaido must be quite “juvenile.” However, the positive  $\epsilon_{\text{Nd}}(t)$  values (+1 to +5) are not so “mantellic”; they are lower than that of the depleted mantle, thus some amount of older crustal contribution is implied in the granite petrogenesis. In addition, the large range of zircon Hf isotope

TABLE 5  
Hf isotopic data of zircons (in-situ analysis by ICP-MS)

Sample	t (Ma)	$1\sigma$	$\frac{^{176}\text{Yb}}{^{177}\text{Hf}}$	$2\sigma$	$\frac{^{176}\text{Lu}}{^{177}\text{Hf}}$	$2\sigma$	$\frac{^{176}\text{Hf}}{^{177}\text{Hf}}$	$2\sigma_m$	$\epsilon_{\text{Hf}}(0)$	$\epsilon_{\text{Hf}}(t)$	$1\sigma$	$f_{\text{Lu/Hf}}$	$T_{\text{DM1}}$	$T_{\text{DM2}}$
<b>OTC-1</b>														
Wt. mean age = $17.9 \pm 0.3$ Ma ( $2\sigma$ )														
OTC-1 03	17.9	0.4	0.1648	0.0031	0.0025	0.0001	0.283084	0.000018	11.0	11.4	0.3	-0.92	247	369
OTC-1 04	18.2	0.4	0.1783	0.0009	0.0028	0.0000	0.283226	0.000016	16.1	16.4	0.3	-0.92	36	46
OTC-1 06	18.8	0.4	0.1241	0.0023	0.0019	0.0000	0.283116	0.000022	12.2	12.6	0.4	-0.94	196	295
OTC-1 07	18.7	0.4	0.0943	0.0009	0.0015	0.0000	0.283095	0.000021	11.4	11.8	0.4	-0.96	224	342
OTC-1 08	18.5	0.5	0.1261	0.0016	0.0019	0.0000	0.283089	0.000020	11.2	11.6	0.4	-0.94	235	357
OTC-1 09	18.3	0.5	0.1711	0.0019	0.0025	0.0000	0.283167	0.000021	14.0	14.3	0.4	-0.92	124	180
OTC-1 14	18.0	0.4	0.1367	0.0030	0.0021	0.0000	0.283093	0.000024	11.3	11.7	0.4	-0.94	232	350
OTC-1 15	17.4	0.5	0.1815	0.0021	0.0026	0.0000	0.283190	0.000022	14.8	15.1	0.4	-0.92	89	128
OTC-1 16	17.5	0.4	0.1710	0.0017	0.0026	0.0000	0.283054	0.000016	10.0	10.3	0.3	-0.92	292	439
OTC-1 18	18.2	0.4	0.1652	0.0015	0.0023	0.0000	0.283103	0.000024	11.7	12.1	0.4	-0.93	217	325
OTC-1 24	17.6	0.4	0.1789	0.0018	0.0023	0.0000	0.283081	0.000022	10.9	11.3	0.4	-0.93	251	376
<b>OTC-2</b>														
Wt. mean age = $18.2 \pm 0.2$ Ma ( $2\sigma$ )														
OTC-2 02	18.0	0.4	0.1217	0.0028	0.0020	0.0000	0.283052	0.000016	9.9	10.3	0.3	-0.94	291	443
OTC-2 06	18.5	0.4	0.1595	0.0007	0.0024	0.0000	0.283006	0.000027	8.3	8.6	0.5	-0.93	362	547
OTC-2 07	18.3	0.5	0.1878	0.0044	0.0026	0.0000	0.283129	0.000029	12.6	13.0	0.5	-0.92	181	267
OTC-2 08	18.1	0.5	0.1786	0.0032	0.0025	0.0001	0.283121	0.000026	12.3	12.7	0.5	-0.92	193	286
OTC-2 10	18.2	0.4	0.1742	0.0019	0.0024	0.0000	0.283131	0.000029	12.7	13.1	0.5	-0.93	177	263
OTC-2 12	18.2	0.4	0.1295	0.0028	0.0018	0.0000	0.283106	0.000019	11.8	12.2	0.3	-0.94	210	318
OTC-2 13	18.5	0.4	0.1741	0.0025	0.0024	0.0000	0.283120	0.000020	12.3	12.7	0.3	-0.93	193	286
OTC-2 15	17.6	0.4	0.1955	0.0049	0.0027	0.0001	0.283165	0.000023	13.9	14.2	0.4	-0.92	128	186
OTC-2 16	18.9	0.4	0.1618	0.0045	0.0023	0.0000	0.283073	0.000023	10.6	11.0	0.4	-0.93	262	395
OTC-2 20	17.8	0.5	0.0963	0.0037	0.0014	0.0000	0.283039	0.000021	9.5	9.8	0.4	-0.96	304	471
OTC-2 21	18.5	0.6	0.1756	0.0005	0.0025	0.0000	0.283247	0.000025	16.8	17.2	0.4	-0.92	5	-2
OTC-2 24	19.1	0.4	0.1994	0.0024	0.0028	0.0000	0.283122	0.000029	12.4	12.8	0.5	-0.92	192	283
<b>ICH-1</b>														
Wt. mean age = $18.5 \pm 0.2$ Ma ( $2\sigma$ )														
ICH-1 06	17.9	0.6	0.1159	0.0004	0.0016	0.0000	0.283091	0.000023	11.3	11.7	0.4	-0.95	231	352
ICH-1 10	18.7	0.4	0.1171	0.0010	0.0017	0.0000	0.283062	0.000026	10.2	10.6	0.5	-0.95	274	419
ICH-1 11	17.8	0.5	0.1116	0.0011	0.0016	0.0000	0.283004	0.000019	8.2	8.6	0.3	-0.95	357	552
ICH-1 12	18.9	0.5	0.1201	0.0020	0.0018	0.0000	0.283135	0.000024	12.8	13.2	0.4	-0.95	168	252
ICH-1 16	19.0	0.5	0.1601	0.0018	0.0023	0.0000	0.283121	0.000027	12.3	12.7	0.5	-0.93	191	284
ICH-1 21	19.2	0.5	0.0869	0.0013	0.0013	0.0000	0.283019	0.000024	8.7	9.1	0.4	-0.96	333	517
ICH-1 24	19.1	0.5	0.1209	0.0014	0.0016	0.0000	0.283061	0.000027	10.2	10.6	0.5	-0.95	274	420

TABLE 5  
(continued)

Sample	t (Ma)	$1\sigma$	$\frac{^{176}\text{Yb}}{^{177}\text{Hf}}$	$2\sigma$	$\frac{^{176}\text{Lu}}{^{177}\text{Hf}}$	$2\sigma$	$\frac{^{176}\text{Hf}}{^{177}\text{Hf}}$	$2\sigma_m$	$\varepsilon_{\text{Hf}}(0)$	$\varepsilon_{\text{Hf}}(t)$	$1\sigma$	$f_{\text{Lw/Hf}}$	$T_{\text{DM1}}$	$T_{\text{DM2}}$
<b>UTT-2</b>														
Wt. mean age = $45.0 \pm 0.5$ Ma ( $2\sigma$ )														
UTT-2 03	45	1	0.1165	0.0004	0.0017	0.0000	0.283127	0.000017	12.5	13.5	0.3	-0.95	180	256
UTT-2 04	45	1	0.1132	0.0015	0.0017	0.0000	0.283099	0.000015	11.6	12.5	0.3	-0.95	220	319
UTT-2 05	47	1	0.1515	0.0017	0.0025	0.0001	0.283224	0.000022	16.0	16.9	0.4	-0.92	39	35
UTT-2 06	46	1	0.1103	0.0021	0.0016	0.0000	0.283172	0.000020	14.1	15.1	0.4	-0.95	114	152
UTT-2 07	46	1	0.0977	0.0008	0.0015	0.0000	0.283052	0.000016	9.9	10.9	0.3	-0.95	287	426
UTT-2 08	46	1	0.1023	0.0008	0.0016	0.0000	0.283123	0.000018	12.4	13.4	0.3	-0.95	185	265
UTT-2 09	45	1	0.1364	0.0004	0.0019	0.0000	0.283165	0.000021	13.9	14.8	0.4	-0.94	125	170
UTT-2 10	44	1	0.1165	0.0016	0.0018	0.0000	0.283160	0.000019	13.7	14.6	0.3	-0.95	132	181
UTT-2 11	46	1	0.0962	0.0016	0.0014	0.0000	0.283059	0.000018	10.1	11.1	0.3	-0.96	276	410
UTT-2 12	45	1	0.1302	0.0013	0.0019	0.0000	0.283086	0.000022	11.1	12.0	0.4	-0.94	240	350
UTT-2 13	45	1	0.1253	0.0028	0.0020	0.0001	0.283139	0.000025	13.0	13.9	0.4	-0.94	162	228
UTT-2 17	44	1	0.1008	0.0026	0.0015	0.0001	0.283037	0.000024	9.4	10.3	0.4	-0.95	309	462
UTT-2 19	47	1	0.0971	0.0010	0.0014	0.0000	0.283057	0.000024	10.1	11.1	0.4	-0.96	278	413
UTT-2 23	43	1	0.0689	0.0005	0.0010	0.0000	0.283099	0.000022	11.6	12.5	0.4	-0.97	215	318
UTT-2 25	45	1	0.1388	0.0019	0.0021	0.0001	0.283117	0.000028	12.2	13.1	0.5	-0.94	195	278
<b>AB-1</b>														
Wt. mean age (rim) = $45.7 \pm 0.5$ Ma ( $2\sigma$ )														
AB-1 13	45	1	0.1750	0.0008	0.0024	0.0000	0.283029	0.000022	9.1	10.0	0.4	-0.93	328	481
AB-1 15	46	1	0.1957	0.0017	0.0028	0.0000	0.283009	0.000023	8.4	9.3	0.4	-0.91	362	526
AB-1 20	45	1	0.1722	0.0016	0.0024	0.0000	0.283110	0.000018	12.0	12.9	0.3	-0.93	207	295
AB-1 27	44	1	0.1923	0.0027	0.0030	0.0000	0.283120	0.000024	12.3	13.2	0.4	-0.91	196	275
AB-1 29	47	1	0.1669	0.0018	0.0027	0.0000	0.283074	0.000026	10.7	11.6	0.5	-0.92	264	378
AB-1 30 (Old core)	104	3	0.0990	0.0019	0.0016	0.0000	0.282668	0.000022	-3.7	-1.5	0.4	-0.95	839	1262
<b>UK-1</b>														
Wt. mean age = $44.8 \pm 0.5$ Ma ( $2\sigma$ )														
UK-1 02	43	1	0.1438	0.0009	0.0026	0.0000	0.282999	0.000048	8.0	8.9	0.8	-0.92	375	550
UK-1 03	45	1	0.1484	0.0062	0.0023	0.0001	0.283167	0.000032	14.0	14.9	0.6	-0.93	123	165
UK-1 04	46	1	0.1272	0.0015	0.0019	0.0001	0.283135	0.000025	12.8	13.8	0.4	-0.94	169	238
UK-1 05	45	1	0.1428	0.0004	0.0020	0.0000	0.283227	0.000034	16.1	17.0	0.6	-0.94	34	28
UK-1 06	45	1	0.1373	0.0016	0.0024	0.0001	0.283016	0.000026	8.6	9.6	0.5	-0.93	347	509
UK-1 07	44	1	0.1462	0.0016	0.0027	0.0000	0.283157	0.000039	13.6	14.5	0.7	-0.92	139	188
UK-1 11	45	1	0.1750	0.0038	0.0033	0.0001	0.283183	0.000026	14.5	15.4	0.5	-0.90	102	131
UK-1 12	46	1	0.1355	0.0013	0.0027	0.0000	0.283105	0.000026	11.8	12.7	0.5	-0.92	218	308
UK-1 13	45	1	0.1411	0.0041	0.0027	0.0001	0.283213	0.000037	15.6	16.5	0.7	-0.92	56	61

TABLE 5  
(continued)

Sample	t (Ma)	$1\sigma$	$\frac{^{176}\text{Yb}}{^{177}\text{Hf}}$	$2\sigma$	$\frac{^{176}\text{Lu}}{^{177}\text{Hf}}$	$2\sigma$	$\frac{^{176}\text{Hf}}{^{177}\text{Hf}}$	$2\sigma_m$	$\epsilon_{\text{Hf}}(0)$	$\epsilon_{\text{Hf}}(t)$	$1\sigma$	$f_{\text{Lu/Hf}}$	$T_{\text{DM1}}$	$T_{\text{DM2}}$
<b>UK-1</b>														
Wt. mean age = 44.8 ± 0.5 Ma (2σ)														
UK-1 14	43	1	0.1555	0.0025	0.0031	0.0000	0.283223	0.000043	16.0	16.8	0.8	-0.91	40	39
UK-1 15	46	1	0.0900	0.0011	0.0015	0.0000	0.283152	0.000022	13.5	14.4	0.4	-0.95	142	197
UK-1 18	44	1	0.1919	0.0031	0.0027	0.0000	0.283205	0.000031	15.3	16.2	0.5	-0.92	67	79
UK-1 19	45	1	0.1279	0.0010	0.0019	0.0000	0.283107	0.000021	11.9	12.8	0.4	-0.94	209	301
UK-1 20	45	1	0.1421	0.0020	0.0022	0.0000	0.283237	0.000033	16.4	17.3	0.6	-0.93	20	7
UK-1 22	43	1	0.1830	0.0013	0.0025	0.0000	0.283191	0.000029	14.8	15.7	0.5	-0.92	88	111
UK-1 23	46	1	0.1882	0.0045	0.0032	0.0001	0.283056	0.000041	10.1	11.0	0.7	-0.90	294	419
UK-1 24	46	1	0.1459	0.0010	0.0020	0.0000	0.283089	0.000035	11.2	12.2	0.6	-0.94	237	343
<b>ST-1</b>														
Wt. mean age = 37.0 ± 0.5 Ma (2σ)														
ST-1 02	37.3	0.8	0.1472	0.0044	0.0019	0.0000	0.283108	0.000022	11.9	12.6	0.4	-0.94	209	304
ST-1 03	38	1	0.1327	0.0033	0.0019	0.0001	0.283142	0.000020	13.1	13.9	0.3	-0.94	158	225
ST-1 08	37.2	0.8	0.1594	0.0029	0.0022	0.0000	0.283062	0.000025	10.2	11.0	0.4	-0.93	278	409
ST-1 09	38.4	0.9	0.0855	0.0008	0.0012	0.0000	0.283129	0.000026	12.6	13.4	0.4	-0.96	174	254
ST-1 11	37.1	0.8	0.1907	0.0011	0.0025	0.0000	0.283262	0.000027	17.3	18.1	0.5	-0.92	-18	-47
ST-1 12	35.9	0.8	0.1187	0.0003	0.0016	0.0000	0.283073	0.000020	10.7	11.4	0.3	-0.95	257	383
ST-1 14	37	0.8	0.1527	0.0024	0.0020	0.0000	0.283175	0.000024	14.3	15.0	0.4	-0.94	110	150
ST-1 16	36.1	0.8	0.1296	0.0008	0.0018	0.0000	0.283187	0.000028	14.7	15.4	0.5	-0.95	93	125
ST-1 19	38	0.9	0.1492	0.0025	0.0020	0.0000	0.283064	0.000029	10.3	11.1	0.5	-0.94	273	404
ST-1 22	36.8	0.8	0.1512	0.0028	0.0019	0.0000	0.283164	0.000021	13.9	14.6	0.4	-0.94	126	176
ST-1 23	35.9	0.8	0.1357	0.0009	0.0019	0.0000	0.283088	0.000030	11.2	11.9	0.5	-0.94	237	349
ST-1 24	38.2	0.8	0.1999	0.0023	0.0027	0.0000	0.283110	0.000024	11.9	12.7	0.4	-0.92	210	301
<b>SRK-1</b>														
Wt. mean age = 19.0 ± 0.2 Ma (2σ) Gabbro														
SRK-1 02	19.4	0.6	0.1185	0.0007	0.0016	0.0000	0.283232	0.000025	16.3	16.7	0.4	-0.95	26	29
SRK-1 03	18.4	0.6	0.1587	0.0025	0.0021	0.0000	0.283282	0.000025	18.0	18.4	0.4	-0.94	-48	-84
SRK-1 04	18.0	0.7	0.1283	0.0028	0.0021	0.0000	0.283295	0.000032	18.5	18.9	0.6	-0.94	-66	-113
SRK-1 05	19.2	0.6	0.1248	0.0023	0.0017	0.0000	0.283252	0.000027	17.0	17.4	0.5	-0.95	-3	-15
SRK-1 07	19.2	0.6	0.1521	0.0046	0.0026	0.0001	0.283274	0.000026	17.8	18.1	0.5	-0.92	-36	-65
SRK-1 08	19.8	0.7	0.0976	0.0010	0.0013	0.0000	0.283199	0.000022	15.1	15.5	0.4	-0.96	74	105
SRK-1 10	18.8	0.5	0.0914	0.0044	0.0013	0.0001	0.283185	0.000022	14.6	15.0	0.4	-0.96	94	137
SRK-1 11	18.8	0.6	0.1883	0.0020	0.0026	0.0000	0.283304	0.000025	18.8	19.2	0.4	-0.92	-81	-134
SRK-1 12	19.8	0.8	0.0851	0.0011	0.0013	0.0000	0.283212	0.000023	15.6	16.0	0.4	-0.96	55	75
SRK-1 13	18.2	0.7	0.0951	0.0019	0.0015	0.0001	0.283246	0.000018	16.8	17.2	0.3	-0.95	5	-2
SRK-1 16	18.2	0.5	0.1528	0.0022	0.0024	0.0001	0.283270	0.000019	17.6	18.0	0.3	-0.93	-30	-56

TABLE 5  
(continued)

Sample	t (Ma)	1σ	$\frac{^{176}\text{Yb}}{^{177}\text{Hf}}$	2σ	$\frac{^{176}\text{Lu}}{^{177}\text{Hf}}$	2σ	$\frac{^{176}\text{Hf}}{^{177}\text{Hf}}$	2σ <sub>m</sub>	ε <sub>Hf</sub> (0)	ε <sub>Hf</sub> (t)	1σ	f <sub>Lu/Hf</sub>	T <sub>DM1</sub>	T <sub>DM2</sub>	
<b>SRK-1</b>	<b>Wt. mean age = 19.0 ± 0.2 Ma (2σ) Gabbro</b>														
SRK-1 17	19.3	0.6	0.1170	0.0016	0.0017	0.0000	0.283246	0.000026	16.8	17.2	0.5	-0.95	6	-1	
SRK-1 18	18.8	0.5	0.1810	0.0037	0.0027	0.0001	0.283237	0.000028	16.5	16.8	0.5	-0.92	19	19	
SRK-1 19	18.7	0.6	0.1497	0.0036	0.0024	0.0001	0.283284	0.000025	18.1	18.5	0.4	-0.93	-50	-87	
SRK-1 20	20.3	0.7	0.0663	0.0014	0.0012	0.0000	0.283192	0.000033	14.9	15.3	0.6	-0.97	83	121	
SRK-1 21	19.2	0.6	0.1440	0.0026	0.0021	0.0000	0.283239	0.000028	16.5	16.9	0.5	-0.94	16	14	
SRK-1 22	19.1	0.6	0.1422	0.0040	0.0021	0.0001	0.283273	0.000027	17.7	18.1	0.5	-0.94	-34	-63	
SRK-1 24	18.6	0.6	0.1180	0.0009	0.0018	0.0000	0.283255	0.000021	17.1	17.5	0.4	-0.95	-7	-22	
<b>SAH-1</b>	<b>Wt. mean age = 18.6 ± 0.2 Ma (2σ)</b>														
SAH-1 17	18.5	0.4	0.1947	0.0029	0.0029	0.0001	0.283096	0.000021	11.5	11.8	0.4	-0.91	231	341	
<b>NS-1</b>	<b>Wt. mean age = 18.2 ± 0.3 Ma (2σ)</b>														
NS-1 03	18.9	0.4	0.1217	0.0022	0.0017	0.0000	0.283215	0.000019	15.7	16.1	0.3	-0.95	51	69	
NS-1 08	18.0	0.4	0.1269	0.0036	0.0018	0.0000	0.283235	0.000024	16.4	16.7	0.4	-0.94	22	25	
NS-1 09	18.8	0.4	0.1622	0.0014	0.0023	0.0000	0.283150	0.000022	13.4	13.8	0.4	-0.93	147	217	
NS-1 10	19.0	0.4	0.1113	0.0014	0.0017	0.0000	0.283183	0.000024	14.5	14.9	0.4	-0.95	98	142	
NS-1 11	17.6	0.4	0.1616	0.0005	0.0023	0.0000	0.283218	0.000024	15.8	16.1	0.4	-0.93	48	64	
NS-1 13	17.3	0.5	0.0861	0.0013	0.0013	0.0000	0.283166	0.000025	13.9	14.3	0.4	-0.96	121	181	
NS-1 14	17.8	0.6	0.1593	0.0044	0.0022	0.0001	0.283202	0.000025	15.2	15.6	0.4	-0.93	71	100	
NS-1 15	18.1	0.4	0.1793	0.0033	0.0028	0.0001	0.283122	0.000029	12.4	12.7	0.5	-0.92	192	284	
NS-1 20	18.8	0.6	0.1321	0.0021	0.0021	0.0000	0.283151	0.000023	13.4	13.8	0.4	-0.94	146	216	
NS-1 22	18.1	0.4	0.1055	0.0022	0.0019	0.0000	0.283179	0.000025	14.4	14.8	0.4	-0.94	104	153	
NS-1 23	18.1	0.6	0.0867	0.0005	0.0015	0.0000	0.283191	0.000017	14.8	15.2	0.3	-0.95	86	125	
NS-1 24	18.3	0.5	0.1040	0.0006	0.0018	0.0000	0.283094	0.000021	11.4	11.8	0.4	-0.95	227	345	

$\epsilon_{\text{Hf}}(0) = 10000 * \left[ \left( \frac{^{176}\text{Hf}/^{177}\text{Hf}}{^{176}\text{Hf}/^{177}\text{Hf}} \right)_{\text{CHUR}(0)} - 1 \right]$   
 $\epsilon_{\text{Hf}}(t) = 10000 * \left[ \left( \frac{^{176}\text{Hf}/^{177}\text{Hf}}{^{176}\text{Hf}/^{177}\text{Hf}} \right)_{\text{S}(0)} - \left( \frac{^{176}\text{Hf}/^{177}\text{Hf}}{^{176}\text{Hf}/^{177}\text{Hf}} \right)_{\text{S}(0)} * (e^{\lambda * t * 10^{-6}} - 1) \right] - 1$ ; t (Ma)  
 $\lambda = \lambda_{176} = 1.867 * 10^{-11} / \text{yr}$  (Söderlund and others, 2004)  
 $f_{\text{cc}} = -0.5482$ ;  $f_{\text{s}} = \left( \frac{^{176}\text{Lu}/^{177}\text{Hf}}{^{176}\text{Lu}/^{177}\text{Hf}} \right)_{\text{sample}(0)} / \left( \frac{^{176}\text{Lu}/^{177}\text{Hf}}{^{176}\text{Lu}/^{177}\text{Hf}} \right)_{\text{CHUR}(0)} - 1$   
 $T_{\text{DM1}} = 1 / \lambda * \ln \left[ 1 + \left( \frac{^{176}\text{Hf}/^{177}\text{Hf}}{^{176}\text{Hf}/^{177}\text{Hf}} \right)_{\text{sample}(0)} - \left( \frac{^{176}\text{Hf}/^{177}\text{Hf}}{^{176}\text{Hf}/^{177}\text{Hf}} \right)_{\text{DM}(0)} \right] / \left( \frac{^{176}\text{Lu}/^{177}\text{Hf}}{^{176}\text{Lu}/^{177}\text{Hf}} \right)_{\text{DM}(0)}$   
 $^{176}\text{Hf}/^{177}\text{Hf}_{\text{DM}(0)} = 0.28325$  (Griffin and others, 2000);  $^{176}\text{Lu}/^{177}\text{Hf}_{\text{DM}(0)} = 0.0384$  (Griffin and others, 2000)  
 $T_{\text{DM2}} = T_{\text{DM1}} - (T_{\text{DM1}} - t) * (f_{\text{cc}} - f_{\text{s}}) / (f_{\text{cc}} - f_{\text{DM}})$ ;  $f_{\text{DM}} = 0.1566$

( $^{176}\text{Hf}/^{177}\text{Hf}$ )<sub>CHUR(0)</sub> = 0.282772 (Blichert-Toft and Albarede, 1997); ( $^{176}\text{Lu}/^{177}\text{Hf}$ )<sub>CHUR(0)</sub> = 0.0332 (Blichert-Toft and Albarede, 1997)

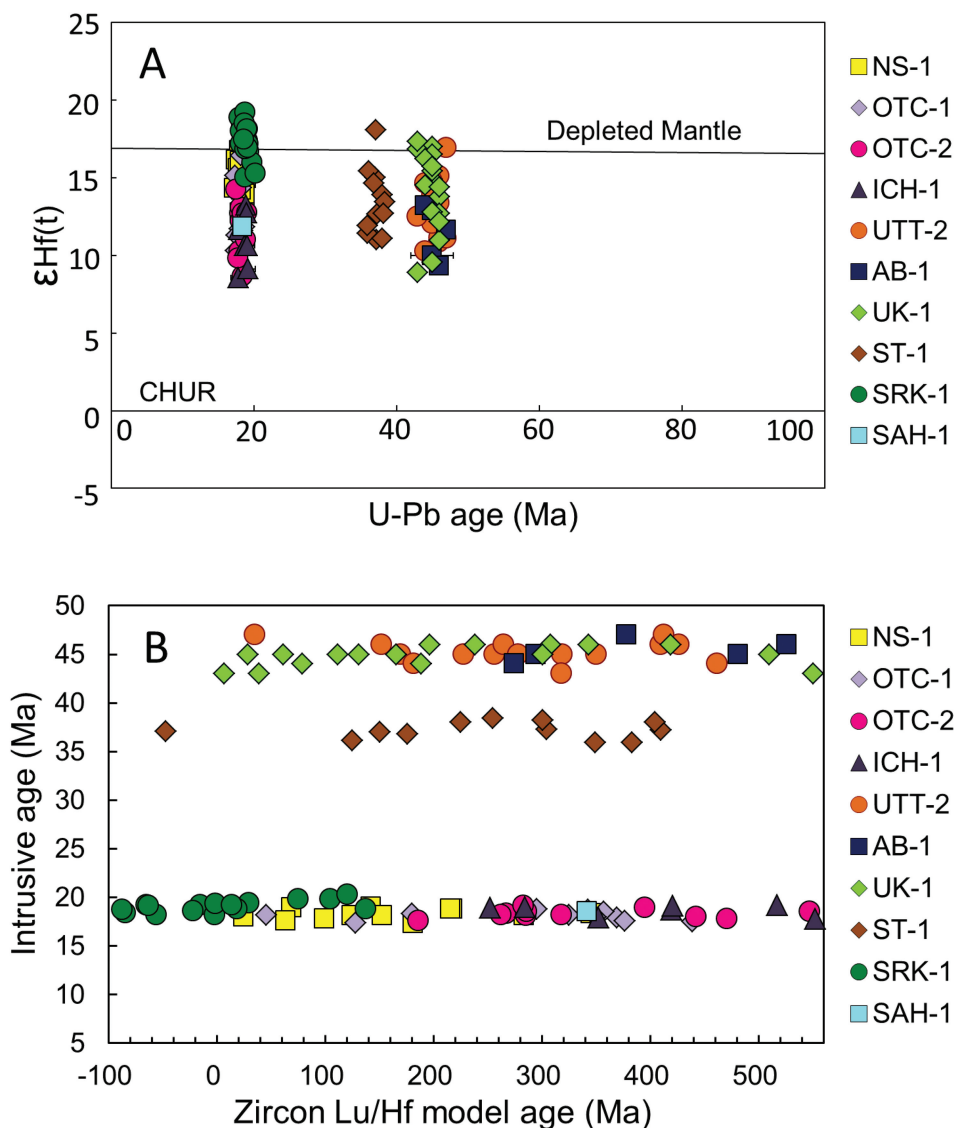


Fig. 10. Zircon Hf isotopic compositions. (A) Zircon grains of the same rock show a significant variation in Hf isotopic composition, suggesting an open-system behavior during the fractional crystallization in the magma chamber. (B) Consequently, the calculated Lu-Hf model ages also vary within a single rock. Nevertheless, the ensemble of the dataset show relatively young model ages and highly positive  $\epsilon_{\text{Nd}}(t)$  values, indicating the broadly juvenile characteristics of the Hokkaido granitoids.

compositions also attests to the contribution of recycled crust. A crude estimate of the proportion of juvenile/recycled components is shown in figure 12. The estimate was done using a simple two-component mixing calculation, assuming the two end-members to be mantle-derived basaltic rocks (= mantle) and old continental crust (= crust). The mixing proportions for all granitoid samples can be calculated using the following equation:

$$X^m = \text{Nd}_c \times (\epsilon^c - \epsilon^r) / [\epsilon^r \times (\text{Nd}_m - \text{Nd}_c) - (\epsilon^m \times \text{Nd}_m - \epsilon^c \times \text{Nd}_c)] \times 100$$

TABLE 6  
*Comparison of new zircon ages (in bold type) with K-Ar and Fission-Track age data*

Pluton	Sample No. (localities)	Rock name	Age (Ma)	Error (2 $\sigma$ ) in Ma)	Methods	Material	data Source
<b>Otchube</b>	<b>OTC-1</b>	<b>granite</b>	<b>17.8</b>	<b>0.3</b>	<b>U-Pb</b>	<b>Zircon</b>	<b>This study</b>
<b>Otchube</b>	<b>OTC-2</b>	<b>granite</b>	<b>18.1</b>	<b>0.3</b>	<b>U-Pb</b>	<b>Zircon</b>	<b>This study</b>
Otchube	74HK09	granodiorite	16.5	2.0	K-Ar	Biotite	Ishihara and Terashima (1985)
Otchube	44N°40'39", 142°36'21" (Amanokawa)	px-amp <b>gabbro</b>	16.0	0.3	K-Ar	Whole-rock	Ishihara and others (1998)
<b>Ichinohashi</b>	<b>ICH-1</b>	<b>granite</b>	<b>18.3</b>	<b>0.3</b>	<b>U-Pb</b>	<b>Zircon</b>	<b>This study</b>
Ichinohashi	74HK26	Hbl-bt granodiorite	18.4	0.6	K-Ar	Biotite	Shibata and Ishihara (1981)
Ichinohashi	74HK26?	Hbl-bt granodiorite	18.6	0.6	K-Ar	Biotite	Shibata and Ishihara (1981)
<b>Utsu-dake</b>	<b>UTT-2</b>	<b>granite</b>	<b>44.7</b>	<b>0.6</b>	<b>U-Pb</b>	<b>Zircon</b>	<b>This study</b>
Utsu-dake	74HK21	Hbl-bt granite	43.4	2.8	K-Ar	Biotite	Shibata and Ishihara (1981)
<b>Aibetsu</b>	<b>AB-1</b>	<b>granite</b>	<b>45.5</b>	<b>0.5</b>	<b>U-Pb</b>	<b>Zircon</b>	<b>This study</b>
Aibetsu	Ab-1 (43N°58'21", 142°38'19")	Bt granodiorite	46.0	1.1	K-Ar	Biotite	Kawakami and others (2006)
Aibetsu	Ab-1 (43N°58'21", 142°38'19")	Bt granodiorite	38.9	2.4	FT	Zircon	Kawakami and others (2006)
Aibetsu	Ab-1 (43N°58'21", 142°38'19")	Bt granodiorite	16.5	1.2	FT	Apatite	Kawakami and others (2006)
<b>Ukishima</b>	<b>UK-1</b>	<b>granite</b>	<b>44.8</b>	<b>0.5</b>	<b>U-Pb</b>	<b>Zircon</b>	<b>This study</b>
<b>Shirakawa</b>	<b>SRK-1</b>	<b>gabbro</b>	<b>18.9</b>	<b>0.2</b>	<b>U-Pb</b>	<b>Zircon</b>	<b>This study</b>
<b>Shirakawa</b>	<b>SRK-2</b>	<b>granodiorite</b>	-	-	<b>U-Pb</b>	<b>Zircon</b>	<b>This study</b>
Shirakawa		granodiorite	19.8	1.5	FT	Zircon	Koshimizu and others (1988)
<b>Shirataki</b>	<b>ST-1</b>	<b>granite</b>	<b>36.7</b>	<b>0.5</b>	<b>U-Pb</b>	<b>Zircon</b>	<b>This study</b>
Shirataki	Sg1 (Kamishiyubetsu river)	biotite granite (sheared)	33.0	2.5	FT	Zircon	Koshimizu and Kim (1986)
Shirataki	Sg2 (Muri river)	biotite granite (sheared)	32.0	2.3	FT	Zircon	Koshimizu and Kim (1986)
<b>Sahoro-dake</b>	<b>SAH-1</b>	<b>granite</b>	<b>18.6</b>	<b>0.3</b>	<b>U-Pb</b>	<b>Zircon</b>	<b>This study</b>
<b>Nissho-toge</b>	<b>NS-1</b>	<b>granite</b>	<b>18.2</b>	<b>0.3</b>	<b>U-Pb</b>	<b>Zircon</b>	<b>This study</b>
Nissho-toge			16.0	4.0	K-Ar	Biotite	Shibata (1968)

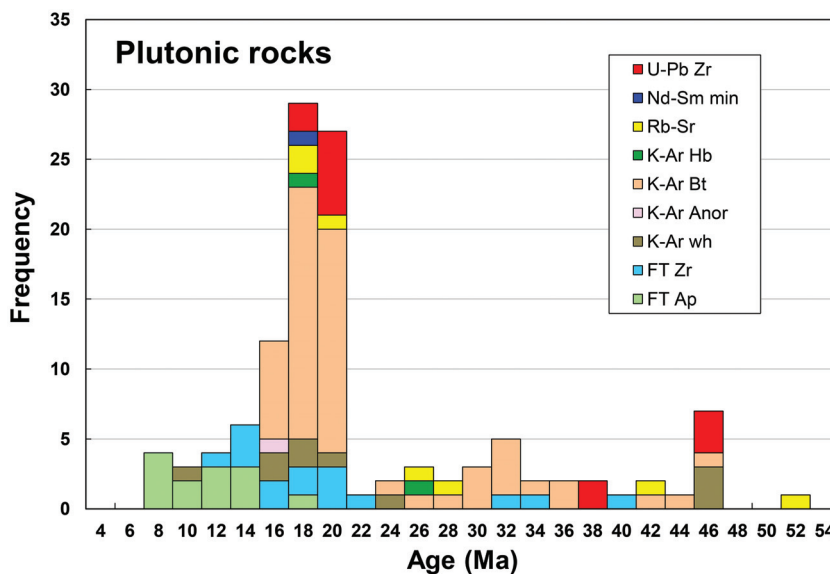


Fig. 11. Summary of the available age data (new and literature) for the intrusive rocks from Hokkaido. Literature data source: Arita and others (1993, 2001), Honma and Fujimaki (1997), Ishihara and Terashima (1985), Ishihara and others (1998), Kawakami and others (2006), Kawano and Ueda (1967), Kemp and others (2007a), Kimbrough and others (1994), Koshimizu and others (1988), Koshimizu and Kim (1986), Kubo and others (1984), Maeda and others (1990), Nakagawa (1992), Okamoto and Honma (1983), Okamura and others (2003), Ono (2002), Owada and others (1997, 2006), Saheki and others (1995), Shibata (1968), Shibata and others (1975), Shibata and Ishihara (1979, 1981), Zeniya and others (1996).

where  $X^m$  = % mantle-derived juvenile component (represented by basalt);  $\epsilon^c$ ,  $\epsilon^r$ ,  $\epsilon^m$  = Nd isotopic compositions of the crust, rock measured, and mantle component, respectively.  $Nd_c$ ,  $Nd_m$  = Nd concentrations in the crust and mantle components, respectively. The inset was taken from Jahn (2004), and the parameters used are:  $\epsilon^m = +8$ ,  $\epsilon^c = -12$  (NE China and Inner Mongolia),  $-30$  (Central Mongolia and Transbaikalia),  $-15$  (Altai Mountains),  $-4$  (Junggar),  $-15$  (Kazakhstan),  $Nd_m = 15$  ppm, and  $Nd_c = 25$  ppm. For the granitoids of Hokkaido,  $\epsilon^m = +10$  and  $\epsilon^c = -10$  were used.

We conclude that the juvenile or mantle component in the protoliths of the Hokkaido granitoids is between 65 to 95 percent. As displayed in the inset of figure 12, among the various tectonic terranes of the CAOB, the Junggar crust, as represented by its Paleozoic granitoids (500-300 Ma), has the most juvenile characteristics, with 60 to 100 percent mantle component. Thus, Hokkaido is most comparable with the Junggar terrane regarding the crustal evolution.

In the earlier review of the geology of Hokkaido (section II), we presented that the central Hokkaido is occupied by the Sorachi-Yezo and Hidaka Belts. The Sorachi-Yezo Belt is a Cretaceous-Paleogene forearc basin and accretionary complex; whereas the Hidaka Belt is a Paleogene arc complex in the north and the Hidaka metamorphic belt in the south. In a crustal section proposed by Ueda (2005), the likely source region for granitoid generation, the lower to middle crust, is composed of subducted oceanic crust (pillowed basalt), seamount, accretionary complex and a sedimentary cover sequence. The accretionary complex includes ophiolite mélangé and other components of "ocean plate stratigraphy." Partial melting of such lithological assemblages would produce granitic magmas with juvenile isotopic characteristics as shown in this study.

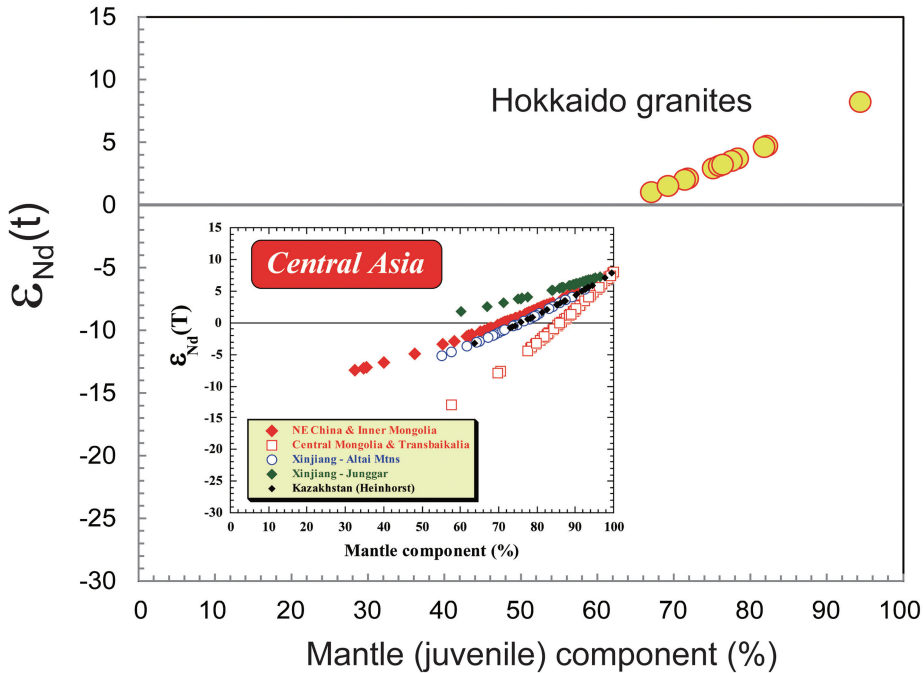


Fig. 12. Proportion of the mantle (juvenile) component involved in the generation of the Hokkaido granitoids. Assumption in the estimate for the Hokkaido rocks: Nd concentrations used for the mantle-derived juvenile component (“m”) and recycled crustal component (“c”) are 15 and 25 ppm, respectively. The Nd isotopic compositions used for  $\epsilon_{\text{Nd}}^{\text{m}} = +10$  and  $\epsilon_{\text{Nd}}^{\text{c}} = -10$ .

Ishihara and others (1998) noted that a distinctive feature of the late Cenozoic plutonism in the north-central Hokkaido is that granitoids and gabbroids occur in an equal amount (120 vs 110 km<sup>2</sup>) and are closely associated. The granitoids tend to occur in the whole region, but the gabbroids are restricted to the western edge of the Hidaka belt. Since the emplacement times of granitoids and gabbroids are similar (*ca.* 18 Ma), the plutonism is considered as bimodal in character. Moreover, bimodal magmatism is generally known to occur in an extensional tectonic regime, therefore, many models are in favor of the generation of the Hokkaido Miocene granitoids in a back-arc setting. On the other hand, the Eocene granotoid magmas were probably produced by melting of subducted accretionary complexes in supra-subduction zones. The accretionary complexes were likely dominated by juvenile or mantle-derived lithological assemblages as argued from the Sr-Nd-Hf isotopic signatures.

#### *Juvenile Crustal Growth and Comparison with Other Parts of Japan*

The formation of the Japanese Islands has been taken as a standard model for accretionary orogeny. It was proposed that the most important cause of the orogeny is the subduction of oceanic ridge, by which the continental mass increases through the transfer of granitic melt from the subducting oceanic crust to the orogenic belt (Maruyama, 1997). Sengor and Natal'in (1996) named the orogenic complexes “Nipponides,” consisting predominantly of Permian to Recent subduction-accretion complexes with few fragments of old continental crust, and further pointed out the resemblance in orogenic style between Japan and the Central Asian Orogenic Belt (CAOB). Consequently, the Japanese Islands are essentially built up by juvenile crust.

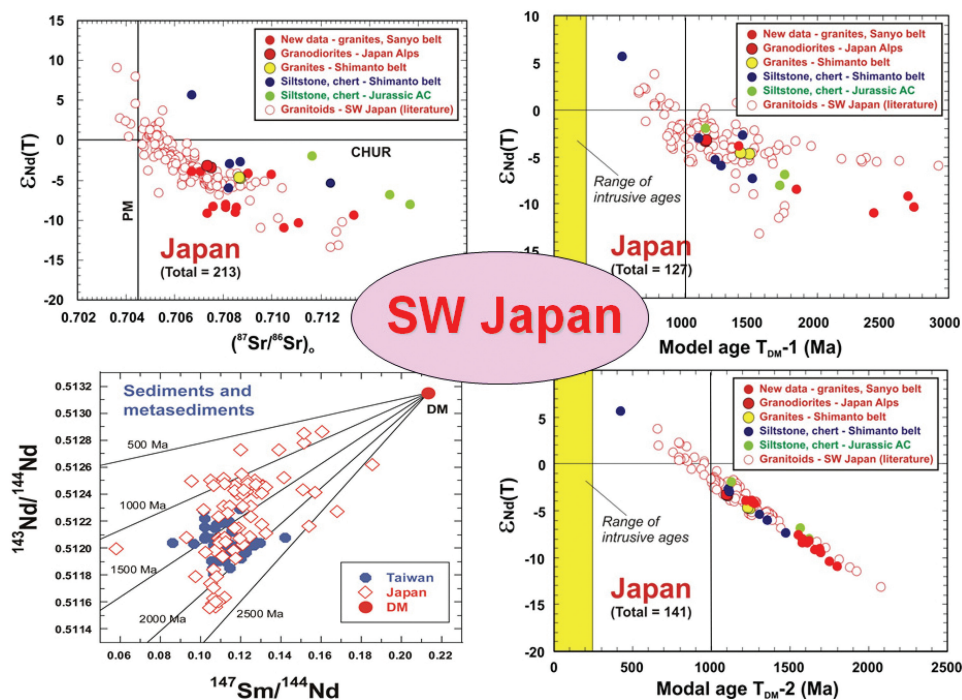


Fig. 13. Nd-Sr isotopic plots of granitoids from SW Japan (original data are from Jahn, 2010 and the cited references).

However, based on the available Sr-Nd isotopic data, Jahn (2010) showed that a large proportion of the granitoids of SW Japan have Proterozoic Sm-Nd model ages, high initial  $^{87}\text{Sr}/^{86}\text{Sr}$  ratios and negative  $\epsilon_{\text{Nd}}(\text{T})$  values (fig. 13). These isotopic data are in strong contrast with those of two celebrated accretionary orogens: the Central Asian Orogenic Belt and Arabian-Nubian Shield, but are quite comparable with those observed in SE China and Taiwan, or in classical collisional orogens in the European Hercynides and Caledonides (Jahn, 2004). This raises questions about the bulk composition or type of material accreted in accretionary complexes, and negates the hypothesis that the Nipponides contains very few fragments of older continental crust (Sengor and Natal'in, 1996). Jahn (2010) concluded that the subduction-accretion complexes in SW Japan were composed in significant amount of recycled continental crust, probably of Proterozoic age. The scenario is comparable with that in Taiwan.

However, further research has revealed that the real juvenile crust was produced in other parts of Japan, rather than in the best-studied SW Japan. As demonstrated in preceding sections, Hokkaido as a whole provides an excellent example of juvenile crustal addition to the global continental crust. Figure 14 illustrates the essential Nd-Sr isotopic plots for the granitoids from NE Japan (Hokkaido included). The data of granitoids (*sensu lato*) from the Kitakami and Abukuma Mountains and the Niigata area are shown for comparison with that of the granites and rhyolites from Hokkaido. Note that many of them are new and unpublished data.

Figure 14 shows that the majority of the data points have positive  $\epsilon_{\text{Nd}}(\text{T})$  values and initial  $^{87}\text{Sr}/^{86}\text{Sr}$  ratios of  $\leq 0.7055$ . The data of Abukuma granitoids straddle the  $\epsilon_{\text{Nd}}(\text{T})$  zero-line but generally form a negative correlation with the rest of the data points. By contrast, the data of the Niigata granitoids (shown in blue squares) seem to

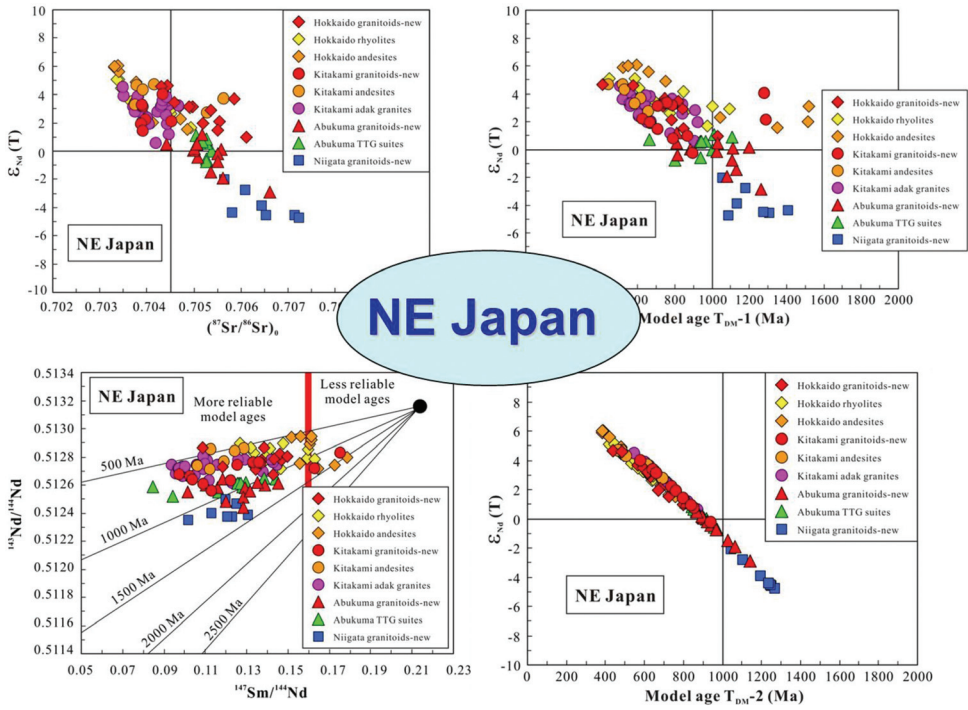


Fig. 14. Nd-Sr isotopic plots of granitoids from NE Japan (Hokkaido included). Individual source of data are not listed herein, but the original data-set used in this compilation is available upon request.

form a separate group distinguished from the rest but is comparable with the data array of SW Japan (fig. 13). Note that the data arrays in figures 13 and 14 are highly contrasted. The juvenile-crust-dominated features in NE Japan are replaced by the recycled-crust-dominated characteristics of SW Japan. This indicates that the architecture and crustal evolution of the two major parts of the Japanese Islands are quite distinguished. Note that the isotopic data displayed in figures 13 and 14 [ $\epsilon_{Nd}(T)$  vs.  $(^{87}Sr/^{86}Sr)_o$ ] involve rocks of different ages, so their display on the same plane is not strictly valid. In theory, we should have adjusted all the data points to the same time line. However, the adjusted vectors for a time difference less than 100 Ma would be too small to be detected in the figures, so the calculated initial ratios were plotted directly on the same plane.

The comparable isotopic compositions and the occurrence of the Niigata granitoids to the west of the Tanakura Tectonic Line lend support to the idea that the tectonic boundary or suture zone between NE and SW Japan before the Cenozoic is more logically represented by the Tanakura Tectonic Line, but not the Itoigawa-Shizuoka Fault.

CONCLUSIONS

The present study leads to the following conclusions:

1. Zircon U-Pb geochronology revealed three distinct periods of granitoid emplacement in central Hokkaido, at 45, 37 and 18 Ma.

2. Geochemical analyses show that the granitoids comprise granodiorite, monzogranite and syenogranite; they are weakly peraluminous and possess volcanic arc characteristics. They are not S-type granites. All the granitoids, regardless of their ages

‘(Eocene or Miocene), have similar REE patterns and spidergrams, typical of Phanerozoic granitoids.

3. Whole-rock Sr-Nd and zircon Hf isotopic data indicate that the granitoids are quite juvenile and likely generated by partial melting of sources dominated by mantle-derived rocks, and in matured arc settings. Recycled ancient crustal rocks are not a significant component in the source regions of the granitoids, and probably the entire Hokkaido crust.

4. The literature data show that the Miocene volcanic rocks (rhyolites, dacites and andesites) from Hokkaido possess Sr-Nd isotopic characteristics comparable with the granitoids, hence the plutonic granitoid and volcanic felsic magmas were probably derived from similar juvenile sources.

5. The crustal development of Hokkaido is most comparable with that of the Junggar Terrane of the Central Asian Orogenic Belt. Together with the Arabian-Nubian Shield, they document the best examples of juvenile crust growth.

#### ACKNOWLEDGMENTS

We have benefitted from frequent communications with Dr. Shunso Ishihara (Geological Survey of Japan/AIST) and Dr. Kazu Okamoto (Saitama University). Shoujie Liu and Jeremy Wu helped in preparation of some figures presented herein. Professor Dunyi Liu and the Beijing SHRIMP Center provided a temporary shelter to BMJ in May 2013 for preparation of the manuscript. Drs. Ishihara, Ueda and Bill Griffin critically reviewed this paper and helped ameliorate the manuscript. Dr. Ueda is particularly thanked for improving the presentation of geology and tectonics of Hokkaido. Bor-ming Jahn acknowledges the support of NSC-Taiwan (NSC100-2116-M-002-024, NSC100-2923-M-002-010 and NSC101-2116-M-002-003).

#### REFERENCES

- Apel, E. V., Bürgmann, R., Steblov, G., Vasilenko, N., King, R., and Prytkov, A., 2006, Independent active microplate tectonics of northeast Asia from GPS velocities and block modeling: *Geophysical Research Letters*, v. 33 (L11303), <http://dx.doi.org/10.1029/2006GL026077>
- Arai, S., 1994, Characterization of spinel peridotites by olivine-spinel compositional relationships: Review and interpretation: *Chemical Geology*, v. 113, n. 3–4, p. 191–204, [http://dx.doi.org/10.1016/0009-2541\(94\)90066-3](http://dx.doi.org/10.1016/0009-2541(94)90066-3)
- Arai, S., and Takahashi, N., 1989, Formation and compositional variation of phlogopites in the Horoman peridotite complex, Hokkaido, northern Japan: implications for origin and fractionation of metasomatic fluids in the upper mantle: *Contributions to Mineralogy and Petrology*, v. 101, n. 2, p. 165–175, <http://dx.doi.org/10.1007/BF00375303>
- Arita, K., Shingu, H., and Itaya, T., 1993, K-Ar geochronological constraints on tectonics and exhumation of the Hidaka metamorphic belt, Hokkaido, northern Japan: *Journal of Mineralogy, Petrology and Economic Geology*, v. 88, n. 3, p. 101–113, <http://dx.doi.org/10.2465/ganko.88.101>
- Arita, K., Ganzawa, Y., and Itaya, T., 2001, Tectonics and uplift process of the Hidaka Mountains, Hokkaido Japan inferred from thermochronology: The University of Tokyo, *Bulletin of the Earthquake Research Institute*, v. 76, p. 93–104 (in Japanese with English abstract).
- Blichert-Toft, J., and Albarède, F., 1997, The Lu–Hf geochemistry of chondrites and the evolution of the mantle–crust system: *Earth and Planetary Science Letters*, v. 148, n. 1–2, p. 243–258, [http://dx.doi.org/10.1016/S0012-821X\(97\)00040-X](http://dx.doi.org/10.1016/S0012-821X(97)00040-X)
- Cawood, P. A., Kröner, A., Collins, W. J., Kusky, T. M., Mooney, W. D., and Windley, B. F., 2009, Accretionary orogens through Earth history, in Cawood, P. A., and Kröner, A., editors, *Earth Accretionary Systems in Space and Time*: Geological Society, London, Special Publications, v. 318, p. 1–36, <http://dx.doi.org/10.1144/SP318.1>
- Chappell, B. W., and White, A. J. R., 1992, I- and S-type granites in the Lachlan Fold Belt. *Transactions of Royal Society of Edinburgh: Earth Sciences*, v. 83, p. 1–26, <http://dx.doi.org/10.1017/S0263593300007720>
- Chen, J. F., and Jahn, B. M., 1998, Crustal evolution of southeastern China: Nd and Sr isotopic evidence: *Tectonophysics*, v. 284, n. 1–2, p. 101–133, [http://dx.doi.org/10.1016/S0040-1951\(97\)00186-8](http://dx.doi.org/10.1016/S0040-1951(97)00186-8)
- Chiu, H. Y., Chung, S. L., Wu, F. Y., Liu, D., Liang, Y. H., Lin, I. J., Iizuka, Y., Xie, L. W., Wang, Y., and Chu, M. F., 2009, Zircon U-Pb and Hf isotopic constraints from eastern Transhimalayan batholiths on the pre-collisional magmatic and tectonic evolution in southern Tibet: *Tectonophysics*, v. 477, n. 1–2, p. 3–19, <http://dx.doi.org/10.1016/j.tecto.2009.02.034>
- De Jong, K., Kurimoto, C., and Ruffet, G., 2009, Triassic  $^{40}\text{Ar}/^{39}\text{Ar}$  ages from the Sakaigawa unit, Kii Peninsula, Japan: implications for possible merger of the Central Asian Orogenic Belt with large-scale

- tectonic systems of the East Asian margin: *International Journal of Earth Sciences*, v. 98, n. 6, p. 1529–1556, <http://dx.doi.org/10.1007/s00531-008-0340-1>
- Editorial committee of GEOLOGY OF JAPAN, editor, 2005, *Geology of Japan: Revised edition*: Tokyo, Kyoritsu Shuppan CO., LTD., 374 p (in Japanese).
- Editorial committee of HOKKAIDO, editor, 1990, *Regional Geology of Japan Part 1: Hokkaido*: Tokyo, Kyoritsu Shuppan CO., LTD., 337 p (in Japanese).
- Eyal, M., Zanzvilevich, A. N., Litvinovsky, B. A., Jahn, B. M., Vapnik, Ye., and Be'eri-Shlevin, Y., 2014, The Katherina ring complex (Sinai Peninsula, Egypt): sequence of emplacement and petrogenesis: *American Journal of Science*, v. 314, p.
- Furukata, C., Nakagawa M., Hirose W., and Adachi Y., 2010, Geochemical character of Early-Middle Miocene volcanic rocks from central Hokkaido: Characterization of magma-related back-arc spreading at the margin of the volcanic field: *The Journal of the Geological Society of Japan*, v. 116, p. 199–218 (in Japanese with English abstract).
- Goldstein, S. L., O'Nions, R. K., and Hamilton, P. J., 1984, A Sm-Nd study of atmospheric dusts and particulates from major river systems: *Earth and Planetary Science Letters*, v. 70, n. 2, p. 221–236, [http://dx.doi.org/10.1016/0012-821X\(84\)90007-4](http://dx.doi.org/10.1016/0012-821X(84)90007-4)
- Goolaerts, A., Mattielli, N., de Jong, J., Weis, D., and Scoates, J. S., 2004, Hf and Lu isotopic reference values for the zircon standard 91500 by MC-ICP-MS: *Chemical Geology*, v. 206, n. 1–2, p. 1–9, <http://dx.doi.org/10.1016/j.chemgeo.2004.01.008>
- Griffin, W. L., Pearson, N. J., Belousova, E., Jackson, S. E., van Achterbergh, E., O'Reilly, S. Y., and Shee, S. R., 2000, The Hf isotope composition of cratonic mantle: LAM-MC-ICPMS analysis zircon megacrysts in Kimberlites: *Geochimica et Cosmochimica Acta*, v. 64, n. 1, p. 133–147, [http://dx.doi.org/10.1016/S0016-7037\(99\)00343-9](http://dx.doi.org/10.1016/S0016-7037(99)00343-9)
- Griffin, W. L., Wang, X., Jackson, S. E., Pearson, N. J., O'Reilly, S. Y., Xu, X., and Zhou, X., 2002, Zircon chemistry and magma mixing, SE China: *In-situ* analysis of Hf isotopes, Tonglu and Pingtan igneous complexes: *Lithos*, v. 61, n. 3–4, p. 237–269, [http://dx.doi.org/10.1016/S0024-4937\(02\)00082-8](http://dx.doi.org/10.1016/S0024-4937(02)00082-8)
- Griffin, W. L., Pearson, N. J., Belousova, E. A., and Saeed, A., 2006, Comment: Hf-isotope heterogeneity in zircon 91500: *Chemical Geology*, v. 233, p. 358–363, <http://dx.doi.org/10.1016/j.chemgeo.2006.03.007>
- GSJ (The Geological Survey of Japan), AIST, editor, 2003, *Seamless digital geological map of Japan Nov 1, 2007 version: Research Information Database DB084*, Geological Survey of Japan, National Institute of Advanced Industrial Science and Technology, scale 1: 200,000.
- 2010, *Memoir of Regional Geology of Japan (1): Hokkaido*, Asakura Publishing Co. Ltd., 631 p. (in Japanese).
- Honma, H., and Fujimaki, H., 1997, Rb-Sr dating and petrological characteristics of a granodiorite dike from the southern Hidaka metamorphic belt, Hokkaido, Japan: *Journal of Mineralogy, Petrology and Economic geology*, v. 92, n. 7, p. 265–272, <http://dx.doi.org/10.2465/ganko.92.265>
- Hoskin, P. W. O., and Black, L. P., 2000, Metamorphic zircon formation by solid-state recrystallization of protolith igneous zircon: *Journal of Metamorphic Geology*, v. 18, n. 4, p. 423–439, <http://dx.doi.org/10.1046/j.1525-1314.2000.00266.x>
- Ireland, T. R., and Williams, I. S., 2003, Considerations in zircon geochronology by SIMS, *in* Hanchar, J. M., and Hoskin, P. W. O., (editors), *Zircon: Reviews in Mineralogy and Geochemistry*, v. 53, p. 215–241, <http://dx.doi.org/10.2113/0530215>
- Ishihara, S., 2007, Origin of the Cenozoic–Mesozoic magnetite-series and ilmenite-series granitoids in East Asia: *Gondwana Research*, v. 11, n. 12, p. 247–260, <http://dx.doi.org/10.1016/j.gr.2006.04.003>
- Ishihara, S., and Terashima, S., 1985, Cenozoic granitoids of central Hokkaido, Japan—An example of plutonism along a collisional belt: *Bulletin of the Geological Survey of Japan*, v. 36, p. 653–680.
- Ishihara, S., Matsuhiya, Y., Tanaka, R., Ihara, H., Nagasaka, A., Koike, T., and Shibata, K., 1998, The timing and genesis of ilmenite-series and magnetite-series granitic magmatism in the north-central Hokkaido, Japan: *Bulletin of the Geological Survey of Japan*, v. 49, p. 605–620.
- Isozaki, Y., 1996, Anatomy and genesis of a subduction-related orogen: A new view of geotectonic subdivision and evolution of the Japanese islands: *The Island Arc*, v. 5, n. 3, p. 289–320, <http://dx.doi.org/10.1111/j.1440-1738.1996.tb00033.x>
- 1997, Contrasting two types of orogen in Permo-Triassic Japan: Accretionary versus collisional: *The Island Arc*, v. 6, n. 1, p. 2–24, <http://dx.doi.org/10.1111/j.1440-1738.1997.tb00038.x>
- Isozaki, Y., and Itaya, T., 1991, Pre-Jurassic klippe in northern Chichibu Belt in west-central Shikoku, Southwest Japan-Kurosegawa Terrane as a tectonic outlier of the pre-Jurassic rocks of the Inner Zone: *Journal of the Geological Society of Japan*, v. 97, 431–450 (in Japanese with English abstract).
- Isozaki, Y., and Maruyama, S., 1991, Studies on orogeny based on plate tectonics in Japan and new geotectonic subdivision of the Japanese Islands: *Journal of Geography*, v. 100, n. 5, p. 697–761, [http://dx.doi.org/10.5026/jgeography.100.5\\_697](http://dx.doi.org/10.5026/jgeography.100.5_697)
- Isozaki, Y., Aoki, K., Nakama, T., and Yanai, S., 2010, New insight into a subduction-related orogeny: A reappraisal of the geotectonic framework and evolution of the Japanese Islands: *Gondwana Research*, v. 18, n. 1, p. 82–105, <http://dx.doi.org/10.1016/j.gr.2010.02.015>
- Iwasaki, T., Adachi, K., Moriya, T., Miyamachi, H., Matsushima, T., Miyashita, K., Takeda, T., Taira, T., Yamada, T., and Ohtake, K., 2004, Upper and middle crustal deformation of an arc-arc collision across Hokkaido, Japan, inferred from seismic refraction/wide-angle reflection experiments: *Tectonophysics*, v. 388, n. 1–4, p. 59–73, <http://dx.doi.org/10.1016/j.tecto.2004.03.025>
- Jacobsen, S. B., and Wasserburg, G. J., 1980, Sm-Nd isotopic evolution of chondrites: *Earth and Planetary Science Letters*, v. 50, n. 1, p. 139–155, [http://dx.doi.org/10.1016/0012-821X\(80\)90125-9](http://dx.doi.org/10.1016/0012-821X(80)90125-9)
- Jahn, B. M., 2004, The Central Asian Orogenic Belt and growth of the continental crust in the Phanerozoic, *in* Malpas, J., Fletcher, C. J. N., Ali, J. R., and Aitchison, J. C., editors, *Aspects of the Tectonic Evolution*

- of China: Geological Society, London, Special Publications, v. 226, p. 73–100, <http://dx.doi.org/10.1144/GSL.SP.2004.226.01.05>
- 2010, Accretionary orogen and evolution of the Japanese Islands: Implications from a Sr-Nd isotopic study of the Phanerozoic granitoids from SW Japan: *American Journal of Science*, v. 310, n. 10, p. 1210–1249, <http://dx.doi.org/10.2475/10.2010.02>
- Jahn, B. M., Zhou, X. H., and Li, J. L., 1990, Formation and tectonic evolution of Southeastern China and Taiwan: Isotopic and geochemical constraints: *Tectonophysics*, v. 183, n. 1–4, p. 145–160, [http://dx.doi.org/10.1016/0040-1951\(90\)90413-3](http://dx.doi.org/10.1016/0040-1951(90)90413-3)
- Jahn, B. M., Litvinovsky, B. A., Zangvilovich, A. N., and Reichow, M., 2009, Peralkaline granitoid magmatism in the Mongolian-Transbaikalian Belt: Evolution, petrogenesis and tectonic significance: *Lithos*, v. 113, n. 3–4, p. 521–539, <http://dx.doi.org/10.1016/j.lithos.2009.06.015>
- Kawakami, G., Ohira, H., Arita, K., Itaya, T., and Kawamura, M., 2006, Uplift history of the Hidaka Mountains, Hokkaido, Japan: A thermochronologic view: *Journal of Geological Society of Japan*, v. 112, n. 11, p. 684–698 (in Japanese with English abstract).
- Kawamura, M., 2004, Forearc tectonics and tentative plate-tectonic synthesis for Jurassic-Cretaceous Hokkaido, Japan, in Mawatari, S. F., and Okada, H., editors, *Neo-Science of Natural History: Integration of Geoscience and Biodiversity Studies: Sapporo, Japan, Proceedings of International Symposium on "Dawn of a New Natural History—Integration of Geoscience and Biodiversity Studies,"* March 5–6, 2004, p. 109–119.
- Kawamura, M., Yasuda, N., Watanabe, T., Fanning, M., and Terada, T., 2000, Composition and provenance of the Jurassic quartzfeldspathic sandstone of the Oshima Accretionary Belt, SW Hokkaido, Japan: *Memoir Geological Society of Japan*, v. 57, p. 63–72 (in Japanese with English abstract).
- Kawano, Y., and Ueda, Y., 1967, K-Ar dating on the igneous rocks in Japan (VI): Granitic rocks, summary: *Journal of Mineralogy, Petrology and Economic Geology*, v. 57, n. 5, p. 177–187 (in Japanese with English abstract).
- Kemp, A. I. S., Shimura, T., Hawkesworth, C. J., and EIMF, 2007a, Linking granulites, silicic magmatism, and crustal growth in arcs: Ion microprobe (zircon) U-Pb ages from the Hidaka metamorphic belt, Japan: *Geology*, v. 35, n. 9, p. 807–810, <http://dx.doi.org/10.1130/G23586A.1>
- Kemp, A. I. S., Hawkesworth, C. J., Foster, G. L., Paterson, B. A., Woodhead, J. D., Hergt, J. M., Gray, C. M., and Whitehouse, M. J., 2007b, Magmatic and crustal differentiation history of granitic rocks from Hf-O isotopes in zircon: *Science*, v. 315, n. 5814, p. 980–983, <http://dx.doi.org/10.1126/science.1136154>
- Kimbrough, D. L., Herzig, C. T., Watanabe, T., Arita, K., Kuriya, M., Kagami, H., Hayasaka, Y., and Tainosho, Y., 1994, Uranium-lead dating of ophiolite, granitoid & high-grade metamorphic rocks, Japan, in *From Paleasian ocean to Paleo-Pacific ocean: Sapporo, Japan, Abstract of an international joint symposium of IGC projects 283, 321, 359, 1994*, p. 48–51.
- Kiminami, K., Komatsu, M., Niida, K., and Kito, N., 1986, Tectonic divisions and stratigraphy of the Mesozoic rocks of Hokkaido, Japan: Monograph of the Association of Geological Collaboration in Japan, v. 31, p. 1–15 (in Japanese with English abstract).
- Kiminami, K., Miyashita, S., and Kawabata, K., 1999, Occurrence and significance of in-situ basaltic rocks from the Rurochi Formation in the Hidaka Supergroup, northern Hokkaido, Japan: *The Memoirs of the Geological Society of Japan*, v. 52, p. 103–112 (in Japanese with English abstract).
- Kimura, G., 1986, Oblique subduction and collision: Forearc tectonics of the Kuril arc: *Geology* v. 14, n. 5, p. 404–407, [http://dx.doi.org/10.1130/0091-7613\(1986\)14\(404:OSACFT\)2.0.CO;2](http://dx.doi.org/10.1130/0091-7613(1986)14(404:OSACFT)2.0.CO;2)
- 1994, The latest Cretaceous-Early Paleogene rapid growth of accretionary complex and exhumation of high pressure series metamorphic rocks in northwestern Pacific margin: *Journal of Geophysical Research*, v. 99, n. B11, p. 22147–22164, <http://dx.doi.org/10.1029/94JB00959>
- Kimura, G., and Kusunoki, K., 1997, The Hidaka orogeny and tectonics of arc-arc junction: *The Memoirs of the Geological Society of Japan*, v. 47, p. 295–305 (in Japanese with English abstract).
- Kimura, G., Sakakibara, M., and Okamura, M., 1994, Plumes in central Panthalassa? Deductions from accreted oceanic fragments in Japan: *Tectonics*, v. 13, n. 4, p. 905–916, <http://dx.doi.org/10.1029/94TC00351>
- Komatsu, M., Osanai, Y., Toyoshima, T., and Miyashita, S., 1989, Evolution of the Hidaka metamorphic belt, Hokkaido, northern Japan, in Daly, J. S., Cliff, R. A., and Yardley, B. W. D., editors, *Evolution of Metamorphic Belts: Geological Society, London, Special Publication*, v. 43, p. 487–493, <http://dx.doi.org/10.1144/GSL.SP.1989.043.01.45>
- Komatsu, M., Shibakusa, H., Miyashita, S., Ishizuka, H., Osanai, Y., and Sakakibara, M., 1992, Subduction and collision related high and low P/T metamorphic belts in Hokkaido: *Geological Survey of Japan, 29th IGC Field Trip Guide Book, C01*, p. 1–61.
- Komatsu, M., Toyoshima, T., Osanai, Y., and Arai, M., 1994, Prograde and anatexis reactions in the deep arc crust exposed in the Hidaka metamorphic belt, Hokkaido, Japan: *Lithos*, v. 33, n. 1–3, p. 31–49, [http://dx.doi.org/10.1016/0024-4937\(94\)90052-3](http://dx.doi.org/10.1016/0024-4937(94)90052-3)
- Koshimizu, S., and Kim, C. W., 1986, Fission-track dating of the Cenozoic formations in central-eastern Hokkaido, Japan (part 1): Kamishiyubetsu and Kitamifujii district: *Journal of Geological Society of Japan*, v. 92, p. 477–487 (in Japanese with English abstract).
- Koshimizu, S., Kawamura, M., and Kato, M., 1988, Fission-track age of granodiorite, west of Sounkyo-Spa, Kamikawa-cho, Hokkaido: *Journal of Geological Society of Japan*, v. 94, p. 711–714 (in Japanese with English abstract).
- Kubo, K., Shibata, K., and Satoh, H., 1984, K-Ar age of lamprophyre in the Urakawa area, Hokkaido: *Bulletin of the Geological Survey of Japan*, v. 35, p. 87–90 (in Japanese with English abstract).
- Lin, I. J., Chung, S. L., Chu, C. H., Lee, H. Y., Gallet, S., Wu, G., Ji, J., and Zhang, Y., 2012, Geochemical and Sr-Nd isotopic characteristics of Cretaceous to Paleogene granitoids and volcanic rocks, SE Tibet:

- Petrogenesis and tectonic implications: *Journal of Asian Earth Sciences*, v. 53, p. 131–150, <http://dx.doi.org/10.1016/j.jseaeas.2012.03.010>
- Lugmair, G. W., and Marti, K., 1978, Lunar initial  $^{143}\text{Nd}/^{144}\text{Nd}$ : Differential evolution of the lunar crust and mantle: *Earth and Planetary Science Letters*, v. 39, n. 3, p. 349–357, [http://dx.doi.org/10.1016/0012-821X\(78\)90021-3](http://dx.doi.org/10.1016/0012-821X(78)90021-3)
- Maeda, J., and Kagami, H., 1994, Mafic igneous rocks derived from N-MORB source mantle, Hidaka magmatic zone, central Hokkaido: Sr and Nd isotopic evidence. *Journal of Geological Society of Japan*, v. 100, p. 185–188.
- 1996, Interaction of a spreading ridge and an accretionary prism: Implications from MORB magmatism in the Hidaka magmatic zone, Hokkaido, Japan: *Geology*, v. 24, p. 31–34, [http://dx.doi.org/10.1130/0091-7613\(1996\)024\(0031:IOASRA\)2.3.CO;2](http://dx.doi.org/10.1130/0091-7613(1996)024(0031:IOASRA)2.3.CO;2)
- Maeda, J., Suetake, S., Ikeda, Y., Tomura, S., Motoyoshi, Y., and Okamoto, Y., 1986, Tertiary plutonic rocks in the axial zone of Hokkaido: distribution, age, major element chemistry, and tectonics: Monograph of the Association of Geological Collaboration in Japan, v. 31, p. 223–246 (in Japanese with English abstract).
- Maeda, J., Miyasaka, S., Ikeda, Y., Suetake, S., Tomura, S., Kawachi, S., and Matsui, M., 1990, K-Ar ages of Tertiary intrusive rocks and spatial and temporal transition of magmatism in Central Hokkaido, northern Japanese islands: *Earth Science*, v. 44, p. 231–244 (in Japanese with English abstract).
- Maruyama, S., 1997, Pacific-type orogeny revisited: Miyashiro-type orogeny proposed: *The Island Arc*, v. 6, n. 1, p. 91–120, <http://dx.doi.org/10.1111/j.1440-1738.1997.tb00042.x>
- Maruyama, S., Isozaki, Y., Kimura, G., and Terabayashi, M., 1997, Paleogeographic maps of the Japanese islands: Plate tectonic synthesis from 750 Ma to the present: *The Island Arc*, v. 6, n. 1, p. 121–142, <http://dx.doi.org/10.1111/j.1440-1738.1997.tb00043.x>
- Mikoshiba, M., 1999, Chemical characteristics of basic metamorphic rocks from the Main Zone of the Hidaka metamorphic belt, Hokkaido: an affinity to mid-ocean ridge basalts: *Bulletin of the Geological Survey of Japan*, v. 50, p. 613–634 (in Japanese with English abstract).
- Miyashita, S., and Katsushima, T., 1986, The Tomuraushi greenstone complex of the central Hidaka zone: contemporaneous occurrence of abyssal tholeiite and terrigenous sediments: *Journal of Geological Society of Japan*, 92, p. 535–57.
- Nakagawa, M., 1992, The age difference between metamorphic rocks and associated leucogranites in the Kamuiokotan zone: abstract for the 216<sup>th</sup> meeting of Geological Survey of Japan: *Bulletin of the Geological Survey of Japan*, v. 43, p. 467 (in Japanese).
- Nakamura, K., 1983, Possible nascent trench along the eastern Japan Sea as the convergent boundary between Eurasian and North American plates: University of Tokyo, *Bulletin Earthquake Research Institute*, v. 58, p. 711–722 (in Japanese with English abstract).
- Niida, K., and Kito, N., 1986, Cretaceous arc-trench systems in Hokkaido: The Association for the Geological Collaboration in Japan Monograph 31, p. 379–402 (in Japanese with English abstract).
- Ogawa, Y., Nishida, Y., and Makino, M., 1994, A collision boundary imaged by magnetotellurics, Hidaka Mountains, central Hokkaido, Japan: *Journal of Geophysical Research-Solid Earth*, v. 99, n. B11, p. 22373–22388, <http://dx.doi.org/10.1029/94JB01129>
- Oh, C. W., 2006, A new concept on the tectonic correlation between Korea, China and Japan: Histories from the late Proterozoic to Cretaceous: *Gondwana Research*, v. 9, n. 1–2, p. 47–61, <http://dx.doi.org/10.1016/j.gr.2005.06.001>
- Okamoto, Y., and Honma, H., 1983, Oxygen and strontium isotope study of granitic and metamorphic rocks of the Hidaka belt, Hokkaido: *Magma*, v. 67, p. 151–155 (in Japanese).
- Okamura, S., Yahata, M., and Nishido, H., 2003, K-Ar ages of late Cenozoic igneous rocks from Aibetsu-Kamikawa region, north Hokkaido, Japan: *Earth Science*, v. 57, p. 129–135 (in Japanese with English abstract).
- Ono, M., 2002, Uplift history of the Hidaka Mountains: Fission-track analyses: The University of Tokyo, *Bulletin of the Earthquake Research Institute*, v. 77, p. 123–130 (in Japanese with English abstract).
- Osanai, Y., Komatsu, M., and Owada, M., 1991, Metamorphism and granite genesis in the Hidaka metamorphic belt, Hokkaido, Japan: *Journal of Metamorphic Geology*, v. 9, n. 2, p. 111–124, <http://dx.doi.org/10.1111/j.1525-1314.1991.tb00508.x>
- Osanai, Y., Owada, M., and Kawasaki, T., 1992, Tertiary deep crustal ultrametamorphism in the Hidaka metamorphic belt, northern Japan: *Journal of Metamorphic Geology*, v. 10, n. 3, p. 401–414, <http://dx.doi.org/10.1111/j.1525-1314.1992.tb00092.x>
- Osanai, Y., Owada, M., Shimura, T., Nakano, N., Kawanami, S., and Komatsu, M., 2006, Partial melting of high-grade metamorphic rocks in lower crustal part of the Hidaka Arc (Main Zone of the Hidaka metamorphic belt), northern Japan: *Journal of Geological Society of Japan*, v. 112, p. 623–638 (in Japanese with English abstract).
- Osanai, Y., Owada, M., and Toyoshima, T., 2007, Metamorphic and deformation processes of lower crustal rocks in the Hidaka Collision Zone, Hokkaido, northern Japan: *Journal of Geological Society of Japan*, v. 113, Supplement, p. 29–50 (in Japanese).
- Owada, M., Osanai, Y., and Kagami, H., 1997, Rb-Sr isochron ages for hornblende tonalite from the southeastern part of the Hidaka metamorphic belt, Hokkaido, Japan: implication for timing of peak metamorphism: *The Memoirs of the Geological Society of Japan*, v. 47, p. 21–27.
- Owada, M., Osanai, Y., Shimura, T., Toyoshima, T., and Katsui, Y., 2003, Crustal section and anatexis of lower crust due to mantle flux in the Hidaka metamorphic belt, Hokkaido, Japan: *Geological Survey of Japan*, Interim Report, v. 28, p. 81–102.
- Owada, M., Yamasaki, T., Osanai, Y., Yoshimoto, K., Hamamoto, T., and Kagami, H., 2006, Poly-metamorphism, anatexis and formation of granitic magma due to intrusion of the Niobetsu complex

- during Miocene, the Nozuka-dake area, Hidaka metamorphic belt, northern Japan: *Journal of the Geological Society of Japan*, v. 112, p. 666–683 (in Japanese with English abstract).
- Pearce, J. A., Harris, N. W., and Tindle, A. G., 1984, Trace element discrimination diagrams for the tectonic interpretation of granitic rocks: *Journal of Petrology*, v. 25, n. 4, p. 956–983, <http://dx.doi.org/10.1093/petrology/25.4.956>
- Rodionov, S. M., Khanchuk A. I., Obolenskiy, A. A., Ogasawara, M., Seminskiy, Z. V., Prokopiiev, A. V., Timofeev, V. F., and Nokleberg, W. J., 2011, Middle Jurassic through Quaternary metallogenesis and tectonics of Northeast Asia, Chapter 8, in Parfenov, L. M., Nokleberg, W. J., and 17 others, editors, *Tectonic and metallogenic model for Northeast Asia*: US Geological Survey Professional Paper 1765 (Open-File Report 2011-1026), 137 p.
- Saheki, K., Shiba, M., Itaya, T., and Onuki, H., 1995, K-Ar ages of the metamorphic and plutonic rocks in the southern part of the Hidaka belt, Hokkaido and their implications: *Journal of Mineralogy, Petrology and Economic Geology*, v. 90, p. 297–309 (in Japanese with English abstract).
- Sengor, A. M. C., and Natal'in, B. A., 1996, Turcic-type orogeny and its role in the making of the continental crust: *Annual Review of Earth and Planetary Sciences*, v. 24, p. 263–337, <http://dx.doi.org/10.1146/annurev.earth.24.1.263>
- Seno, T., Sakurai, T., and Stein, S., 1996, Can the Okhotsk plate be discriminated from the North American plate?: *Journal of Geophysical Research-Solid Earth*, v. 101, n. B5, p. 11305–11315, <http://dx.doi.org/10.1029/96JB00532>
- Shibata, K., 1968, K-Ar age determinations on granitic and metamorphic rocks in Japan: Reports, Geological Survey of Japan, v. 227, 73 p.
- Shibata, K., and Ishihara, S., 1979, Rb-Sr whole-rock and K-Ar mineral ages of granitic rocks in Japan: *Geochemical Journal*, v. 13, n. 3, p. 113–119, <http://dx.doi.org/10.2343/geochemj.13.113>
- 1981, K-Ar ages of granitoids of the Hidaka belt: Tokyo, Japan, Abstract issue, 88<sup>th</sup> Annual Meeting of the Geological Society of Japan, p. 342.
- Shibata, K., Yamaguchi, S., and Satoh, H., 1975, K-Ar ages of the Miocene to Pleistocene series in the Tokachi region, Hokkaido: *Bulletin of the Geological Survey of Japan*, v. 26, p. 491–496 (in Japanese with English abstract).
- Shimura, T., Owada, M., Osanai, Y., Komatsu, M., and Kagami, H., 2004, Variety and genesis of the pyroxene-bearing S- and I-type granitoids from the Hidaka Metamorphic belt, Hokkaido, northern Japan: *Transactions of the Royal Society of Edinburgh, Earth Sciences*, v. 95, n. 1–2, p. 161–179, <http://dx.doi.org/10.1017/S0263593300000997>
- Söderlund, U., Patchett, P. J., Vervoort, J. D., and Isachsen, C. E., 2004, The <sup>176</sup>Lu decay constant determined by Lu-Hf and U-Pb isotope systematics of Precambrian mafic intrusions: *Earth and Planetary Science Letters*, v. 219, n. 3–4, p. 311–324, [http://dx.doi.org/10.1016/S0012-821X\(04\)00012-3](http://dx.doi.org/10.1016/S0012-821X(04)00012-3)
- Stern, R. J., 1994, Arc assembly and continental collision in the Neoproterozoic East African orogen: Implications for the consolidation of Gondwanaland: *Annual Reviews of Earth Planetary Sciences*, v. 22, p. 319–351, <http://dx.doi.org/10.1146/annurev.earth.22.050194.001535>
- Streckeisen, A., and Le Maitre, R. W., 1979, A chemical approximation to the modal QAPF classification of the igneous rocks: *Neues Jahrbuch für Mineralogie, Abhandlungen*, v. 136, p. 169–206.
- Suetake, S., 1997, Heterogeneous structures in a plutonic complex: Inferences from the Tottabetsu plutonic complex, the Main zone of the Hidaka metamorphic belt, Hokkaido: The memoirs of the Geological Society of Japan, v. 47, p. 57–74 (in Japanese with English abstract).
- Taira, A., 2001, Tectonic evolution of the Japanese island arc system: *Annual Review of Earth and Planetary Sciences*, v. 29, p. 109–134, <http://dx.doi.org/10.1146/annurev.earth.29.1.109>
- Takagi, T., Orihashi, Y., Naito, K., and Watanabe, Y., 1999, Petrology of a mantle-derived rhyolite, Hokkaido, Japan: *Chemical Geology*, v. 160, n. 4, p. 425–445, [http://dx.doi.org/10.1016/S0009-2541\(99\)00111-4](http://dx.doi.org/10.1016/S0009-2541(99)00111-4)
- Takahashi, N., 1991, Origin of three peridotite suites from Horoman peridotite complex, Hokkaido, Japan: Melting, melt segregation and solidification processes in the upper mantle: *Journal of Mineralogy, Petrology and Economic Geology*, v. 86, n. 5, p. 199–215, <http://dx.doi.org/10.2465/ganko.86.199>
- Takanashi, K., Shuto, K., and Sato, M., 2011, Origin of late Paleogene to Neogene basalts and associated coeval felsic volcanic rocks in Southwest Hokkaido, northern NE Japan arc: Constraints from Sr and Nd isotopes and major- and trace-element chemistry: *Lithos*, v. 125, n. 1–2, p. 368–392, <http://dx.doi.org/10.1016/j.lithos.2011.02.020>
- Takanashi, K., Kakihara, Y., Ishimoto, H., and Shuto, K., 2012, Melting of crustal rocks as a possible origin for Middle Miocene to Quaternary rhyolites of northeast Hokkaido, Japan: Constraints from Sr and Nd isotopes and major- and trace-element chemistry: *Journal of Volcanology and Geothermal Research*, v. 221–222, p. 52–70, <http://dx.doi.org/10.1016/j.jvolgeores.2011.11.008>
- Takashima, R., Nishi, H., and Yoshida, T., 2002, Geology, petrology and tectonic setting of the Late Jurassic ophiolite in Hokkaido, Japan: *Journal of Asian Earth Sciences*, v. 21, n. 2, p. 197–215, [http://dx.doi.org/10.1016/S1367-9120\(02\)00028-7](http://dx.doi.org/10.1016/S1367-9120(02)00028-7)
- Takazawa, E., Frey, F. A., Shimizu, N., Saal, A., and Obata, M., 1999, Polybaric petrogenesis of mafic layers in the Horoman peridotite complex, Japan: *Journal of Petrology*, v. 40, n. 12, p. 1827–1851, <http://dx.doi.org/10.1093/ptrology/40.12.1827>
- Takazawa, E., Frey, F. A., Shimizu, N., and Obata, M., 2000, Whole-rock compositional variations in an upper mantle peridotite (Horoman, Hokkaido, Japan): are they consistent with a partial melting process?: *Geochimica et Cosmochimica Acta*, v. 64, n. 4, p. 695–716, [http://dx.doi.org/10.1016/S0016-7037\(99\)00346-4](http://dx.doi.org/10.1016/S0016-7037(99)00346-4)
- Tamaki, K., and Honza, E., 1985, Incipient subduction and obduction along the eastern margin of the Japan Sea: *Tectonophysics*, v. 119, n. 1–4, p. 381–406, [http://dx.doi.org/10.1016/0040-1951\(85\)90047-2](http://dx.doi.org/10.1016/0040-1951(85)90047-2)
- Ueda, H., 2005, Accretion and exhumation structures formed by deeply subducted seamounts in the

- Kamuiokotan high-pressure/temperature zone, Hokkaido, Japan: *Tectonics*, v. 24, p. 1–17, TC2007, <http://dx.doi.org/10.1029/2004TC001690>
- Ueda, H., Kawamura, M., and Niida, K., 2000, Accretion and tectonic erosion processes revealed by the mode of occurrence and geochemistry of greenstones in the Cretaceous accretionary complexes of the Idonnappu zone, southern central Hokkaido, Japan: *Island Arc*, v. 9, n. 2, p. 237–257, <http://dx.doi.org/10.1046/j.1440-1738.2000.00275.x>
- Usuki, T., Kaiden, H., Misawa, K., and Shiraiishi, K., 2006, Sensitive high resolution ion microprobe U-Pb ages of the latest Oligocene-Early Miocene rift-related Hidaka high-temperature metamorphism in Hokkaido, northern Japan: *The Island Arc*, v. 15, n. 4, p. 503–516, <http://dx.doi.org/10.1111/j.1440-1738.2006.00547.x>
- Wen, D. R., Liu, D. Y., Chung, S. L., Chu, M. F., Ji, J. Q., Zhang, Q., Song, B., Lee, T. Y., Yeh, M. W., and Lo, C. H., 2008, Zircon SHRIMP U-Pb ages of the Gangdese Batholith and implications for Neotethyan subduction in southern Tibet: *Chemical Geology*, v. 252, n. 3–4, p. 191–201, <http://dx.doi.org/10.1016/j.chemgeo.2008.03.003>
- Whalen, J. B., Currie, K. L., and Chappell, B. W., 1987, A-type granites: geochemical characteristics, discriminations and petrogenesis: *Contributions to Mineralogy and Petrology*, v. 95, n. 4, p. 407–419, <http://dx.doi.org/10.1007/BF00402202>
- Woodhead, J., Hergt, J., Shelley, M., Eggins, S., and Kemp, R., 2004, Zircon Hf-isotope analysis with an excimer laser, depth profiling, ablation of complex geometries, and concomitant age estimation: *Chemical Geology*, v. 209, n. 1–2, p. 121–135, <http://dx.doi.org/10.1016/j.chemgeo.2004.04.026>
- Woodhead, J. D., and Hergt, J. M., 2005, A preliminary appraisal of seven natural zircon reference materials for *in situ* Hf isotope determination: *Geostandards and Geoanalytical Research*, v. 29, n. 2, p. 183–195, <http://dx.doi.org/10.1111/j.1751-908X.2005.tb00891.x>
- Wu, F. Y., Yang, Y. H., Xie, L. W., Yang, J. H., and Xu, P., 2006, Hf isotopic compositions of the standard zircons and baddeleyites used in U-Pb geochronology: *Chemical Geology*, v. 234, n. 1–2, p. 105–126, <http://dx.doi.org/10.1016/j.chemgeo.2006.05.003>
- Xie, L. W., Zhang, Y. B., Zhang, H. H., Sun, J. F., and Wu, F. Y., 2008, *In situ* simultaneous determination of trace elements, U-Pb and Lu-Hf isotopes in zircon and baddeleyite: *Chinese Science Bulletin*, v. 53, n. 10, p. 1565–1573, <http://dx.doi.org/10.1007/s11434-008-0086-y>
- Yamada, N., Saito, E., and Murata, Y., editors, 1990, Computer-generated geologic map of Japan: The Geological Survey of Japan, 1:2,000,000 geological map, v. 22, scale 1:2,000,000.
- Yoshikawa, M., Nakamura, E., and Takahashi, N., 1993, Rb-Sr isotopic systematics in a phlogopite-bearing spinel lherzolite and its implications for age and origin of metasomatism in the Horoman peridotite complex, Hokkaido, Japan: *Journal of Mineralogy, Petrology and Economic Geology*, v. 88, n. 3, p. 121–130.
- Zeniya, R., Maeda, J., Itaya, T., and Kagami, H., 1996, Isotopic age of ferrogabbro in the Pankenushi gabbroic intrusion in the northern Hidaka Mountains, Hokkaido: *Abstracts of the Annual Meeting of the Geological Society of Japan*, v. 103, p. 133 (in Japanese).
- Zhao, D., Wang, Z., Umino, N., and Hasegawa, A., 2007, Tomographic imaging outside a seismic network: Application to the northeast Japan arc: *Bulletin of Seismological Society of America*, v. 97, n. 4, p. 1121–1132, <http://dx.doi.org/10.1785/0120050256>
- Zhao, D., Yu, S., and Ohtani, E., 2011, East Asia: Seismotectonics, magmatism, and mantle dynamics: *Journal of Asian Earth Sciences*, v. 40, n. 3, p. 689–709, <http://dx.doi.org/10.1016/j.jseas.2010.11.013>